MEMOIRS

OF THE

COLLEGE OF SCIENCE

KYOTO IMPERIAL UNIVERSITY

SERIES A

VOL. XXIII, NO. 5

AUGUST 1941

KYOTO

On the Refined Structure of the Silver-rich Aluminium-Silver Alloys[1]

By **Hajime Kotô**

(Received November 1, 1940)

Abstract

Microscopic examination was made in connection with various quenched specimens of the aluminium-silver alloys containing 6.5 per cent. of aluminium and of the same with the addition of a small quantity of Sn and Sb respectively and also of the alloy with 7 per cent. of aluminium. The X-ray investigation was then carried out, to test the crystal structures and the crystalline configurations of the same alloys.

As the consequence of these researches, it was found on the one hand that the micro-structures of those alloys both normal and modified are considerably refined, depending on differences in the quenching temperatures, and the quenching agents and in the concentrations of the added metal; and on the other hand that the micro-structures of these specimens were proved not to be always in agreement with their crystalline configurations.

Introduction

Among the investigations of the refined structures of the alloys, much has been done with those of the Silumin-structure, but up to the present little has been done with those of the other alloys.

Several years ago, in connection with the normal and modified Si-Al alloys the writer[2] reported that the micro-structures in these specimens were not always in agreement with their inner crystalline configurations. Furthermore, with regard to the eutectic alloys, such as antimony-lead, lead-bismuth and tin-bismuth,[3] their refined structures were studied using the method that had been used earlier with Si-Al alloys.

Among the aluminium-silver alloys under consideration, those which bear either $\alpha+\beta$ or β above 600°C, exhibit the refined structure or not, according to the differences in the quenching temperatures and in the quenching media. In the case of the brasses, Bauer and Hansen[4]

1. A part of this paper was read at the 61 st annual meeting of the Chemical Society of Japan, April, 1939.

2. H. Kotô; These Memoirs, A, **18**, 17 (1935); The Report of the Institute for Chemical Research, Imperial University, Kyoto, **5**, 104 (1935).

3. Presented at the Autumn Meeting of the Institute for Chemical Research, December 11, 1937. These Memoirs, A, **23**, 298 (1941).

4 Der Aufbau der Kupfer-Zinklegierungen (1927) S. 92.

have previously attempted similar experiments, investigating their micro-structures only.

In the present experiment, the writer made more precise investigation in connection with the aluminium-silver alloys which give rise to such refined structures as described above, and moreover examined their crystalline configurations and crystal structures with X-rays.

Specimens

The silver used was of the highest purity (1000/1000), especially prepared at the Imperial Mint, Osaka ; the aluminium was also of the utmost purity (99.996%). Under a layer of sodium chloride the alloys were prepared in a graphite crucible, carefully protected from oxidation and introduction of impurities. After the silver was melted the aluminium was added, then the mixture well stirred, and the alloy cast into an iron mould (6.5 mm. in inner diameter and 60 mm. long). The specimens used were prepared by cutting these ingots to suitable size.

Micro-structures

After several trials, the electrolytic etching process using a 10 per cent. solution of citric acid, was found to give the best results, particularly for the development of the refined structure. A mixture of chromic and nitric acids is suitable for etching the homogeneous alloy. Moreover, for the convenience of comparison all the micro-photographs were taken with a magnification of 160 diameters.

From the constitutional diagram of the system Al-Ag in Fig. 1, it is conceivable that a specimen of the alloy containing 7 per cent. of aluminium gives rise to the transformation of $\beta \rightleftarrows \alpha+\beta$ between 665° and 670°C ; i. e., at this temperature of transformation it converts, when quenched, into β or $\alpha+\beta$. The numbers in Fig. 1 correspond to those of the annexed micro-photographs and are only appended to represent the positions of the specimens in the constitutional diagram.

To examine the differences of the micro-structures according to the variations in the annealing times, the quenching temperatures and the quenching media, the annealing time was fixed for convenience sake as one hour and the quenching medium as ice-water, while the quenching temperature was varied.

As can be seen in Photo 1, Plate I, the micro-structure of the alloy containing 7 per cent. of aluminium quenched from 750°C in ice-water is composed only of the β-phase. While Photo 2 indicates that the

Fig. 1

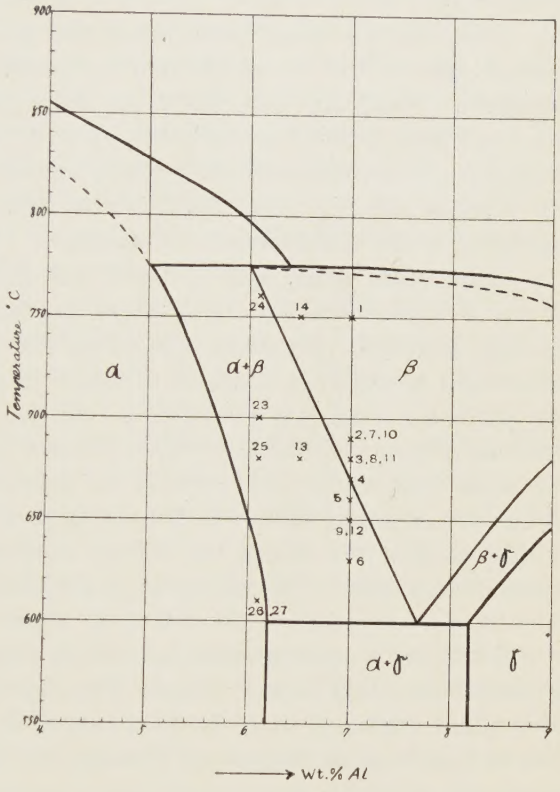

alloy containing 7 per cent. of aluminium quenched from 690°C in ice-water consists of a small amount of α-crystals finely separated in the ground mass of β-phase. This fact may be explained in the following manner :- When the alloy is plunged into ice-water, its temperature suddenly falls to that of the solubility curve as $\alpha+\beta \backsim \beta$, so that the separation represented by $\beta \rightarrow \alpha$ instantly sets in, and the separated α-crystals cannot grow and consequently they are fine. Since the quenching temperature in this case is a little high, the larger portion of the specimen enters into the quenching medium before the temperature falls to that of the solubility curve and consequently the separated α-crystals are very slight. While the specimen quenched from 680°C in ice-water, as can be seen in Photo 3, Plate I, is composed of a large amount of α finely separated throughout the β-grains.

The mechanism of such a refined structure is explainable and will be described below. When the specimen is immersed in the quenching liquid, the temperature of the larger portion of the specimen arrives at just the transition temperature, because the difference between the quenching-and transition-temperatures is only higher or lower than 10°C, and suddenly the separation as $\beta \rightarrow \alpha$ takes place for a moment throughout the specimen, and consequently such refined structure is given rise to. Photo 4 shows the micro-structure of the

specimen quenched from 670°C in ice-water. When the specimen is plunged into the quenching medium, a large part of it passes through the transformation temperature, since the quenching temperature just corresponds to the transformation temperature. Consequently, the separated crystals are very slight, as shown in Photo 4. While as is seen in Photo 5, when quenched from 660°C in ice-water, the insoluble α-crystals already remain in the β-phase and the α-crystals separated from the β-phase are also very slight, because this temperature of quenching is below the transformation temperature. Moreover, as the quenching temperature is lowered to 650°C and also to 630°C, the amounts of the α-crystals insoluble in β-phase gradually increase, and the α-crystals separated in β-phase almost do not appear. The fact above mentioned is observed in Photo 6, which shows the micro-structure of the specimen quenched from 630°C. As the micro-photograph of the specimen quenched from 650°C is similar to that of the specimen quenched from 630°C, the former is not here reproduced. In the above cases, the annealing time was always fixed at an hour, but even when it was fixed at five hours, the refined structures of the present specimens did not alter. Therefore, for convenience sake the annealing time was fixed at an hour in the following experiments.

Next, for a more gradual quenching castor-oil was used in place of ice-water. In Photo 7, Plate I, the alloy containing 7 per cent. of aluminium quenched from 690°C in castor-oil is observed to consist of the α-crystals finely separated throughout the β-grains, presenting a somewhat different aspect from that quenched from the same temperature in ice-water. Such a refined structure is given rise to by the fact that the greater part of the specimen passes slowly through the transformation temperature in the quenching medium, owing to the heat conductivity of the castor-oil which is smaller than that of ice-water and also to other facts. As can be seen in Photo 8, Plate I, the alloy quenched from 680°C in castor-oil bears nearly the same micro-structure as that quenched from the same temperature in ice-water. In Photo 9, Plate I, the micro-structure of the alloy containing 7 per cent. of aluminium quenched from 650°C in castor-oil is observed to consist of the insoluble α-crystals and those finely separated throughout the β-grains.

Lastly, for the most gradual quenching, boiling water was used. Photos 10 and 11 show the refined structures of the alloys containing 7 per cent. of aluminium quenched from respectively 690° and 680°C in boiling water; each of them is observed to consist of the α-crystals

finely separated throughout the β-grains, similar to those quenched in castor-oil, while the separated crystals in the former are much larger than in the latter. This may be explainable by the fact that the separated crystals have time to grow, owing to the slow rate of cooling of the specimen after being immersed in the quenching medium. As can be seen in Photo 12, the insoluble α-crystals remain in the β-phase in the case of the specimen quenched from 650°C, similarly as in the case of those quenched in the previous quenching media and the state of separation of α-crystals in the β-phase is also very similar, even though the separated α-crystals come to appear very large.

As is seen in Photo 13, the specimen quenched from 680°C in ice-water consists of a considerable amount of the insoluble α-crystals and the finely separated ones in the β-phase. Photo 14 shows the micro-photograph of the specimen quenched from 750°C in ice-water; no insoluble α-crystals remain, since this temperature is a little higher than that of the solubility curve $\alpha+\beta\sim\beta$. The reason why the finely separated α-crystals in the β-phase should be given rise to, is the fact that as soon as the specimen is immersed in the quenching medium, its temperature falls to that corresponding to the solubility curve above mentioned.

Microscopic examinations have been carried out in our laboratory by T. Ôtsubo,[1] in connection with the specimens of alloys quenched from 680°C in ice-water and containing about 1 per cent. of As, Cd, Cu, Mg, Mn, Sb, Sn and Zn respectively in addition to 6.5 per cent. of aluminium. By these examinations, the micro-structure of the alloys, especially of the specimens containing Sb and Sn, was found to be fine, similar to the Silumin structure. Therefore, further investigation was made by the present writer to see whether their micro-structures are fine or not with regard to the specimens quenched from 680°C and containing 0.1~2% of Sn and Sb respectively besides 6.5% of aluminium.

The micro-photographs of some of the specimens quenched from 680°C and containing tin in addition to 6.5 per cent. of aluminium, are reproduced in Photos 15, 16 and 18.

The micro-structure of the specimen quenched from 680°C in ice-water and containing 0.1 per cent. of tin in addition to 6.5 per cent. of aluminium (not reproduced) scarcely differs from that of the previous

1. This was read by T. Ôtsubo at the meeting of the Chemical Society of Japan, April, 1938.

specimen quenched in the same way and containing 6.5 per cent. of aluminium modified with 0.1 per cent. of tin shown in Photo 13. The micro-structure of the specimen quenched from 680°C in ice-water and containing 0.5% Sn besides 6.5 per cent. of aluminium (not reproduced) bears fair resemblance to that of the specimen containing 0.1 per cent. of tin besides 6.5 per cent. of aluminium quenched in the same way, except that the insoluble α-crystals increase with the increment of tin-content in the specimen.

While in the specimen quenched from 680°C in ice-water and containing 1% of Sn in addition to 6.5% of aluminium, as shown in Photo 15, no insoluble α-crystals exist, and rather the separation of the fine α-crystals takes place throughout the β-phase. The micro-structure of the specimen quenched from 680°C in castor-oil and containing 1% of Sn besides 6.5% of aluminium is almost the same as that of the specimen containing 1% of Sn besides 6.5% of aluminium quenched from 680°C in ice-water. The micro-structure of the two specimens above mentioned bears marked similarity to that of the specimen containing 7% of aluminium quenched from 690°C in boiling water (see Photo 10); the separated α-crystals have a tendency to become somewhat coarse. In Photo 16, Plate II, which shows the micro-structure of the specimen containing 1% of Sn in addition to 6.5% of aluminium quenched from 680°C in boiling water, the separated α-crystals in the β-phase are observed to have become more coarse. Moreover, as is seen in Photo 17, when the alloy containing 0.1% of aluminium and 1% of tin in addition to 6.5% of aluminium was quenched from 680°C in boiling water, the separation of the α-crystals in the β-phase decreased markedly. When the same alloy is quenched from 680°C in castor-oil, its micro-structure bears close resemblance to Photo 17. Consequently, it may be considered that with the increase of only 0.1%Al, the temperature corresponding to the solubility curve falls at least 10°C. Moreover, in connection with the effect of added metal on the refinement of the micro-structure, it may be concluded from the results of these experiments that aluminium was found to be more efficacious than tin. Photo 18 shows the micro-photograph of the specimen containing 2% of tin in addition to 6.5% of aluminium quenched from 680°C in ice-water; no separation of α-crystals in the β-phase takes place.

Photo 19, 20 and 22 show micro-photographs of some of the specimens containing 0.1~2 per cent. of antimony in addition to 6.5 per cent. of aluminium quenched from 680°C.

The micro-structures of the specimens quenched from 680°C in ice-water and containing 0.1 and 0.5 per cent. of antimony in addition to 6.5 per cent. of aluminium (not reproduced), scarcely differ from that of the similarly quenched specimen containing 6.5 per cent. of aluminium shown in Photo 13; i. e., the insoluble α-crystals remain in the β-phase and also the fine α-crystals separate in that phase. The field of the insoluble α-crystals increases with the increment of antimony-content, similarly to the case of tin-content. Moreover, as is seen in Photo 19, the micro-structure of the specimen quenched from 680°C in ice-water and containing 1 per cent. of antimony in addition to 6.5 per cent. of aluminium, bears fair resemblance to that of the specimen containing 7 per cent. of aluminium quenched in the same manner (Photo 3). The micro-structure of the specimen quenched from 680°C in castor-oil and containing 1 per cent. of antimony in addition to 6.5 per cent. of aluminium also bears close resemblance to that of the specimen containing 7 per cent. of aluminium quenched in the similar way. Photo 20 shows the micro-photograph of the specimen quenched from 680°C in boiling water; the separated α-crystals in the β-phase seem to become somewhat coarse. As may be seen in Photo 21, when the alloy containing 0.1 per cent. of aluminium besides 6.5 per cent. of aluminium and 1 per cent. of antimony is quenched from 680°C in boiling water the separated α-crystals decrease remarkably. Consequently, in this case, as in the case where tin is added, the aluminium may be easily supposed to be more conspicuous than the antimony, as to the effect on the separation of the α-crystals in the β-phase. Furthermore, in Photo 22, which is taken with the specimen containing 2 per cent. of antimony quenched from the same temperature in ice-water, the separation of the α-crystals from the β-phase can scarcely be observed; but if we inspect the micro-photograph in Photo 22 more precisely, its aspect differs somewhat from that caused by tin: i. e., since the amount of antimony in this case is comparatively large (2 per cent.), some separation, which may be supposed to be given rise to by the other phase of the ternary system, seems to take place at the grain boundaries of β. The fact above mentioned, is analogous to the fact that in the case of brasses the separation takes place at the grain boundaries, as was pointed out by Bauer and Hansen.[1] Photos 23~27 show the micro-photographs of the specimens containing 6.1 per cent. of aluminium quenched from various tem-

1. Loc. cit.

peratures respectively in ice-water, after annealing at 700°C for 2 hours; each of them consists of $\alpha+\beta$. Photo 23 shows the micro-structure of the specimen quenched from 700°C, after annealing at 700°C for 2 hours; the quantities of α-and β-phases are nearly equal. Photo 24 shows the micro-photograph of the specimen quenched from 760°C in ice-water, raising the temperature up to 760°C in 4 minutes, after annealing at 700°C for 2 hours; it is observed that the insoluble α-crystals, though heated for such a short time, considerably decrease, owing to their solubility in the β-phase, and the separation of the α-crystals in the β-phase is more markedly increased than when quenched from 700°C as above described. Photo 25 shows the micro-photograph of the specimen quenched from 680°C in ice-water, lowering the temperature to 680°C in 2.5 minutes, after annealing at 700°C for 2 hours; although the quenching temperature differs only 20°C from that in the case of Photo 23, the separation of the α-crystals from the β-phase has already a tendency to decrease, and also the number of insoluble α-crystals in the β-phase seems to increase to some extent. Photo 26 shows the micro-photograph of the specimen quenched from 610°C in ice-water, lowering the tempeature down to 610°C in 1 minute, after annealing at 700°C for 2 hours; the separation of the α-crystals from the β-phase almost does not take place, and notwithstanding the fact that the quenching temperature differs 70°C from that in the case of Photo 25, the quantity of insoluble α-crystals in the β-phase in these specimens does not differ. This is due to the decreasing mobility of atoms in the space lattice with falling temperature. Even in such a case as this, the insoluble α-crystals in the β-phase increase, when the rate of cooling is sufficiently slow. Photo 27 represents the micro-photograph of the specimen quenched from 610°C in ice-water, after being allowed to cool from 700° to 610°C in 8.5 minutes; the α-crystals are observed to be greatly increased.

Crystalline Configuration

X-ray examination was first carried out by means of Laue's method, to see whether the micro-structure of the specimens above mentioned gives any accurate information in connection with the actual size and configuration of the micro-crystals. In this research, the same ingots used for the microscopic examination above described, were used as specimens. To utilize the specimens in this examination, two series of thin plates were cut out transversely and longitudinally from each ingot, respectively and etched by conc. nitric acid until they were

reduced to about 0.08 mm. in thickness to remove the mechanical distortions of their surfaces. Then the planed surface of each specimen was set perpendicularly to the incident heterogeneous X-ray beam emitted from the molybdenum anticathode. Now, two series of the diffraction patterns could be obtained; the one is given rise to by the incidence of X-rays perpendicular to the transverse section of ingot, while the other corresponds to the incidence perpendicular to the longitudinal section.

Some of the diffraction patterns thus obtained are reproduced in Plate III. It is noticed that not only those here reproduced, but all the patterns due to the incidence of X-rays perpendicular to respectively the transverse and longitudinal sections of the same specimen, were found not to differ essentially from each other.

As can be seen in Photos 28 and 29, Plate III, both diffraction patterns produced by the alloy containing 7 per cent. of aluminium quenched from 680°C in ice-water (see Photo 3), consist of an irregular assemblage of somewhat elongated Laue's spots. We may conclude from this fact that the specimen under examination is composed of crystals of comparatively large size, and bears a fibrous nature of weak degree. The above conclusion does not agree closely with the results of the microscopic examinations; as can be seen in Photo 3, Plate I, the size of crystallites is rather small.

Photos 30 and 31, Plate III, are the diffraction patterns taken with the alloy containing 6.5 per cent. of aluminium and quenched in a similar way to Photos 28 and 29, Plate III. The prominent parts of these patterns consist of a set of the discontinuous Debye-Hull rings and a number of radiating bands. Thus from the presence of Debye-Hull rings in Photos 30 and 31, Plate III, it can be concluded that the specimen under consideration is partly composed of an irregular aggregation of micro-crystals of comparatively small dimension (about 10^{-2}mm. in diameter): but the presence of radiating bands shows us that the larger portion of it has a fibrous structure.

The diffraction patterns occurring upon the specimen containing 0.1 per cent. of tin in addition to 6.5 per cent. of aluminium scarcely differ from those in the former specimen containing only 6.5 per cent. of aluminium. The diffraction patterns in Photos 32 and 33, Plate III, which were produced by the specimen containing 0.5 per cent. of tin besides 6.5 per cent. of aluminium consist mainly of a number of radiating bands. The predominance of such radiating bands in Photos 32 and 33, shows us without doubt that the larger portion of this

specimen has an incomplete fibrous structure. As is seen in Photos 34 and 35, Plate III, both diffraction patterns produced by the alloy containing 1 per cent. of tin in addition to 6.5 per cent. of aluminium, consist mainly of an irregular assemblage of somewhat elongated Laue's spots. Thus, we may conclude from the presence of such Laue's spots that contrary to the results of the microscopic examination (Photo 15), its crystalline structure is comparatively coarse, and has a somewhat fibrous nature. The diffraction patterns in Photos 36 and 37, Plate III, which were taken with the specimen containing 2 per cent. of tin, consist of somewhat regular Laue's spots. Thus it may be said that the crystallites constituting the specimens with 2 per cent. of tin, are of large size, as was concluded from the results of the microscopic examination (Photo 18).

The diffraction patterns occurring upon the specimens containing respectively 0.1 and 0.5 per cent. of antimony in addition to 6.5 per cent. of aluminium, differ almost none from those in the specimen containing 6.5 per cent. of aluminium, consistent with the results of the microscopic examination.

As can be seen in Photos 38 and 39, Plate III, the diffraction patterns taken with the alloy containing 1 per cent. of aluminium, consist mainly of a number of the discontinuous Debye-Hull rings. From the predominance of such Debye-Hull rings in Photos 38 and 39 it can be conculuded that this specimen is nothing but an aggregation of the finer micro-crystals without any regularity. The above conclusion agrees with the results of the microscopic examinations; as shown in Photo 19, Plate III, the micro-structure is very fine. Photos 40 and 41, Plate III are the diffraction patterns taken with the alloy containing 2 per cent. of antimony besides 6.5 per cent. of aluminium. The prominent parts of these patterns consist of a number of radiating bands. Thus, the predominance of radiating bands in Photos 40 and 41 shows us that this specimen has a fibrous structure.

Crystal Structure

It has been already reported[1] that in the present alloy, when quenched, the β-phase is converted into either $\alpha+\gamma$ or γ according to the composition. To learn whether any change in the β-phase may or may not be observable with the quenched specimens containing 0.1～2

1. H. Kotô and S. Nakamura; Bull. Chem. Soc., Japan, **58**, 694 (1937); The Report of the Institute for Chemical Research, Imperial University, Kyoto, **8**, 79 (1938).

per cent. of tin or antimony, the writer repeated the X-ray examination. In this examination, adopting the Debye-Scherrer method photographs were taken with the aid of a cylindrical camera of 7.03 cm. in diameter.

Utilizing K_α-radiation of copper some of the spectra thus obtained, are reproduced in Photos 42~50, Plate IV.

As can be seen in Photo 42, the spectral lines of the specimen containing 6.5 per cent. of aluminium quenched from 680°C in ice-water, are composed of lines due to both the α- and γ-phases in diffraction patterns. Photos 43~46 show the powder photographs taken with the alloys containing tin, and Photos 47~50, those taken with the alloys containing antimony. By comparing these figures with Photo 42, it was found that all the spectral lines of these specimens are composed of lines due to both the α- and γ-phases in diffraction patterns. Besides, increasing the amount of tin or antimony contained in the specimens from 0.1 to 2 per cent. gradually intensifies the lines corresponding to the γ-phase.

Thus it was concluded that according to the composition the β-phase converts, when quenched, into either $\alpha+\gamma$ or γ, in connection with the specimens containing tin or antimony ; i. e., amounts, at least of less than 2 per cent. of tin or antimony, constitute the ternary solid solution with aluminium and silver.

Conclusion

The experimental results which have hitherto been described, in connection with various specimens of the alloys of aluminium-silver and of those containing a small quantity of tin or antimony as the third metal besides aluminium and silver, led us to the following conclusions :—

(1) Contrary to the result of the microscopic examination, the specimen containing 7 per cent. of aluminium quenched from 680°C in ice-water, was found in the X-ray examination to be composed of crystals of comparatively large size.

(2) Such a discrepancy between the crystalline configuration and the micro-structure, could also be observed in the specimen containing 1 per cent. of tin in addition to 6.5 per cent. of aluminium.

(3) Contrary to the above, the crystalline configurations in the specimens containing respectively 1 per cent. of antimony and 2 per cent. of tin, is in good accordance with their micro-structures.

Thus the crystalline configuration in the specimens above men-

tioned, is not always in fair agreement with their micro-structure, as was found to be the case in the Silumin[1] and also in the binary eutectic alloys,[2] such as antimony-lead, lead-bismuth and tin-bismuth.

(4) It was concluded by the X-ray analysis that according to its composition, the alloy consisting of the β-constituent is converted, when quenched, into either $\alpha+\gamma$ or γ alloy, and also that with respect to the specimens containing tin or antimony, a similar bearing exists.

In conclusion, the writer wishes to express his heartiest thanks to Prof. D. Uno for his kind guidance, during the progress of this investigation and to Ass. Prof. H. Hirata for his valuable advice in the X-ray analysis. The expense for the experiments has been defrayed from a grant made to Prof. D. Uno by the Ministry of Education for the Promotion of Scientific Research, to which the author's thanks are due.

Institute of Metallography,
Department of Science,
Kyoto Imperial University.

1. Loc. cit.
2. Loc. cit.

Plate I

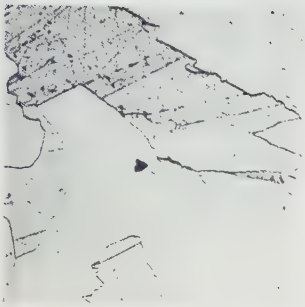

Photo 1. 7.0% Al
Quenched from 750°C in ice-water.

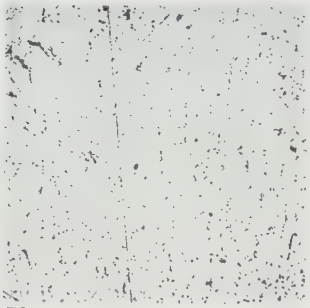

Photo 2. 7.0% Al
Quenched from 690°C in ice-water.

Photo 3. 7.0% Al
Quenched from 680°C in ice-water.

Photo 4. 7.0% Al
Quenched from 670°C in ice-water.

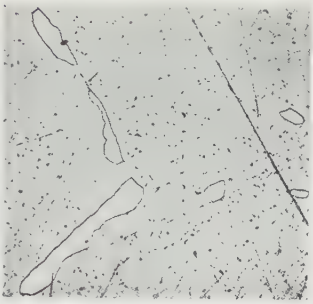

Photo 5. 7.0% Al
Quenched from 660°C in ice-water.

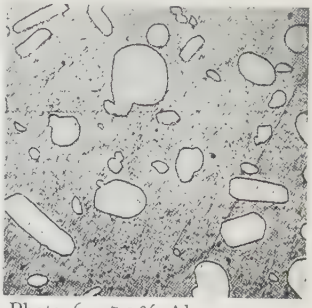

Photo 6. 7.0% Al
Quenched from 630°C in ice-water.

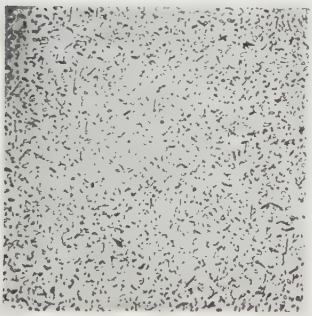

Photo 7. 7.0% Al
Quenched from 690°C in castor-oil.

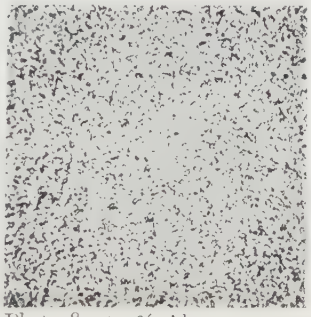

Photo 8. 7.0% Al
Quenched from 680°C in castor-oil.

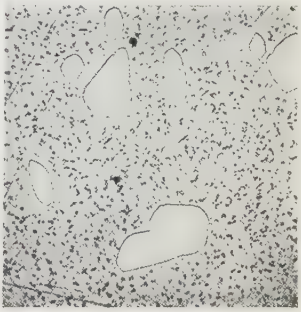

Photo 9. 7.0% Al
Quenched from 650°C in castor-oil.

Photo 10. 7.0% Al
Quenched from 690°C in boiling water.

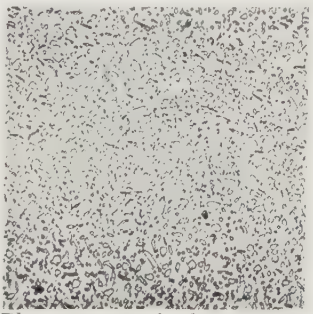

Photo 11. 7.0% Al
Quenched from 680°C in boiling water.

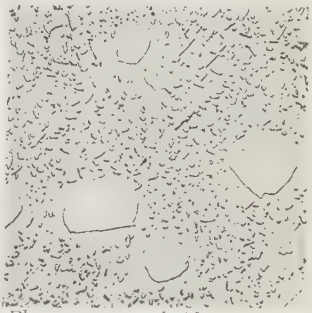

Photo 12. 7.0% Al
Quenched from 650°C in boiling water.

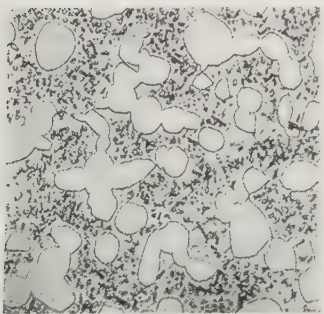

Photo 13. 6.5% Al
Quenched from 680°C in ice-water.

Photo 14. 6.5% Al
Quenched from 750°C in ice-water.

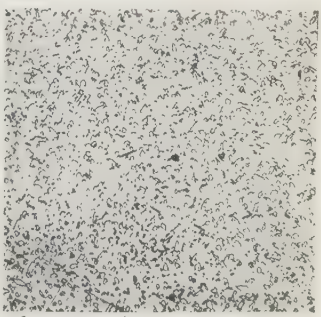

Photo 15. 6.5% Al, 1.0% Sn
Quenched from 680°C in ice-water.

Plaet II

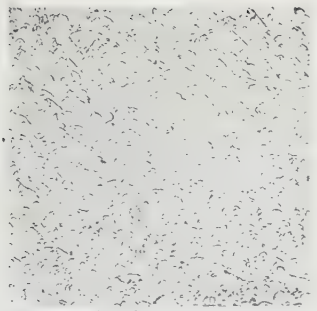

Photo 16. 6.5% Al, 1.0% Sn
Quenched from 680°C in boiling water.

Photo 17. 6·6% Al, 1.0% Sn
Quenched from 680°C in boiling water.

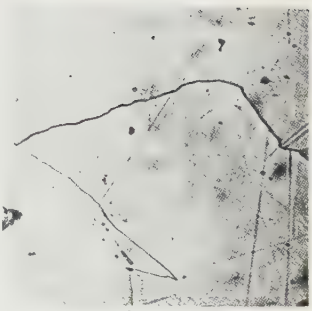

Photo 18. 6.5% Al, 2.0% Sn
Quenched from 680°C in ice-water.

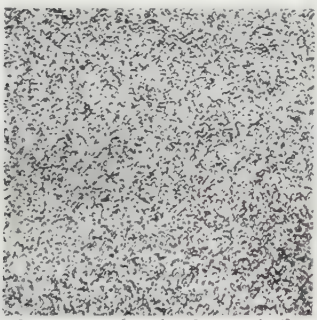

Photo 19. 6.5% Al, 1.0% Sb
Quenched from 680°C in ice-water.

Photo 20. 6.5% Al, 1.0% Sb
Quenched from 680°C in boiling water.

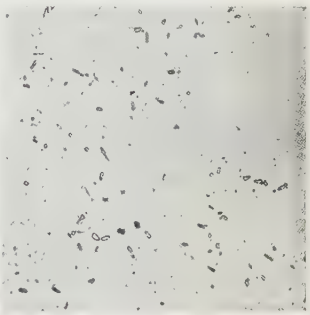

Photo21. 6.6%Al, 1.0% Sb
Quenched from 680°C in boiling water.

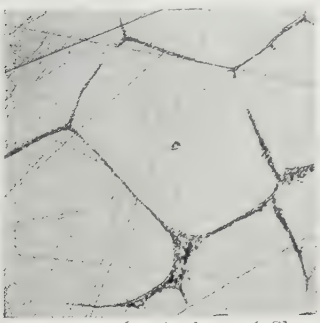

Photo 22. 6.5% Al, 2.0% Sb
Quenched from 680°C in ice-water.

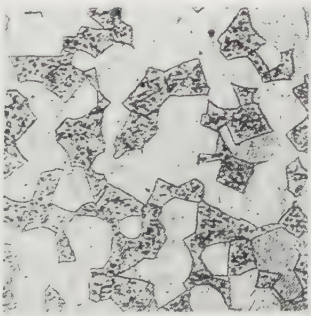

Photo 23. 6.1% Al
Quenched from 700°C in ice-water, after annealing for 2 hrs. at 700°C.

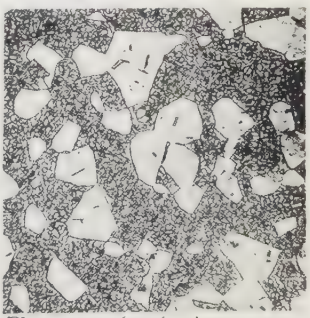

Photo 24. 6.1% Al
Quenched from 760°C in ice-water, after annealing for 2 hrs. at 700°C.

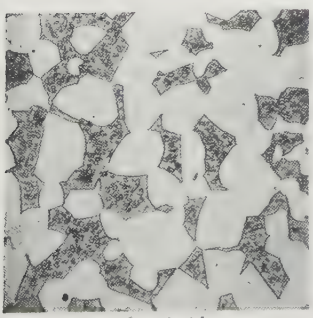

Photo 25. 6.1% Al
Quenched from 680°C in ice-water, after annealing for 2 hrs. at 700°C.

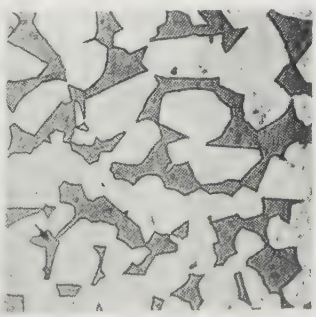

Photo 26. 6.1% Al
Quenched from 610°C in ice-water, after annealing for 2 hrs. at 700°C.

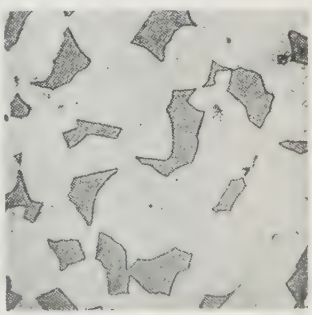

Photo 27. 6.1% Al
Slowly cooled to 610°C after annealing for 2 hrs. at 700°C and quenched from 610°C in ice-water.

Plate III

(Quenched from 680°C in ice-water, after annealing for an hour.)

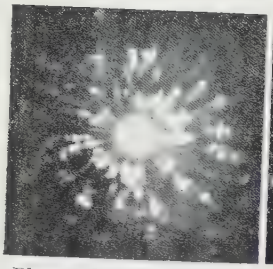

Photo 28. 7.0% Al
(Transversal section)

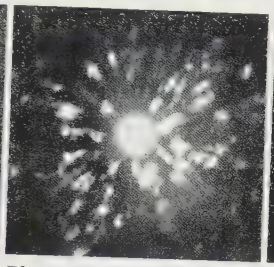

Photo 29. 7.0% Al
(Longitudinal section)

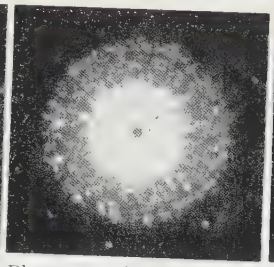

Photo 30. 6.5% Al
(Transversal section)

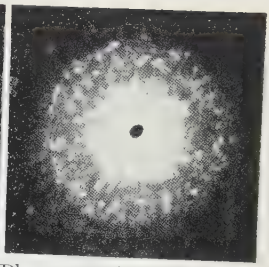

Photo 31. 6.5% Al
(Longitudinal section)

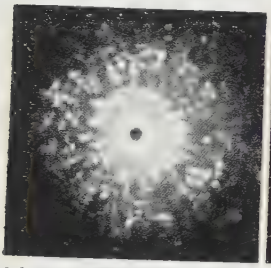

Photo 32. 6.5%Al, 0.5%Sn
(Transversal section)

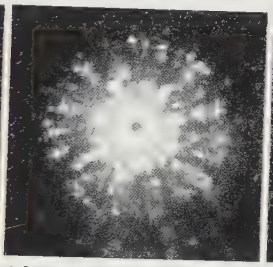

Photo 33. 6.5%Al, 0.5%Sn
(Longitudinal section)

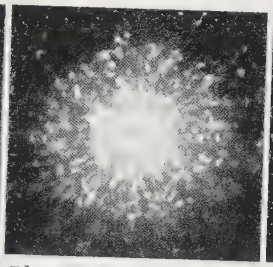

Photo 34. 6.5%Al, 1.0%Sn
(Transversal section)

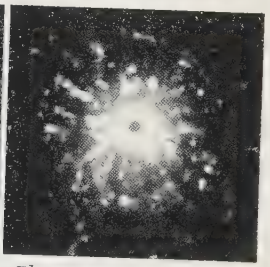

Photo 35. 6.5%Al, 1.0%Sn
(Longitudinal section)

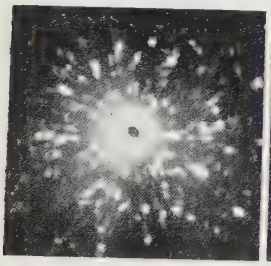

Photo 36. 6.5%Al, 2.0%Sn
(Transversal section)

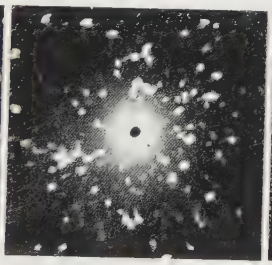

Photo 37. 6.5%Al, 2.0%Sn
(Longitudinal section)

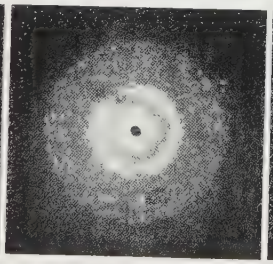

Photo 38. 6.5%Al, 1.0%Sb
(Transversal section)

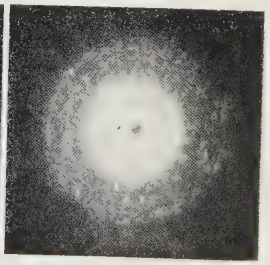

Photo 39. 6.5%Al, 1.0%Sb
(Longitudinal section)

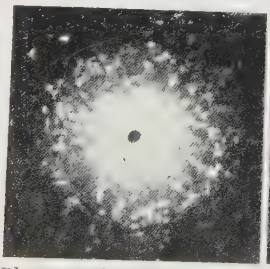

Photo 40. 6.5%Al, 2.0%Sb
(Transversal section)

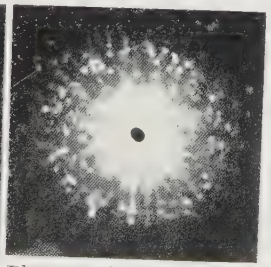

Photo 41. 6.5%Al, 2.0%Sb
(Longitucinal section)

Plate IV

(Quenched from 680°C in ice-water, after annealing for an hour.)

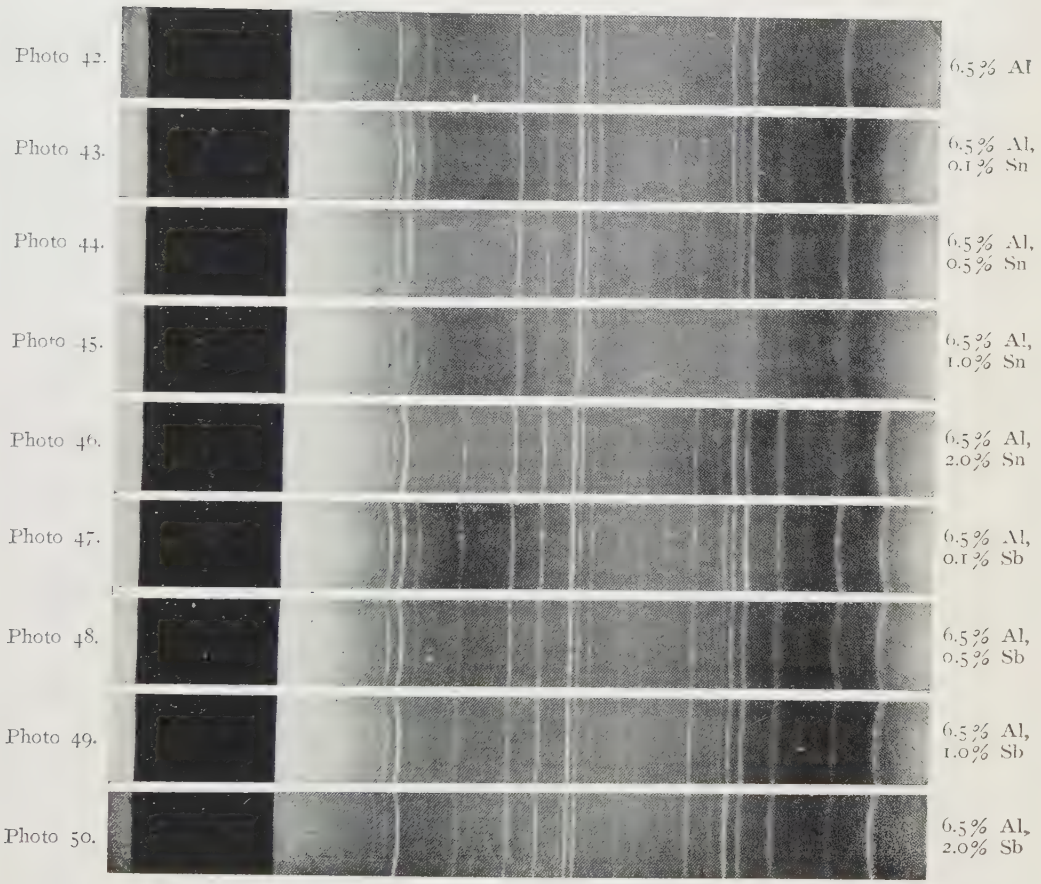

On the Refinement of the Eutectic-structure of Some Alloys by the Addition of a Small Quantity of Foreign Metal[1]

By **Kaoru Kase** and **Hajime Kotô**

(Received November 1, 1940)

Abstract

By microscopic and also by X-ray analyses, the normal and modified eutectic structures were examined in connection with various sand-cast and a few chill-cast specimens of lead-bismuth, tin-bismuth and antimony-lead alloys. Moreover, to make clear the mechanism of the modification especially in the case of Sb–Pb alloy, the thermal change, the influence of gas and the amounts of remaining aluminium were determined with regard to the normal and modified alloys.

As the consequence of these examinations, the micro-structures of the alloys of antimony-lead, lead-bismuth and tin-bismuth were found to be considerably refined with the addition of a small quantity of aluminium and calcium respectively.

Introduction

Improvement in the mechanical properties of casting alloys has been made by refining their micro-structure. Especially, it is well known that the eutectic structure of the sand-cast silicon-aluminium alloy becomes strikingly finer by the modifying process of adding a small quantity of sodium, alkali fluorides or the elements analogous to sodium. One of the writers[2] has previously reported in detail on the modified structure of silicon-aluminium alloy. The writers have undertaken the present investigation, supposing that such phenomena as characterize Si-Al alloys, may also be found in connection with the other eutectic alloys.

Specimens

Under powdered carbon or a mixture of 38%NaCl and 62%$CaCl_2$, the alloys were prepared in a graphite crucible. In sand moulds (15 mm. in inner diameter, 70 mm. long and about 25 mm. in thickness) castings were carried out at temperatures, respectively, of 450°~500°C in the case of Sb-Pb alloys, and of 300°~400°C in the cases of Sn-Bi

1. This paper was read at the meetings of the Kinki Branch of the Chemical Society of Japan, May, 1937, and of the Institute for Chemical Research, December, 1937.

2. H. Kotô; These Memoirs, A, **18**, 17 (1935).

and Pb-Bi alloys. For the microscopical examiation, Sb-Pb alloys were cut out longitudinally, but in the cases of Sn-Bi and Pb-Bi alloys transversely at the central part. Each of these specimens was well polished and then etched with a 2～4 per cent. alcoholic solution of nitric acid.

Micro-structures

I. The Sb-Pb System

In the antimony-lead system,[1] the eutectic point lies at 12.5～13%Sb and 247°～250°C, and a slight range of solid solution exists at both ends of the system. Photos 1～7, Plate I, show the micro-photographs of the specimens containing 12.5%Sb, in which the light areas represent the β-constituent (a saturated solid solution at Sb end) and the dark the more readily etched α-constituent (a saturated solid solution at Pb end). It can be seen from Photos 1 and 2 that there is a great difference in grain-size between the micro-structures of the chill- and sand-cast specimens.

(1) *The Effect of Na*

Sodium, as is well-known, is very efficacious for the modification of Si-Al alloy: but contrary to our supposition, this was found not to be effective for the modification of Sb-Pb alloy: e. g., the eutectic is composed of β crystallized in a needle-shape of considerable dimensions. Here, it is noticed that there are various methods of procedure in adding sodium to the melt; among these, the best is to plunge it suddenly into the melt, the sodium being fixed at the end of a carbon rod; and the suitable temperatures, for the melt when it is plunged in, are 600°～700°C.

Sodium gives rise to so slight a modification as to be hardly appreciable with the addition of 0.03% or even 0.1%; but its modifying effect can be detected with the addition of 0.3%: e. g., as shown in Photo 3, the modified alloy is of the coarse micro-structure, in which the β-constituent comes to appear in needle-shaped crystals of considerable dimensions and to be disposed in part in a radiating manner.

(2) *The Effect of Li*

The modifying effect due to the addition of lithium was also microscopically examined. But no sign of the modification could be observed,

1. H. Endô; Kinzoku no Kenkyu, **2**, 691 (1925).

even when 0.1 or 0.3% of lithium was added at 650°C, except that part of the light cubical crystals of β appear somewhat enlarged.

(3) *The Effect of Ca*

The calcium used is of small scale-like shape, and the part which is ready to undergo a change into CaO is observed. Accordingly, it is very difficult to plunge it thoroughly into the melt; so, under a mixture of 38%NaCl and 62%$CaCl_2$, calcium enclosed in a thin plate of lead was quickly plunged into the melt at about 850°C. In this way, all exposure to the atmosphere is avoid and the surface of the alloy is perfectly protected from oxidation. Photo 4, Plate I, shows the micro-structure of the specimen, to which 0.5 per cent. of calcium is added, and it is observed to be very fine.

(4) *The Effect of Al*

Aluminium is immiscible to lead even in the melt. Accordingly, when aluminium is to be added, it is reduced to small pieces and thrown into the melt, which is then well stirred, so that it may be uniformly mixed.

Gwyer and Phillips[1] have already found that the aluminium is very effective for the modification of Sb-Pb alloy. The modifying effect due to the addition of aluminium is most efficacious from 0.1 to 0.4%, but almost inappreciable with the addition of more than 0.5%, because the compound between aluminium and antimony is thought to have a tendency to form at the surface of the melt or, if formed below, to float up to the surface, solidifying immediately after forming, so that the aluminium does not remain in the melt. 700°~750°C is the most suitable temperature for adding the aluminium. It is necessary to stir the melt well just before casting. Moreover the casting temperature, efficacious for the modification, is 400°~550°C, but above 550°C or below 400°C, the micro-structure can never be fine. Photo 5 shows the micro-photograph of the specimen with the addition of 0.3%Al.

(5) *The Effect of Mg*

A mixture of 38%NaCl and 62%$CaCl_2$ was used as a flux. The modifying effect due to the addition of magnesium seems to be almost inappreciable up to 0.4%, but with the addition of a comparatively large amount (0.8%), the micro-structure is seen to become coarse, and the aspects of α and β crystals are somewhat varied, as shown in Photo 6.

(6) *The Effect of Cd*

As can be seen in Photo 7, the micro-structure of the specimen,

1. Gwyer and Phillips; J. Inst. Met., **36**, 283 (1926).

to which 0.3 per cent. of cadmium is added, is certainly finer than that of the normal one.

(7) *The Effect of As*

When arsenic is added at about 600°C, the effect is not only to curve the surface of the melt to a great extent, but to produce a highly fluid alloy. But the effect on the micro-structure is very slight.

(8) *The Effect of Te and Se*

When 0.2% of tellurium is added at about 600°C, its modifying effect was found to be somewhat appreciable, but almost inappreciable with the addition of more than 0.2%. That of selenium seems to be almost inappreciable.

From the results of this experiment it became clear that the metals such as sodium and lithium, which were very efficacious for the modification of Si-Al alloy, are never efficacious for the modification of Sb-Pb alloy: on the contrary, calcium, aluminium and cadmium are most efficacious for the modification. Especially, sodium gives rise to a coarser micro-structure, according to the amount added.

With regard to the modifying effects of some other elements belonging to the same group as Ca in the periodic table, such as Ba and Sr, no examination was made, but we may suppose that modification similar to that caused by calcium might be observed.

II. The Sn-Bi System

In the tin-bismuth system,[1] the eutectic point lies at 42%Sn and 140°C, and a solid solution exists on each side of tin[2] or bismuth, respectively. As can be seen in Photo 8, Plate I, the micro-structure of the sand-cast specimen is very coarse, in which α-crystal (a saturated solid solution at Sn end) appears in the characteristic large rounded dendritic form and β-crystal in a cubical form. But in an alloy containing 42 per cent. of tin, the β-crystal very seldom appears in such a form, and only the α-crystal is markedly developed. Consequently, this alloy seems to bear the micro-structure of an alloy containing an excess of tin above the eutectic proportion.

(1) *The Effect of Na*

Sodium acts to make coarse the micro-structure of the Sb-Pb alloy, and conversely to make that of the Sn-Bi alloy to some extent fine.

1. H. Endô; Kinzoku no Kenkyu, **2**, 682 (1925).
   A. C. Davidson; Techn. Publ. Intern. Tin Res. & Devel. Council, A, No. 77 (1938).
2. T. Satô, T. Matuhasi; Japan Institute of Metals, **2**, 592 (1938).

This fact has already been reported by Felice de Carli.[1] On the whole, such a conspicuous modifying action of sodium seems to be dependent on the formation of the ternary eutectic. As can be seen in Photo 9, Plate I, the micro-structure of the specimen containing 0.3 per cent. of sodium shows that contrary to the case of Sb-Pb alloy, sodium is very efficacious for the modification of Sn-Bi alloy.

(2) *The Effect of Al*

Aluminium is very efficacious for the modification of Sn-Bi alloy, as it is in the case of Sb-Pb alloy. As shown in Photo 10, the amount of added aluminium is sufficient with only 0.3 per cent.

(3) *The Effect of Ca*

As shown in Photo 11, calcium is very efficacious for the modification with the addition of 0.3 per cent. Moreover, if we inspect the micro-photograph more precisely, the α-and β-crystals develop a tendency to arrange themselves generally having a definite orientation towards the centre of the field.

(4) *The Effect of Te*

As is seen in Photos 12 and 13, the micro-structures of Sn-Bi alloys are refined to some extent by the addition of 0.25 per cent. of tellurium; but on the contrary, they are rendered very coarse when the proportion of tellurium is increased to 0.7 per cent. In this case, the light cubical crystals represent the well-developed β-ones.

Study was also made of the modifying effects of the addition of 0.3% Li, of 0.1% Se and of 0.5% Se. But these elements were all found not to be efficacious for modification.

III. The Pb-Bi System

In the lead-bismuth system,[2] the eutectic point lies at 43.5% Pb and 124°C, and the solid solution extends rather widely on each side of lead or bismuth. As can be seen in Photo 15, Plate II, the micro-

---

1. Felice de Carli: Atti III Congr. naz. chim. pura appl. Filenze e Toscana, 432 (1929).

2. W. Herold; Z. anorg. Chem., **112**, 131 (1920).

Here, it is noticed that at the 1st great meeting of the Japan Institute of Metals, opened in Tokyo on the 15th of May, 1937, immediately before the present writers read this paper at the regular meeting of the Kinki Branch of the Chemical Society of Japan, opened in Osaka on the 21st of May, 1937, this system was reported by Prof. K. Takahashi and Mr. T. Takase, not to be a simple eutectiferous series as hitherto supposed, but to have a series of solid solution formed by a peritectic reaction.

T. Takase; Japan Institute of Metals, **1**, 143 (1937).

Hans v. Hofe u. H. Hanemann; Zeits. f. Metallk., **32**, 112 (1940).

structure of the sand-cast specimen is considerably coarser, the α-(at Pb end) and β-(at Bi end) crystals appearing in the peculiar angular form. Photo 14, Plate I, shows the micro-structure of the chill-cast specimen; the α-and β-constituents crystallize out only in small dimensions, owing to the rapid cooling.

(1) *The Effect of Li*

As shown in Photo 16, Plate II, the addition of 0.1 per cent. of lithium provides the very fine micro-structure of Pb-Bi alloy.

(2) *The Effect of Na*

Photo 17 shows the micro-structure of the specimen in the case of addition of 0.1%Na, which is refined to some extent. The modifying effect of adding 0.3 per cent. of sodium was also found to be nearly the same as in the previous case. In this case, the α-constituent (the dark) characteristically crystallizes out in a much rounded form.

(3) *The Effect of Mg*

The modifying effect of the addition of 0.3% of magnesium was examined. As is seen from Photo 18, the β-constiuent crystallizes in a rather large shape, and consequently the micro-structure came on the whole to be rather coarse.

(4) *The Effect of Ca*

Photo 19 shows the micro-structure of the specimen in the case of addition of only 0.1 per cent. of calcium, and it will be observed to be very fine.

(5) *The Effect of Al*

The micro-structures of the specimens, which were produced by the addition of 0.1~0.3 per cent. of aluminium are all very fine, as was the case with calcium described above.

(6) *The Effect of Se*

Photo 20 represents the micro-structure of the specimen after the addition of about 0.6% of selenium, which is coarser than normal, the β-constituent crystallizing out in a rather large shape.

(7) *The Effect of As*

Photo 21 shows the micro-structure of the specimen produced by adding 0.15 per cent. of arsenic, and it is observed to be very fine. On the contrary, that of the specimen formed by adding 0.45 per cent. of arsenic is very coarse, as is shown in Photo 22.

(8) *The Effect of Te*

The micro-structure of the specimen in the case of adding 0.2%Te is observed to be somewhat fine; while that of the specimen produced by adding 0.5% of Te is coarse, similar to that of the original.

From the results of the experiments above described, both aluminium and calcium were found to be very efficacious for the modification of the alloys of antimony-lead, tin-bismuth and lead-bismuth.

To make clear the mechanism of modification of Sb-Pb alloy, the following experiments were carried out in connection with the normal and modified alloys.

Thermal Analysis

The specimen (12.5%Sb, the remainder Pb) weighing 40~50 grams was first melted in a Tammann tube placed in an electric resistance furnace, and after being transferred into a low temperature furnace previously prepared, it was subjected to thermal analysis under the powdery carbon, being somewhat rapidly cooled. Here it must be remarked that on solidifying pure lead does not show any tendency to undergo undercooling, while antimony generally undergoes very marked undercooling, and even when cooled in furnace, sometimes suffers the undercooling as much as about 60°C lower than its melting point. Consequently slight undercooling is also observed in the normal alloys of antimony and lead.

The curves obtained in the case of the alloys modified with aluminium or sodium indicate greater tendency to undercooling of the specimens at the temperatures of eutectic crystallization, than the curves corresponding to the normal ones do; besides, the eutectic temperature of the former is also somewhat lower than that of the latter. Furthermore, the alloy modified with calcium also has undergone nearly the same undercooling phenomena as was observed with those modified with aluminium or sodium.

Thus the modified structure of Sb-Pb alloys, caused by adding aluminium and calcium respectively can be considered to be due to the undercooling on solidifying. But the alloy modified with sodium, notwithstanding it has undergone the undercooling, is of larger microstructure. Consequently, it may not be confirmed that the undercooling is the only cause of the formation of the refined structure of Sb-Pb alloy.

The Influence of Gases on the Eutectic Structure

All the molten alloys always contain a small quantity of gases. Therefore the following experiments were made in connection with the Sb-Pb alloys, to examine the effect of gases upon their microstructure.

(1) Assuming that the fine structure caused by adding aluminium is due only to the strong deoxidizing action of aluminium, hydrogen was passed into the melt and the oxygen expelled; then the molten alloy was cast into the sand-mould, with the expectation that the fine structure might be obtained. Contrary to our assumption, the larger micro-structure was obtained, as shown in Photo 23, Plate II.

(2) The molten Sb-Pb alloy with the eutectic, first modified with 0.2 per cent. of aluminium and then treated by hydrogen, was cast from 450°C into the sand-mould at the ordinary temperature. As shown in Photo 24, no refinement of the micro-structure was observed, but the β-crystal was observed to segregate at the periphery of the ingot.

(3) In contrast to the former experiment (2), the molten Sb-Pb alloy with the eutectic, first treated by hydrogen and then modified with aluminium, was cast at 450°C. The micro-structure thus obtained is considerably refined, as is seen in Photo 25.

From the results of the experiments above described, it may be concluded that the refined micro-structure of Sb-Pb alloy caused by adding aluminium, is not due only to the deoxidizing action of aluminium, but also to some other effect, such as the change in the surface tension of the melted aluminium on the molten Sb-Pb alloy.

The Amounts of Aluminium Remaining in the Sb-Pb Alloy Modified with It

It is manifestly important to make clear, whether or not the aluminium remains in the alloy modified with it, and if it does, what are both its proportion and state. Therefore, the modified alloy and its slag were both analysed.

It became clear from the results of the chemical analysis that most of the added aluminium was found in the slag, and little or none in the alloy. Consequently, the modified structure in this case seems shown not to be due to the formation of the ternary eutectic of Sb-Pb-Al alloy.

Crystalline Configuration

In this research, the Sb-Pb, Sn-Bi and Pb-Bi alloys of the normal and modified forms with eutectic composition before mentioned were used as the specimens.

The specimens utilized in this examination were prepared as follows: two series of thin plates (about 3 mm. in thickness) were cut out transversely and longitudinally from each ingot, and etched with

conc. nitric acid in the cases of Sn-Bi and Pb-Bi alloys, and with the aqueous solution of 50%HNO_3 and 50%HCl in the case of Sb-Pb alloys, until they were reduced to about 0.15 mm. in thickness to remove the mechanical distortions of the surfaces. When the planed surface of the specimens was set perpendicularly to the incident heterogeneous X-ray beam emitted from the molybdenum anticathode, two series of diffraction patterns were obtained; the one is given rise to by the incidence of X-rays perpendicular to the transverse section of ingot, while the other corresponds to the incidence perpendicular to the longitudinal section.

Some of the diffraction patterns thus obtained are reproduced in Plate III. It is noticed that not only those here reproduced, but all the patterns, produced respectively by the incidence of X-rays perpendicular to the transverse and longitudinal sections of the same specimen, were found not to be essentially different from each other.

Hence only one of the diffraction patterns for the transverse or longitudinal section of a given specimen is here reproduced.

I. The Sb-Pb System

As can be seen in Photo 26, Plate III, the diffraction pattern produced by the normal alloy containing 12.5 per cent. of antimony, consists of a number of radiating bands. We may conclude from the presence of radiating bands, that the larger portion of the specimen is composed of a complex fibrous structure. The micro-structures of the alloys modified respectively with calcium and aluminium are finer than that of the normal one; while that of the alloy modified with sodium is very coarse. All the diffraction patterns taken with these specimens are composed of a number of radiating bands, similar to those of the normal one. This shows us that the larger portion of each of the specimens consists of a complex fibrous structure. Photos 27 and 28 show the diffraction patterns taken with the alloys modified with 0.5%Ca and 0.3%Na, respectively.

II. The Sn-Bi System

Photo 29, Plate III is the diffraction pattern taken with the normal alloy containing 42 per cent. of tin. This pattern consists mainly of of a number of radiating bands. It can be concluded from the presence of radiating band, that the larger portion of the specimen is composed of a fibrous structure. The micro-structures of the alloys modified respectively with sodium, aluminium and calcium are smaller than that of the normal one, while that of the alloy modified with

tellurium is coarse or very coarse depending upon the amount of tellurium. As can be seen in Photos 30, 31, 32 and 33, all the diffraction patterns occurring upon these specimens are composed of a number of radiating bands. Thus we may conclude from these patterns that all the specimens are mostly made up of a fibrous structure. Especially, the alloy modified with tellurium has a micro-structure coarser than that modified with calcium, and accordingly may be conceived to consist of crystal-grains of comparatively large size. While, by comparing the radiating bands in their diffraction patterns with each other, it was found that the crystalline configuration with tellurium is not necessarily more regular than with calcium.

III. The Pb-Bi System

As shown in Photo 34, Plate III, the diffraction pattern produced by the normal alloy containing 43.5 per cent. of lead is composed of a number of radiating bands. From this diffraction pattern it can be concluded that the larger portion of the specimen consists of a complex fibrous structure. although all the alloys modified with sodium, calcium or aluminium, are of fine micro-structures, all the diffraction patterns of these specimens have the radiating bands increasing in size and decreasing in number. (See Photos 35, 36 and 37.) Thus we may conclude that the crystalline configuration is somewhat more regular in these specimens than in the normal one.

In consequence of these X-ray analyses in connection with the three eutectiferous specimens of alloys above mentioned, we may conclude that the micro-structure of the specimens concerned does not necessarily give accurate information about the actual size and configuration of the micro-structures: i. e., there are some discrepancies between the actual crystalline configuration in the specimens and their micro-structure.

Conclusion

The experimental results in this research may be summarized as follows:—

(1) The micro-structures of the Pb-Bi, Sn-Bi and Sb-Pb alloys with the eutectic composition, are considerably refined with the addition of a small quantity of aluminium or calcium.

(2) The micro-structure of the Sn-Bi alloy with the eutectic composition is refined by the addition of a small quantity of sodium:

contrary to the above, that of the Sb-Pb alloy with the eutectic composition becomes very coarse.

(3) All the micro-structures of the Sb-Pb, Pb-Bi and Sn-Bi alloys with the eutectic composition become decidedly coarse with the addition of more than 0.5 per cent. of magnesium, selenium or tellurium.

(4) The thermal change, the influence of gas and the amount of remaining aluminium were especially determined in connection with the Sb-Pb alloy with the eutectic composition, and on the basis of the results obtained, the mechanism of modification of Sb-Pb alloy was described.

(5) There are some discrepancies between the actual crystalline configuration in the specimens and their micro-structure.

In conclusion, the writers wish to express their cordial thanks to Prof. D. Uno for his kind guidance, during the present investigations and to Ass. Prof. H. Hirata for his valuable advice in the X-ray analysis.

Institute of Metallography,
Department of Science,
Kyoto Imperial University.

Plate I

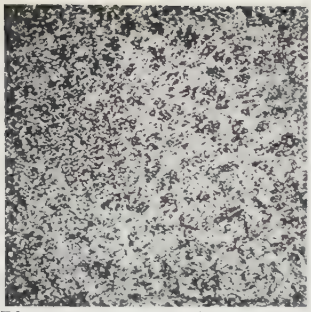

Photo 1. Sb (12.5%)-Pb alloy. Chill cast ×100

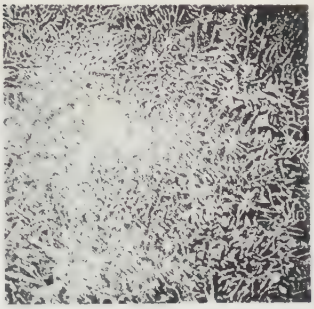

Photo 2. Sb (12.5%)-Pb alloy. Sand cast ×100

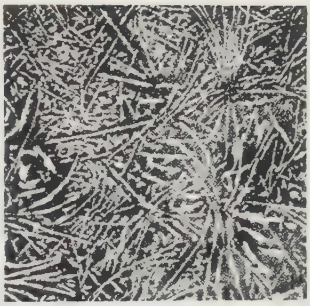

Photo 3. Modified with 0.3% Na ×100

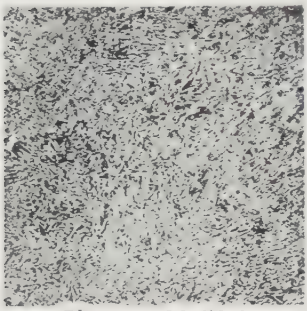

Photo 4. Modified with 0.5% Ca ×100

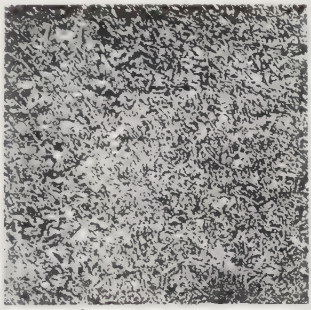

Photo 5. Modified with 0.3% Al ×100

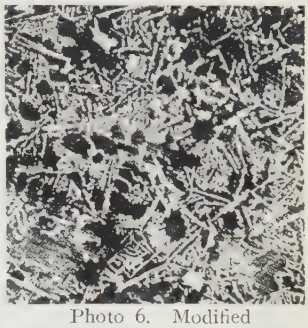

Photo 6. Modified with 0.8% Mg ×100

Photo 7. Modified with 0.3% Cd ×100

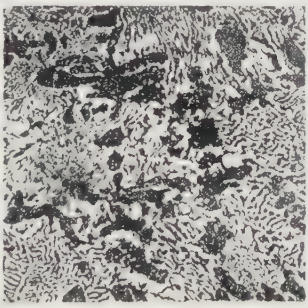

Photo 8. Sn (42%)-Bi alloy. Sand cast ×100

Photo 9. Modified with 0.3% Na ×100

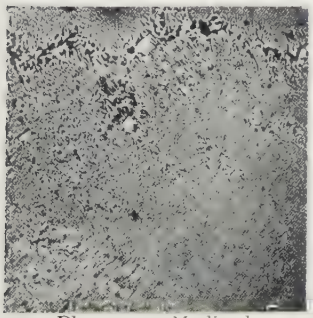

Photo 10. Modified with 0.3% Al ×100

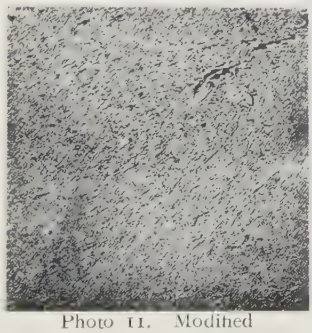

Photo 11. Modified with 0.3% Ca ×100

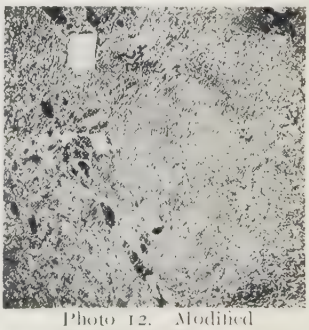

Photo 12. Modified with 0.25% Te ×100

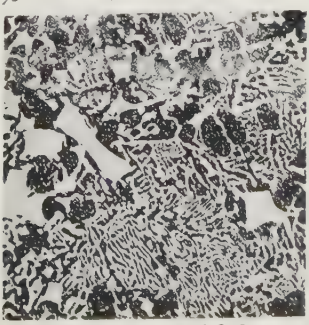

Photo 13. Modified

Photo 14. Pb (43.5%)-Bi alloy. Chill cast ×100

Plate II

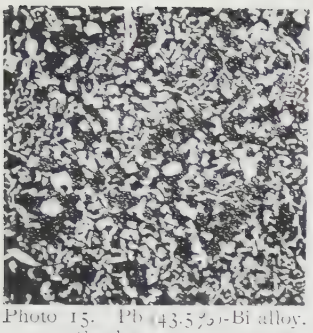

Photo 15. Pb (43.5%)-Bi alloy. Sand cast ×100

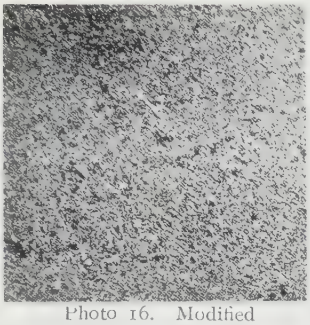

Photo 16. Modified with 0.1% Li ×100

Photo 17. Modified with 0.1% Na ×100

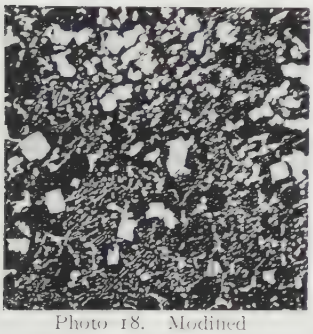

Photo 18. Modified with 0.3% Mg ×100

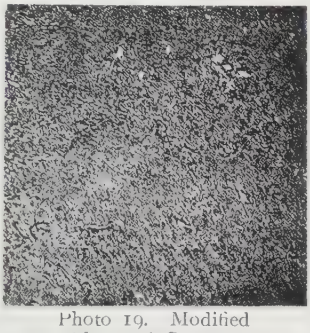

Photo 19. Modified with 0.1% Ca ×100

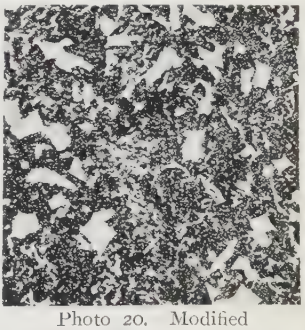

Photo 20. Modified with 0.6% Se ×100

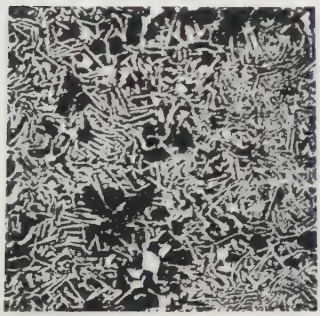

Photo 21. Modified with 0.15% As ×100

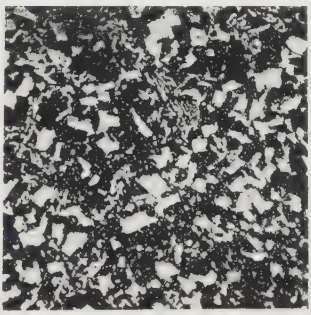

Photo 22. Modified with 0.45% As ×100

Photo 23. Sb (12.5%)-Pb alloy (H_2-treated) ×100

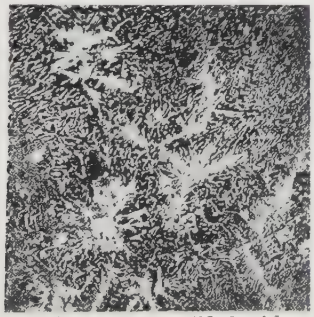

Photo 24. Modified with 0.2% Al (H_2-treated) ×100

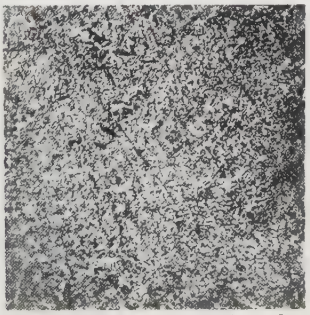

Photo 25. Treated by H_2, then modified with 0.2% Al. ×100

Plate III

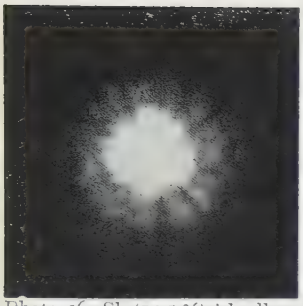

Photo 26. Sb (12.5%)-Pb alloy.
Sand cast.
(Longitudinal section)

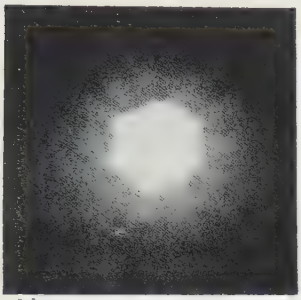

Photo 27.
Modified with 0.5% Ca.
(Longitudinal section)

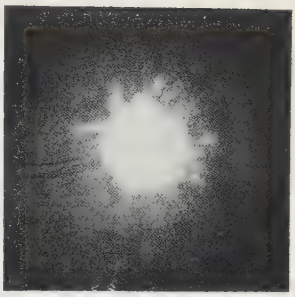

Photo 28.
Modified with 0.3% Na.
(Longitudinal section)

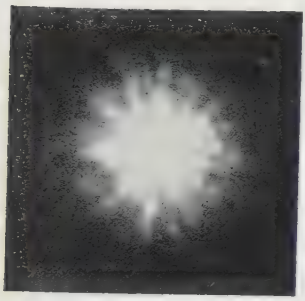

Photo 29. Sn (42%)-Bi alloy.
Sand cast.
(Transversal section)

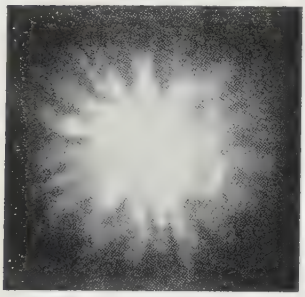

Photo 30.
Modified with 0.3% Na.
(Longitudinal section)

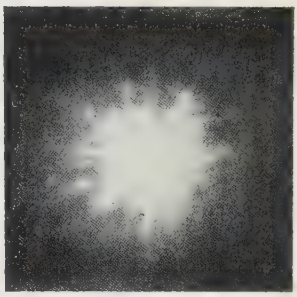

Photo 31.
Modified with 0.3% Al.
(Longitudinal section)

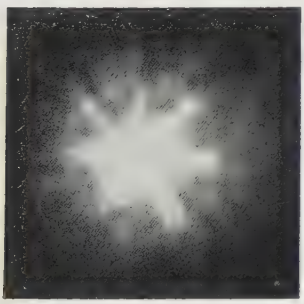

Photo 32.
Modified with 0.3% Ca.
(Longitudinal section)

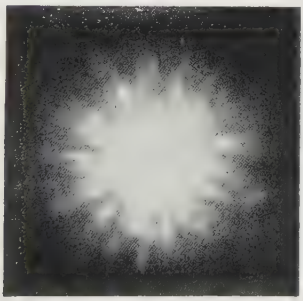

Photo 33.
Modified with 0.7% Te
(Transversal section)

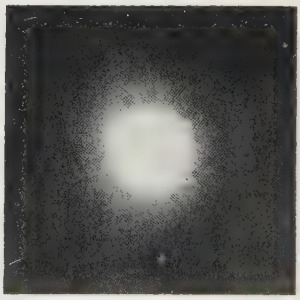

Photo 34. Pb (43.5%)-Bi alloy.
Sand cast.
(Transversal section)

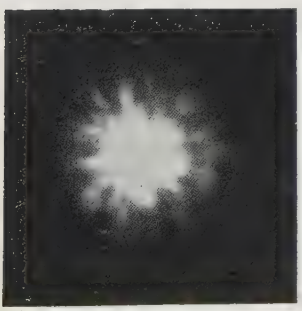

Photo 35.
Modified with 0.3% Na.
(Transversal section)

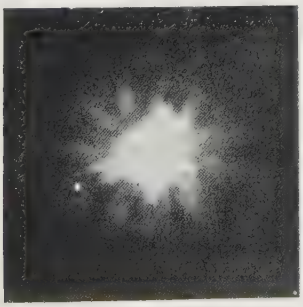

Photo 36.
Modified with 0.3% Ca.
(Transversal section)

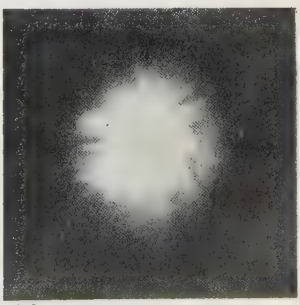

Photo 37.
Modified with 0.1% Al.
(Transversal section)

On the Crystalline Configurations of Zinc and Cadmium Deposited by Electrolysis[1]

By Hideki Hirata, Hajime Kotô and Mituo Hara

(Received November 1, 1940)

Abstract

To make clear the geometrical peculiarities of the inner structures of zinc and cadmium deposited electrolytically, the crystalline configurations of the electrolytic specimens of these two metals were examined with X-rays by the Laue method. From the diffraction patterns obtained, it was found that some of these specimens are composed mostly of a few crystals of considerable size; but the others are of an incomplete fibrous nature in which the micro-crystals of zinc or cadmium rotate within a certain angle around the direction normal to their common plane. In either case, the crystals forming these specimens were proved to be so arranged that each of them has one of its $(2\bar{1}\bar{1}0)$ planes in common. Moreover, it was also found that the normal either to this common plane or to another $(2\bar{1}\bar{1}0)$ plane inclined by an angle 60° to the aforesaid common plane of the crystals, coincides with the direction of the maximum growth of these electrolytically deposited specimens. This seems to explain why electrolytic specimens of zinc and cadmium grow in a dendritic form with many branchlets, which make an angle of 60° to each other.

Introduction

During the last ten years and more, the crystalline configurations of various electro-deposited metals have been investigated with X-rays by Glocker, Kaupp,[2] Bozorth[3] and many others.[4] But in connection with the metals belonging to the hexagonal system, as zinc and cadmiun, very few X-ray examinations have been carried out up to the present time.[5] So the late Mr. Y. Tanaka,[6] who had previously found in our

1. This paper was read at the meeting of the Japan Institute of Metals, April, 1940.

2. R. Glocker & E. Kaupp: Zeits. f. Phys., **24**, 121 (1924).

3. R. M. Bozorth: Phys. Rev., **26**, 390 (1925).

4. e. g., P. K. Fröhlich & G. L. Clark: Zeits f. Elektrochem., **31**, 649 (1925), P. K. Fröhlich, G. L. Clark & R. A. Aborn: Zeits. f. Elektrochem., **32**, 295 (1926), H. Hirata & H. Komatsubara: Zeits. f. anorg. allg. Chem., **158**, 137 (1926). H. Hirata: These Memoirs, **11**, 429 (1928).

5. As is well known from the experimental results of numerous investigators (e. g., E. A. Owen & J. Iball: Phil. Mag., **16**, 479 (1933). E. A. Owen & E. L. Yates: Phil. Mag., **17**, 113 (1934). J. Weigle: Helv. Phys. Acta., **7**, 51 (1933). W. Stenzel & J. Weerts: Zeits. f. Krist., **84**, 20 (1932).), the crystal structures of zinc and cadmium belong to the hexagonal closed-pack of the lateral axes $a_0=2.6589$ Å and 2.9736 Å long, and of the axial ratios $c'=1.856_3$ and 1.885_9 respectively.

6. H. Hirata & Y. Tanaka: Rep. Chem. Res. Inst., Kyoto Imp. Univ., **3**, 45 (1933).

laboratory that under a certain condition the micro-crystals of zinc have a tendency to be electrolytically deposited in a fibrous way, with one of their lateral axes ⟨100⟩—i. e., the normal to one of the lateral faces $(2\bar{1}\bar{1}0)$ of the hexagonal prism of the second order—arranged parallel to a definite common direction, was induced to give a more complete report of his investigation. But as he died young before the completion of his work, the present writers undertook to repeat his investigation, in order to make the report he would have made had he lived to write it. Accordingly before going into detail, it should be emphasized that the main part of this work is the record of the efficient and painstaking labour of the late Mr. Tanaka.

Specimens

In the present experiment, specimens of electro-deposited zinc and cadmium prepared at the laboratory of the Imperial Mint, Osaka, were examined similarly as before. It was reported that these specimens were deposited by applying 3 volts to both electrodes of the electrolytic bath, under the following conditions:—

Zinc

Specimen A:

Electrolyte; H_2O solution of $Zn(C_2H_3O_2)_2$ containing 9.13% of Zn.

Anode; zinc plate of 3 cm. × 4 cm. in area.

Cathode; platinum wire 1 mm. in diameter and 4 cm. long.

Electrolytic current; initially amounting to 0.3 ampere, but gradually increased up to 1.0 ampere due to the augmentation of the electrolytic deposition.

Temperature; 13.5°C.

Cadmium

Specimen A:

Electrolyte; H_2O solution of $Cd(C_2H_3O_2)_2$ containing 12.31% of Cd.

Anode; cadmium wire 5 mm. in diameter, and 10 cm. long.

Cathode; platinum wire 1 mm. in diameter, and 1.5 cm. long.

Electrolytic current; 0.2 amp.~1.0 amp.

Temperature; 13.5°C.

Specimen B

Electrolyte; H_2O solution of $CdSO_4$ containing 11.00% of Cd.

Anode; the same as in the case of Specimen A.

Cathode; platinum wire 1 mm. in diameter and 3 cm, long.
Electrolytic current; 0.5 amp.~1.0 amp.
Temperature; 15.0° C.

The specimens of zinc and cadmium thus obtained from the solutions of acetic acid (called Specimen A for convenience sake), were observed to have a dendritic form with many branchlets which make an angle of 60° with one another in one plane; while the specimen of cadmium deposited from the solution of sulphuric acid (called Specimen B), is of an acicular form without any branchlet. In Figs. 1, 2 and 3, Plate I, the macro-structures of some of these two kinds of specimens are reproduced.

Experimental Results

(i) Zinc

With a fragment of Specimen A of the electrolytic zinc above indicated, the present experiment was begun after the Laue method, making use of the heterogeneous X-ray beam emitted from the molybdenum anticathode. To take a diffraction pattern, the specimen was so situated, unless otherwise stated, that the face of the dendrite took the orientation perpendicular to the incident X-ray beam, having its stem parallel to the vertical direction: while the photographic film was always placed perpendicular to the incident beam, 3 cm. behind the specimen.

The diffraction patterns thus obtained are usually seen to consist of a number of short radiating bands as shown in Figs. 4 and 5, Plate I. But the figures made up of a set of Laue spots as reproduced in Fig. 6, Plate I, were also found to be given rise to by some specimens belonging to this category. This shows us without doubt, that most of these specimens under examination are of an incomplete fibrous nature, in which the micro-crystals of zinc rotated within a certain angle around their common axis: but some of the specimens are seen to be composed of one or a few single crystals of considerable size.

Having thus ascertained these facts, the writers tried by the aid of an improved Yoshida's crystallographic scale,[1] to determine more precisely the crystalline configurations corresponding to the various figures. As the consequence of this determination, each micro-crystal

1. U. Yoshida: Japanese J. Phys., **4**, 133 (1927), and S. Takeyama: These Memoirs, **11**, 467 (1928).

in the fibrous specimens which gave rise to Figs. 4 and 5, Plate I, was confirmed to arrange itself having the normal to one of its $(2\bar{1}\bar{1}0)$ planes—i. e., one of the lateral faces of hexagonal prism of the second order—parallel to a definite common direction. Moreover, it also became clear that either this common axis of the micro-crystals or the normal to another $(2\bar{1}\bar{1}0)$ plane inclined by an angle 60° to the aforesaid common axis, coincides with the direction of the maximum growth of deposited zinc.

To give a particular account of the foregoing statements, the orientations of the micro-crystals of zinc, confirmed to produce Figs. 4 and 5, Plate I, are projected stereographically in the annexed figure, Fig. 7, with reference to the directions of the incident X-ray beams. These directions of incident X-ray beams corresponding to the diffraction patterns, Figs. 4 and 5, were respectively found parallel to the directions of the arrows X_1 and X_2 in this figure, the common axis of the micro-crystals being assigned to take the direction projected at the point F. Further, G_1 and G_2 are the projections of the direction of the maximum growth of the zinc, which coincide respectively with the vertical directions marked by the arrows G in Figs. 4 and 5, Plate I. In Figs. 8 and 9, the theoretical curves representing the positions of the prominent radiating bands expected to appear due to the incomplete rotation of the micro-crystals from the initial orientations projected in Fig. 7, are compared with the copies of the diffraction patterns reproduced from Figs. 4 and 5, Plate

Fig. 7

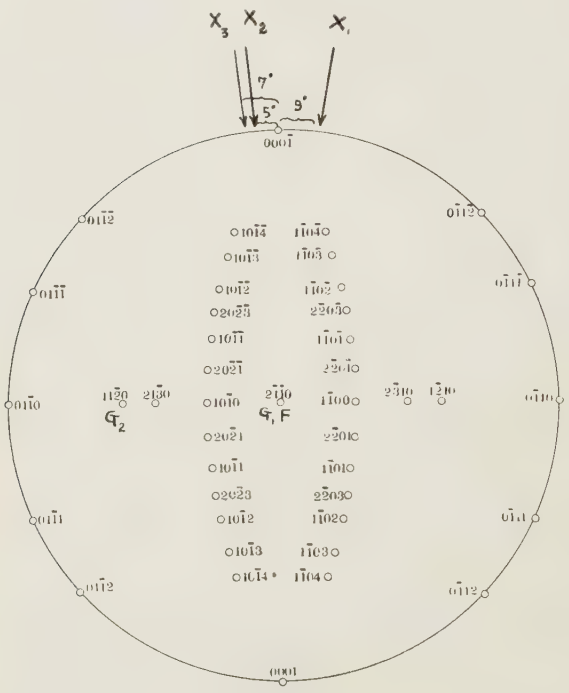

I.[1] To draw the theoretical curves in these two figures, Figs. 8 and 9, the micro-crystals were assumed to rotate to the angles 20° and 17° respectively in the clockwise sense form the intial orientations above stated, around the direction represented by F. The fair agreement between the theoretical positions of the radiating bands and those observed, as may be seen in Figs. 8 and 9, seems to confirm our foregoing statements, that the electro-deposited specimens of zinc giving rise to the diffraction patterns, Figs. 4 and 5, are of an incomplete fibrous structure in which the micro-crystals rotate within a certain angle around the direction normal to their common plane of the indices $(2\bar{1}\bar{1}0)$. Here, it is noticed that the rotations of micro-crystals now under consideration take place in the vicinity of the orientation, in which (0001) plane of the micro-crystals coincides with the largest face of the specimen situated perpendicular to the incident X-ray

Fig. 8

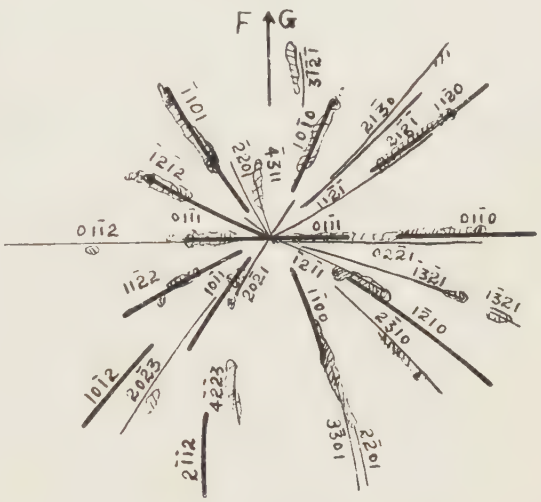

Fig. 9

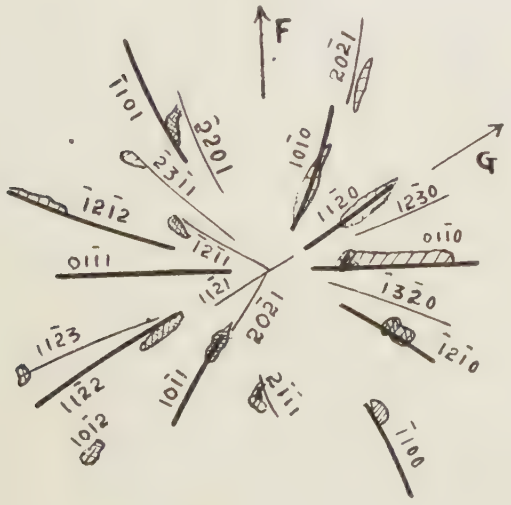

1. To transcribe these copies, the original films of Figs. 4 and 5 were respectively placed upon Figs. 8 and 9, in such a way that the direction represented by F and the centre of the central spot in both figures coincide with each other.

beam. Furthermore, from Fig. 4, Plate I, it is also found that the direction of the maximum growth of electrolytic-deposited zinc is roughly parallel to the direction of the common axis of micro-crystals, as was previously suggested by Tanaka ; but this direction of the maximum growth is seen in Fig. 5, Plate I, to coincide with the normal to another $(2\bar{1}\bar{1}0)$ plane, which makes an angle 60° with the aforesaid common axis.

The above consideration in connection with the inner structures of the electro-deposited zinc, deduced from Figs. 4 and 5, Plate I, was also found to be consistent with the other diffraction patterns corresponding to the different orientation of the specimens. Fig. 10, Plate I shows the diffraction pattern taken with the same specimen used in the case of Fig. 5, Plate I, when the common axis of the micro-crystals was tilted 45° from its normal direction towards the incident X-ray beam. In the annexed figure, Fig. 11, this diffraction pattern is reproduced by the shaded parts, while the full lines in the same figure are the theoretical positions of the prominent radiating bands, expected to appear in the present configuration. As can be seen from Fig. 11, the agreement between the calculated positions and those observed is quite satisfactory. The slight discrepancy of the positions found in Fig. 11, is fully explained by the difficulty of setting the common axis of the micro-crystals in the strictly right position. Accordingly, the above consideration was again confirmed, and we may conclude that our foregoing statements are correct, at least with regard to the inner structures of the specimens responsible for the formation of Figs. 4 and 5, Plate I.

Fig. 11

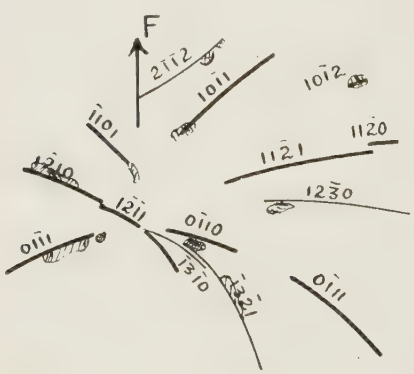

Next, the writers extended their consideration to the specimen giving rise to the diffraction figure, Fig. 6, which consists of a number of Laue spots. By a procedure similar to that used before, it was concluded that the specimen under consideration is mostly composed of two crystals of zinc, situated with reference to each other, in the way shown in the annexed figure Fig. 12.

Fig. 12

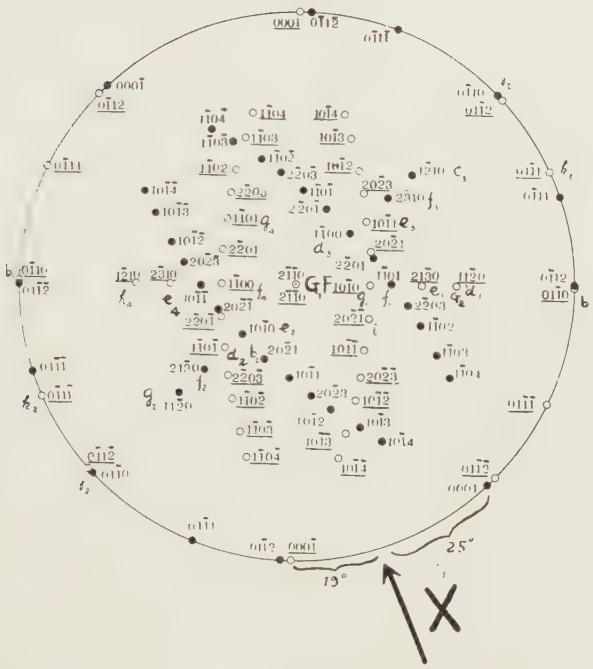

In Fig. 12, various atomic planes belonging to these two crysals are projected stereographically, as in Fig. 7. To distinguish the atomic planes of one of these two crystals from those of the other, their points of projection are indicated in Fig. 12 by white circles, and those corresponding to the other by black ones. The point F in this figure is the projection of the direction normal to the common plane of these two crystals, which was confirmed to coincide with the direction of the maximum growth of deposited zinc represented by G_1, in the present case. Moreover, the small letters a_1, b_1, c_2,....., i_4, j_4, k_4, in Fig. 12 mark respectively the prominent atomic planes of small glancing angles, which were found by calculation to give rise to the Laue spots on the photographic film, just at the positions of the spots represented by the same letters in Fig. 6, Plate I, when the incident X-ray beam was made to strike the specimen perpendicularly to its stem, taking the direction parallel to the arrow X.[1] As may be seen from Fig. 12,

1. The following correspondence was found to exist between the Laue spots in Fig. 6, Plate I and the indices of the atomic planes of these two crystals :—

a_1, $03\bar{3}1$; b_1, $01\bar{1}0$ & $01\bar{1}2$; c_1, $12\bar{3}0$; d_1, $11\bar{2}0$, e_1, $21\bar{3}0$; f_1, $1\bar{1}01$; g_1, $10\bar{1}0$; h_1, $30\bar{3}1$;

the specimen with which Fig. 6, Plate I was obtained, can be concluded to be of a crystalline configuration essentially the same with that corresponding to Fig. 4, Plate I: i. e., the specimen giving rise to Fig. 6, Plate I, is found to be mostly, if not entirely, composed of two crystals of zinc having one of their $(2\bar{1}\bar{1}0)$ planes in common, and the direction normal to this common plane is parallel to the direction of the maximum growth of deposited zinc.

With regard to a few metals, it was previously found in our laboratory that the common axis of the micro-crystals in electro-deposited specimens, does not always coincide with the direction of their maximum growth.[1] The angle between these two directions indicated by the general notations F and G in the present case, was confirmed to be able to take a finite set of values besides O°. Nevertheless, according to the experimental results obtained by Yamamori[2] and others[3] with various specimens of electro-deposited lead, the aforesaid two directions F and G are noticed always to be crystallographic equivalent, even when the parallelism between them is violated. A similar geometrical relation as stated above, has also been seen with the electro-deposited zinc in the present experiment, each one of these two directions F and G in the electro-deposited zinc coinciding with one of the normals to $(2\bar{1}\bar{1}0)$ planes of its micro-crystals. Thus we may infer that the crystalline configuration of the electro-deposited zinc, is of the same category with that of electro-deposited lead, in connection with the geometrical relation between the direction of the common axis of the micro-crystals and the direction of the maximum growth of the specimens.

(ii) Cadmium

(a) Specimen A: Next the writers investigated the crystalline

---

r_1, $\underline{20\bar{2}\bar{1}}$; j_1, $3\bar{1}\bar{2}\bar{1}$ & $3\bar{2}\bar{1}2$; k_1, $2\bar{1}\bar{1}1$; a_2, $\bar{2}111$; b_2, $20\bar{2}1$; c_2, $30\bar{3}1$; d_2, $\underline{\bar{1}101}$; e_2, $\underline{\bar{5}301}$ & $10\bar{1}0$; f_2, $21\bar{3}0$; g_2, $11\bar{2}0$; h_2, $12\bar{3}1$; i_2, $12\bar{3}0$; j_2, $01\bar{1}0$ & $\underline{0\bar{1}1\bar{2}}$; k_2, 0331 & $\underline{01\bar{1}1}$; a_3, $\bar{1}3\bar{2}0$; b_3, $\underline{11\bar{2}2}$; c_3, $\bar{1}2\bar{1}0$ & $\underline{11\bar{2}3}$; d_3, $1\bar{1}00$; e_3, $\underline{10\bar{1}1}$; f_3, $2\bar{3}10$; g_3, $\underline{10\bar{1}2}$; h_3, $\bar{4}311$; i_3, $\bar{3}301$; j_3, $\bar{2}201$; k_3, $\underline{4\bar{2}\bar{2}3}$; l_3, $\underline{2\bar{1}\bar{1}1}$; a_4, $\bar{2}111$; b_4, $\bar{2}112$; c_4, $\underline{3\bar{2}\bar{1}2}$; d_4, $\bar{4}223$; e_4, $10\bar{1}\bar{1}$; f_4, $\underline{1\bar{1}00}$; g_4, $\underline{1\bar{1}01}$; h_4, $\underline{\bar{1}2\bar{1}0}$; i_4, $\underline{\bar{1}3\bar{2}0}$; j_4, $\underline{\bar{1}4\bar{3}0}$; k_4, $\underline{\bar{1}3\bar{2}1}$;

It must be frankly accepted, that only the very diffuse Laue spot marked by g_4, is found to take a position where no reflected beam from any prominent atomic plane of these two crystals of zinc, strikes the photographic film. Consequently, it may be thought probable that this spot is given rise to by the crystallite immersed between two crystals above stated. But for the present, we have attributed this spot to the reflection of $1\bar{1}01$ plane, notwithstanding it deviates considerably (about 6°) from the theoretical position of the spot produced by the aforesaid atomic plane.

1. H. Hirata & Y. Tanaka: These Momoirs, **15**, 9 (1932) and **17**, 144 (1934).
2. S. Yamamori & S. Yoshimoto: These Memoirs, **21**, 75 (1938).
3. H. Hirata, Y. Tanaka & H. Komatsubara: Bull. Chem. Soc., Japan, **10**, 391 (1935).

configuration of electro-deposited cadmium, by the same procedure as in the case of zinc above described. Some diffraction patterns thus obtained with Specimen A of the electro-deposited cadmium, are reproduced in Figs. 13 and 14, Plate II. Not only the patterns here reproduced, but all those given rise to by the specimens belonging to this category, were found always to consist of a number of short radiating bands, similarly to those shown in Figs. 13 and 14, Plate II. Thus it is clear beyond question that all the specimens designated as Specimen A, are equally of some incomplete fibrous-like structure, in which the micro-crystals rotate within a certain angle.

To make the crystalline configuration of Specimen A more precisely clear, a calculation similar to the previous one was carried out in connection with Figs. 13 and 14, Plate II. As the consequence of this calculation, it became evident that the former figure, Fig. 13, was produced by the micro-crystals of cadmium rotated within an angle 19° in the clockwise sense, from their initial orientation represented in Fig. 7[1] with reference to the direction of the incident X-ray beam X_3, around their common axis F. The fair agreement between the theoretical positions of the prominent radiating bands corresponding to the aforesaid configuration and the observed ones reproduced from Fig. 13, Plate II, may be seen in the annexed figure, Fig. 15. It is noticed in Fig. 15, that the direction of the common axis F deduced from Fig. 13, Plate II, coincides with the direction of the maximum growth of the electrolytic deposition G, similarly to the case of Fig. 4, Plate I.

With regard to the latter figure, Fig. 14, the crystalline configuration corresponding to it, was confirmed to be essentially the same as that of the specimen of electro-deposited zinc giving rise to Fig. 6, Plate I: i. e., Fig. 14, Plate II was given rise to by the rotations of two sets of the micro-crystals situated with reference to each other and to the direction of the incident X-ray beam X as shown in Fig. 12, around their common axis F, which coincide with the normal to one of $(2\bar{1}\bar{1}0)$ planes. One of these two sets of the micro-crystals of cadmium were found to rotate within an angle 19° in the clockwise

1. Strictly speaking, the stereographic projections of the crystals of zinc given in Figs. 7 and 12, are of course as they stand, not applicable to those of cadmium. But the crystal lattices formed by the aforesaid two kinds of metals having already been known to be of the same type and of nearly equal axial ratio, these projections which dealt with the former are referred to here again in considerations concerning the latter.

sense, from their initial orientation represented by the white circles in Fig. 12. While the angle of rotation of the other set of the microcrystals corresponding to the black circles, was estimated to amount to 19° ahd 1° in the clockwise and counter-clockwise senses respectively. By the aforesaid rotations of these two sets of microcrystals, the atomic planes represented by the white and black circles in Fig. 12, were respectively deemed to produce the intensity maxima of the diffracted X-rays at the positions on the photographic film shown in Figs. 16_a and 16_b; the prominent radiating bands should consequently be expected to appear taking the positions designated by the curves in Fig. 17, which were obtained by combining Figs. 16_a and 16_b. As may be seen in Fig. 17, the theoretical positions of radiating bands thus obtained, would agree quite well with the observed ones reproduced from Fig. 14, Plate II, if the direction of the maximum growth of deposited cadmium on the photographic film is assumed to be parallel to the direction of the arrow G in the theoretical curves. Here, it must specially be mentioned that this direction G in Fig. 17, which makes an angle of 60° with the direction of the common axis F normal to one of the $(2\bar{1}\bar{1}0)$ planes, is also seen to coincide with the normal to another $(2\bar{1}\bar{1}0)$ plane marked G_2 in Fig. 12, where the indices of

Fig. 15

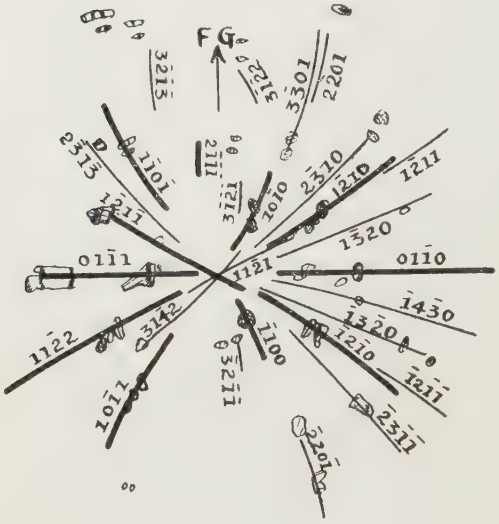

Fig. 16_a

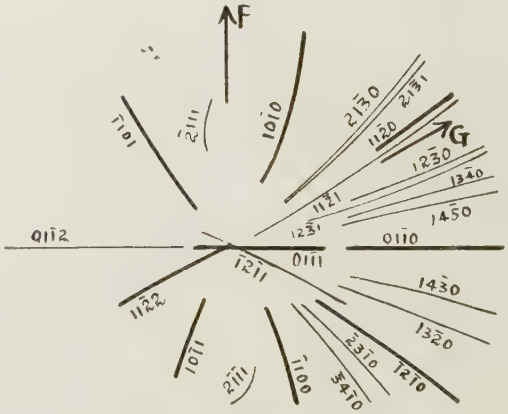

these two atomic planes perpendicular to the directions F and G are respectively designated $2\bar{1}\bar{1}0$ and $\bar{1}\bar{1}20$. The facts adduced above, lead us to conclude that the specimen giving rise to Fig. 14, Plate II, is composed of two sets of micro-crystals of cadmium having one of their $(2\bar{1}\bar{1}0)$ planes in common, and the normal to another $(2\bar{1}\bar{1}0)$ plane inclined by an angle of 69° to the aforesaid common axis parallel to the direction of the maximum growth of deposited cadmium.

Fig. 16b

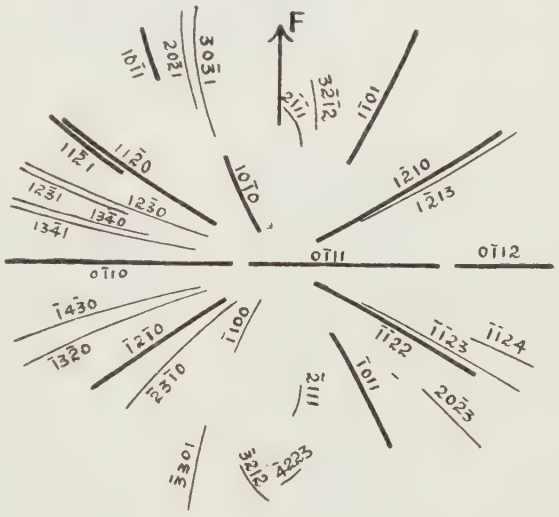

From the conclusions which have already been drawn with regard to Specimen A, it can be inferred that the electrolytic specimens of cadmium are of a similar crystalline configuration to those of zinc referred in the preceding article, i. e., the direction of the common axis in the electro-deposited cadmium does not always coincide with the direction of its maximum growth; but in any case, these two directions are situated normal to some one of the atomic planes $(2\bar{1}\bar{1}0)$.

Fig. 17

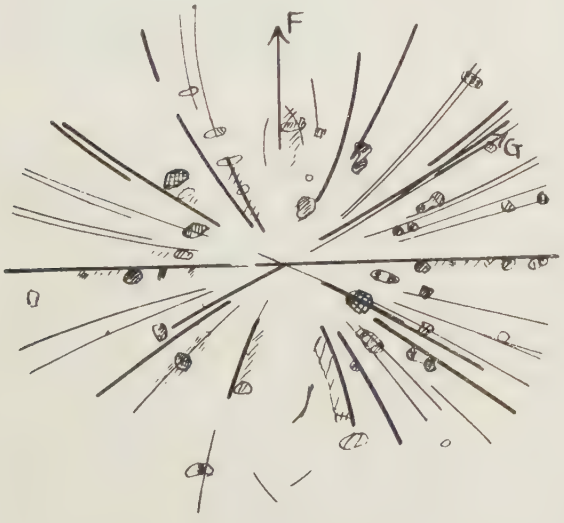

(b) Specimen B: Fig. 18, Plate II is the diffraction figure obtained with a fragment of Specimen B of the electro-deposited cadmium, by

setting the axis of the acicular perpendicular to the incident X-ray beam. Not only Fig. 18, Plate II here reproduced, but all the diffraction patterns given rise to by the specimens of this category were found to be essentially the same, each one of them consisting of a complicated assemblage of radiating bands. Nevertheless, these diffraction patterns differed slightly from one another in the elongation of their radiating bands, but no systematic relation could be found between them. Thus we may conclude that each fragment of Specimen B of electro-deposited cadmium, is made up of an irregular aggregation of many fibrous-like structures.

Conclusion

The arguments which have hitherto been advanced in connection with the crystalline configurations of electrolytic zinc and cadmium, lead us to the following conclusions:—

(1) Some of the specimens of these two metals are composed mostly of a few crystals of considerable size; but the others are of an incomplete fibrous-like structure in which the micro-crystals of zinc or cadmium rotate within a certain angle around the direction normal to their common plane. In either case, the crystals forming the specimens were so arranged that each of them has one of its $(2\bar{1}\bar{1}0)$ planes in common.

(2) The normal either to the aforesaid common plane or to another $(2\bar{1}\bar{1}0)$ plane inclined by an angle of 60° to this common plane of the crystals, coincides with the direction of the maximum growth of these electrolytically deposited specimens.

From the statements above mentioned, it may be inferred that the lateral faces $(2\bar{1}\bar{1}0)$ of the hexagonal prism of the second order of zinc and cadmium crystals, have a distinctive physical nature. Furthermore, these statements seem to elucidate the reason why the branchlets of the electrolytic specimens of zinc and cadmium make an angle of 60° with each other.

In conclusion, the writers wish to express their sincere thanks to Professor Denzo Uno for his constructive suggestions and the interest he has taken in this investigation. Their thanks are also due to Dr. Hisaji Komatsubara of the Imperial Mint, who kindly supplied all the specimens required, and to Mr. Toshio Yawata for his continual aid during the progress of the experiment.

Institute of Metallography,
Department of Science,
Kyoto Imperial University.

Plate I

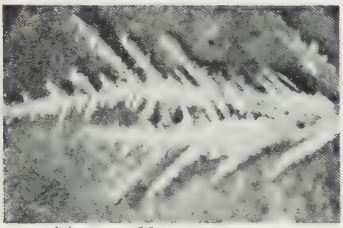

Fig. 1. Macro-structure of *Zn*(A) ×19

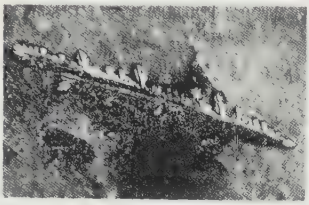

Fig. 2. Macro-structure of *Cd*(A) ×19

Fig. 3. Macro-structure of *Cd*(B) ×15

Fig. 4. *Zn*(A)

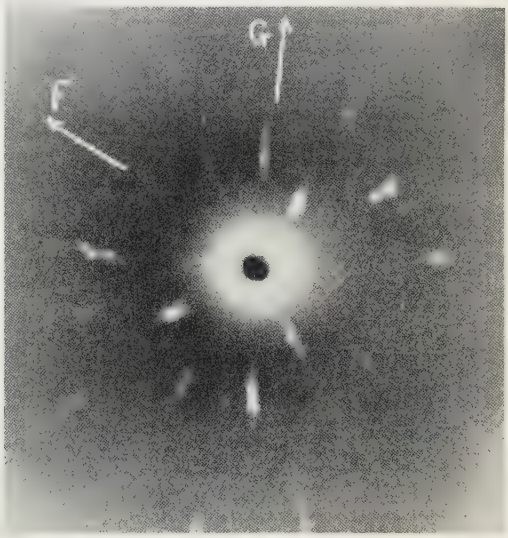

Fig. 5. *Zn*(A)

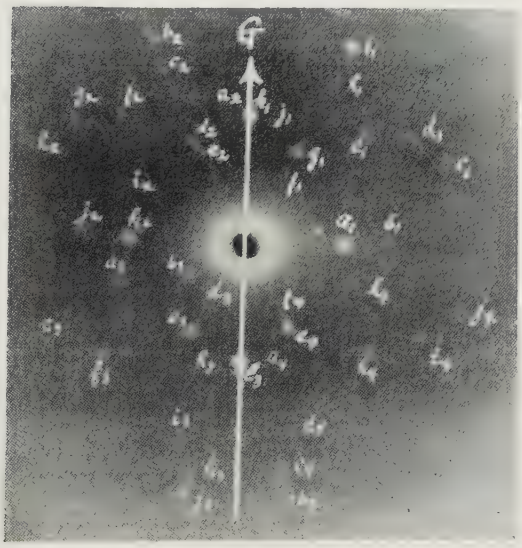

Fig. 6. *Zn*(A)

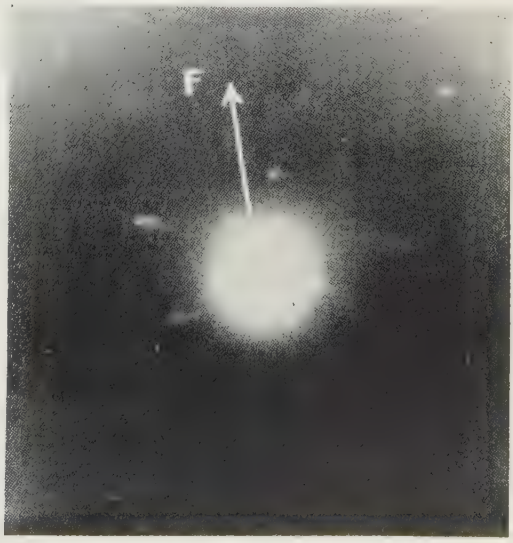

Fig. 10. *Zn*(A) (oblique incidence)

Plate II

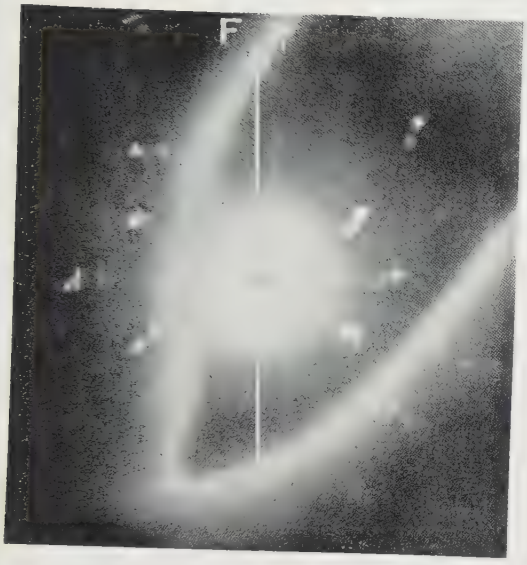

Fig. 13. *Cd*(A)

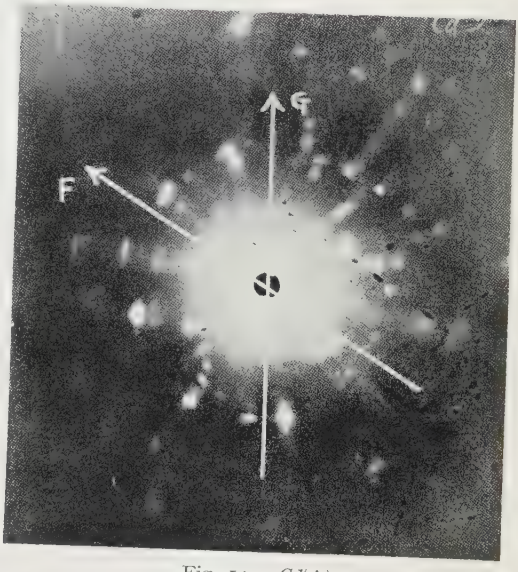

Fig. 14. *Cd*(A)

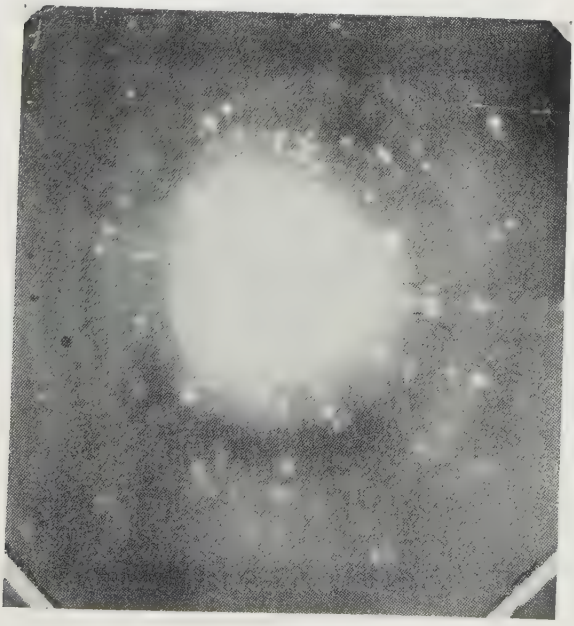

Fig. 18. *Cd*(B)

On the Constitution of the so-called Intermetallic Compound, "Ag_3Al" in the Silver-rich Aluminium-Silver Alloys[1]

By Hajime Kotô

(Received November 1, 1940)

Abstract

Microscopic examination, X-ray analysis and accurate chemical analysis were made with regard to specimens of various compositions corresponding to and also near to the so-called intermetallic compound, "Ag_3Al."

As the result of these researches, it was concluded that the intermetallic compound represented by the formula, Ag_3Al has a narrow range of homogeneity for composition of about 0.24% Al, and its composition is rather close to the formula $Ag_{16}Al_5$.

Introduction

In the aluminium-silver alloys, two intermetallic compounds are generally recognized; the one corresponds to Ag_3Al (β'-phase) which is of the complex cubic structure belonging to the β-manganese type and the other, Ag_2Al (γ-phase) which is of the close-packed hexagonal type.

In the present experiment, the constitution of the former was determined by microscopical examination, X-ray analysis and accurate chemical analysis, as will be described below.

Specimens

The silver used was of the utmost purity (1000/1000), especially prepared at the Imperial Mint, Osaka; the aluminium was also of the highest purity, (99.996%) made in France. Under a layer of sodium chloride, the silver was first melted in a graphite crucible, and then aluminium was thrown into the melt. The mixture was well stirred, and cast into an iron mould (6.5 mm. in inner diameter and 60 mm. long). Alloys of various compositions were prepared in this way, as shown in Table 1.

The alloys thus obtained were first quenched from 350° and 200°C respectively in ice-water after annealing at 700°C for an hour and slow

1. This paper was read at the April meeting of the Chemical Society of Japan (1938) and also at the meeting of the Japan Institute of Metals (1939).

Table 1

By Synthesis Wt. —% Al	By Analysis Wt. —% Al.
7.6920	7.56
7.6000	7.54
7.5000	7.34
7.4074	7.33
7.3000	7.09
7.2000	6.84

cooling down to 350° or 200°C. Then they were again quenched from 350° and 200°C respectively in ice-water, after annealing at 350° and 200°C for 15 and 70 days respectively in a vacuum glass tube. As can be seen in Table 1, the compositions of the specimens thus obtained were precisely determined by estimation of the silver content by the Gay-Lussac method.

The Micro-structure

The micro-photographs of some of the specimens quenched from 350°C in ice-water are reproduced in Photos 1~6, Plate I.

As can be seen in Photo 1, Plate I, the micro-structure of the specimen containing 6.84 per cent. of aluminium shows that it is mainly composed of the β' phase, except for a small quantity of α phase. Moreover, the micro-structures of the specimens quenched from 350°C containing 7.09 and 7.33 per cent. of aluminium respectively, both consist of the homogeneous phase, as shown in Photos 2 and 3. While Photos 4~6 indicate that all the specimens quenched from 350°C containing respectively 7.34, 7.54 and 7.56 per cent. of aluminium, bear the γ-and β'-phases.

Photos 7~11 in the same Plate show the micro-structures of the specimens quenched from 200°C in ice-water.

As is seen from these photographs, when quenched from 200°C, the specimens containing respectively 7.09 and 7.33 per cent. of aluminium are homogeneous, while those containing respectively 6.84, 7.34 and 7.54 per cent. of aluminium are heterogeneous, similarly to the case of those quenched from 350°C.

From the result of the microscopical examination mentioned above, the composition of the so-called intermetallic compound, "Ag_3Al" may be said to be 7.21 per cent. of aluminium, which is the mean value of 7.33 and 7.09 per cent. of aluminium. Thus we may consider from the above data and also various formulae as shown in Table 2 that the composition of the so-called intermetallic compound, "Ag_3Al" is rather close to the formula, $Ag_{16}Al_5$, corresponding to 7.22 per cent. of aluminium.

Table 2

The Formula	Wt. —% Al
Ag_3Al	7.69
$Ag_{34}Al_{11}$	7.51
$Ag_{31}Al_{10}$	7.46
$Ag_{28}Al_9$	7.44
$Ag_{25}Al_8$	7.41
$Ag_{22}Al_7$	7.37
$Ag_{19}Al_6$	7.32
$Ag_{16}Al_5$	**7.22**
$Ag_{13}Al_4$	7.14
$Ag_{10}Al_3$	6.98
Ag_7Al_2	6.67
Ag_4Al	5.88

Fig. 1

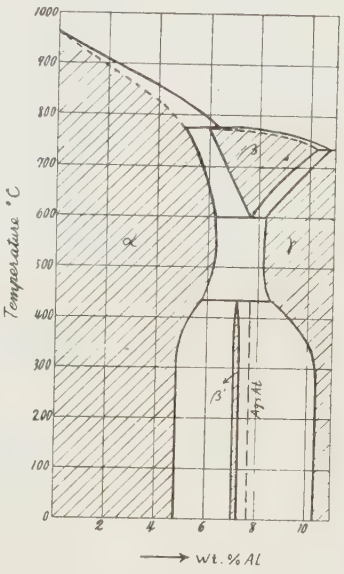

Moreover, when quenched from 350° or 200°C, the specimens respectively containing 7.33 and 7.09 per cent. of aluminium are both homogeneous. Consequently it may be considered that the β' phase has a narrow range of homogeneity for the composition of about 0.24%Al, as shown in Fig. 1.

The Crystal Structure

Adopting K_α radiation of copper, photographs were taken, by the Debye-Scherrer method, and with the aid of a cylindrical camera of 7.03 cm. in diameter. Some of the spectra thus obtained are reproduced in Photos 12~21, Plate II.

As can be seen in Photo 14, the spectral lines of the specimen quenched from 350°C in ice-water containing 6.84 per cent. of aluminium, are composed of many lines on the diffraction pattern of the β'-phase, and also several lines due to the planes (200) and (113) of the α-phase. Photos 15 and 16 show the photographs taken by the powder method with the microscopically homogeneous alloys quenched from 350°C in ice-water containing respectively 7.09 and 7.33 per cent. of aluminium. In these photographs, Photos 15 and 16, spectral lines of the γ-phase could hardly be detected, since many of the spectral lines of the γ-and β'-phases overlap. While in Photos 17~19, which

are taken with the alloys quenched from 350°C in ice-water containing 7.34, 7.54 and 7.56 per cent. of aluminium respectively, a faint spectral line due to the plane $(1\bar{1}\bar{2}2)$ of γ-phase is observed besides that of β'-phase. Accordingly, the γ-phase was distinguished from the β'-phase. Furthermore, in Photo 20 taken with the specimen containing 9 per cent. of aluminium, the β'-and γ-phases were clearly detected. It will be noticed that the spectra taken with the specimens quenched from 200°C, are not here reproduced; they were essentially the same as those from specimens quenched from 350°C.

Though the result of the microscopical examination is not clearly confirmed by that of the X-ray analysis, we may conclude that the former is substantially in agreement with the latter.

Conclusion

The experimental results which have hitherto been described in connection with the specimens of the aluminium-silver alloys quenched from 350° and 200°C respectively in ice-water, lead us to the following conclusion :—

(a) The constitutional formula of the so-called intermetallic compound, "Ag_3Al" is rather near to $Ag_{16}Al_5$.

(b) According to the previous constitutional diagram, the so-called intermetallic compound, "Ag_3Al" is insoluble in both aluminium and silver in the solid state, but it was now found that the so-called "Ag_3Al" is slightly soluble in these two elements.

In conclusion, the writer wishes to express his sincere thanks to Prof. D. Uno for his kind guidance, during the progress of this investigation and to Ass. Prof. H. Hirata for his valuable advice in the X-ray analysis. His thanks are also due to Dr. H. Komatsubara and Mr. G. Chikauchi at the Imperial Mint, Osaka, for their kind efforts with respect to the chemical analysis of the specimens, and to Mr. S. Nakamura for his efficient aid throughout the present research. The expense for the experiments has been defrayed from a grant made to Prof. D. Uno by the Ministry of Education for the Promotion of Scientific Research, to which the author's thanks are due.

Institute of Metallography,
Department of Science,
Kyoto Imperial University.

Plate I

(Quenched from 350°C in ice-water, after annealing for 15 days in vacuum.)

Photo 1. 6.84%Al ×160

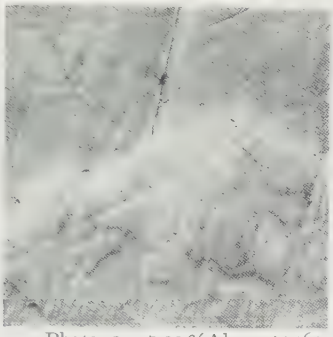

Photo 2. 7.09%Al ×160

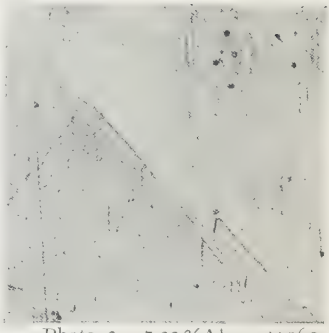

Photo 3. 7.33%Al ×160

Photo 4. 7.34%Al ×160

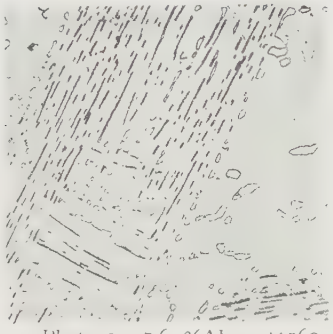

Photo 5. 7.64%Al ×160

Photo 6. 7.56% ×160

(Quenched from 200°C in ice-water, after annealing for 70 days in vacuum.)

Photo 7. 6.84%Al ×160

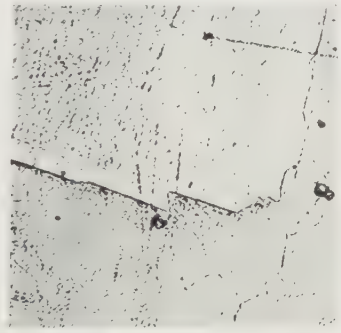

Photo 8. 7.09%Al ×160

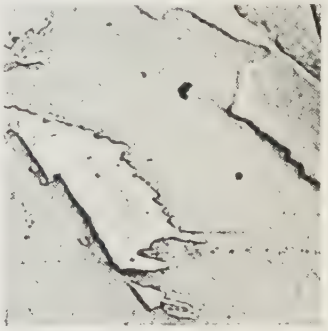

Photo 9. 7.33%Al ×160

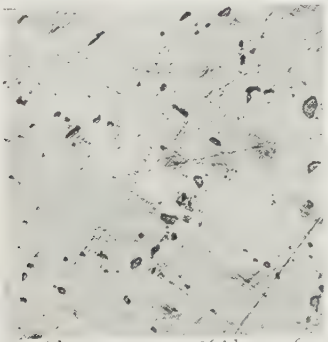

Photo 10. 7.34%Al ×160

Photo 11. 7.54%Al ×160

Plate II

(Quenched from 350°C in ice-water, after annealing for 15 days in vacuum.)

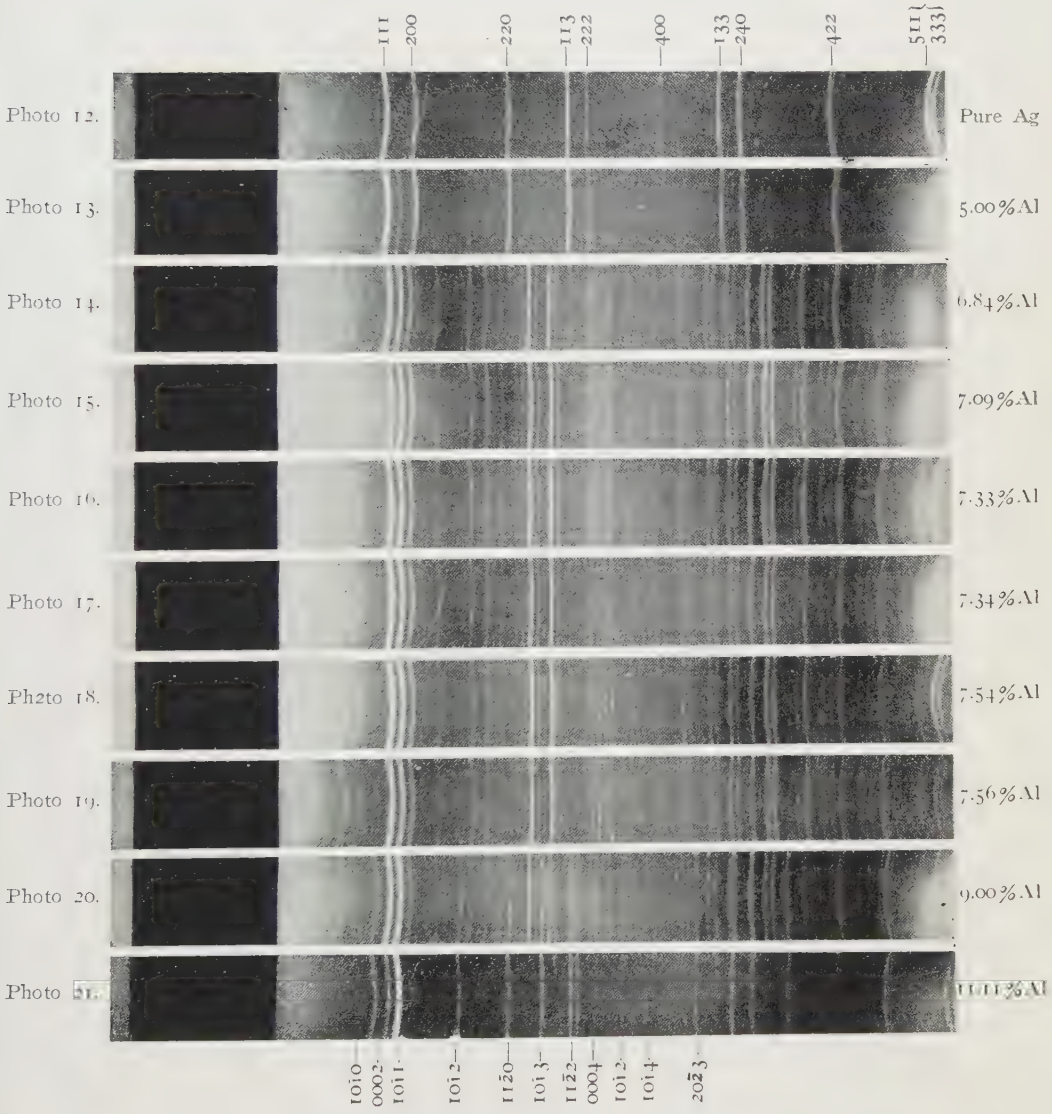

Structure of the Crystal Boundaries of Metals and the Phenomenon of Recrystallization

By **Usaburo Yoshida**

(Received December 4, 1940)

Abstract

The presence of the cybotactic amorphous layer at the boundaries of the metal crystals formed by crystallization in the melt and at the intercrystalline boundaries developed by the process of slipping at the slip plane by the plastic deformation is inferred. Assuming the permanency of the intercrystalline amorphous layer, the theory of recrystallization of metals, proposed by the writer and K. Koyanagi some years ago, was reviewed.

Introduction

In other papers[1] recently published, the writer proposed a cybotactic theory concerning the manner of molecular grouping in liquid and in amorphous solid; and it has been found that this theory, though a rough one, is very fruitful in understanding qualitatively various physical properties of liquids and amorphous solids. In connection with it, the mechanism of crystallization and of melting of a substance was also considered; and the possibility was inferred of formation of the Beilby's amorphous layer on a metal surface by polishing and at an intercrystalline boundary developed between the atomic planes of a metal crystal by the process of slipping by a plastic deformation. Ordinarily, in an amorphous solid, individual molecules are supposed to be distributed entirely at random. But according to the writer's cybotactic idea, some of the molecules are in an aggregated state as cybotactic crystals; every one of these consists of a certain number of the molecules arranged in the same crystal lattice as in the adult crystal of the same substance, and is comparable in size with that of the unit cell of the crystal. These cybotactic crystals have no permanent stability. They are formed and decomposed suddenly by chance among the free molecules in a random distribution. Thus the proportion of the number of molecules in the state of the cybotactic crystals as compared with that of the free molecules is conceivable only in a statistical sense, and it increases continuously with decrease

1. U. Yoshida; These Memoirs A, **23** 207, 225 (1941).

of the temperature, without any discontinuity such as is seen at the melting point of adult crystals. When the temperature is lowered without forming crystal nuclei of any considerable size below the melting point of the substance, which is peculiar to the adult crystal of the substance, it has become super-cooled; and by a further continued cooling it comes at last to a glassy state or a state of amorphous solid consisting partly of free molecules but very largely of cybotactic crystals, both being arranged and distributed entirely at random.

Structure of the Crystal Boundary of Metals

It is well known that the crystal boundary of a metal is harder at low temperatures and is softer at high temperatures than the interior of the crystal. This fact is explained if we assume the presence of the amorphous layer at the crystal boundary as is described above. As the melting point of the metal is approached by raising the temperature, the amorphous layer exhibits the property of the liquid by virtue of the increased proportion of the free molecules as compared with the cybotactic crystals. On the contrary, at low temperatures, the amorphous layer comes to the state of amorphous solid due to an enormously increased proportion of the cybotactic crystals oriented entirely at random. The average life of the cybotactic crystals is now very much increased and the motion of the free molecules constrained in narrow interstices between neighbouring cybotactic crystals is so much restricted that they cannot behave freely any more as they did in the liquid state. In such a state the amorphous layer has no slip plane and slip direction, which is the direction of the minimum resistance in the crystal against an external stress applied; and it is endowed with uniform strength for all directions which is higher than the minimum resistance in the slip direction.

Plastic deformation of a metal is considered to be caused mainly by the slip along a slip direction in a slip plane. But the process of the ideal slip alone, seems to be insufficient to account for the plastic deformation. We know from X-ray examination, that the metal crystals become finer and scattered in their orientation by cold working even in the simplest case of a single crystal stretched or compressed plastically in one direction. This seems to imply that some other precess such as separation and consequent mutual rotation of neighbouring portions of the crystal at a certain atomic plane at some localities takes place simultaneously with the ideal slip in plastic

deformation. The reason for the forcible process such as separation and mutual rotation can be sought for in the imperfection of the crystal lattice and in the coercionary stress called forth near the rather irregular crystal boundary by the slip interference at the crystal boundary where two crystals of different crystallographic orientation are bound together firmly. By such forcible process accompanying the crystal slip some part of the crystals will be smashed into extreme fineness comparable with the cybotactic crystals and will suffer considerable lattice distortion. By virtue of the enormous lowering of the melting point caused by these two facts the local heating caused by the process of the crystal slip will be sufficient to melt at least some of the fine and distorted crystals. If this occurs during the process of the slip, mutual cohesion between two parts of the crystal which are separated by such a thin molten layer will be very much weakened, and this will call forth an irregular and forcible stress distribution in their vicinity even in the simplest case of a single crystal stretched or compressed plastically in one direction. This again will cause at some localities smashing and distortion and consequently melting of the crystallites in the interior of the crystal; and at the same time separation and mutual rotation of the two parts separated by the molten layer may take place as long as the slipping process is continued. When the slipping process is stopped by removing the external stress, the melted portions will be cooled so suddenly that they come to the supercooled solid state or the cybotactic state as is stated before. Thus after the slip, the crystal is divided into finer crystallites of scattered orientation, and the boundaries of the crystallites become cemented to a considerable degree by the amorphous layer. This way of explaining the formation of the Beilby's amorphous layer by the crystal slip was proposed in the former paper.[1)]

Next let us consider as before the growth of the crystals of a substance in its melt. The growth in this case takes place only at the boundary surface of the crystals with the melt. Let N_l be the surface density of the liquid molecules at the crystal boundary, and N_c be that of the molecules situated at the crystal lattice on the boundary surface of the crystal. Then at a certain temperature a certain proportion β which may by called the melting factor, of the molecules

1. loc. cit.
2. loc. cit.

N_c situated at the crystal lattice will be released and enter the liquid phase; and at the same time a certain proportion α, which may be called the crystallizing factor, of the liquid molecules N_l will be bound to the crystal lattice. Thus so far as $\alpha N_l > \beta N_c$ the growth of the crystals will continue until the stage is reached where neighbouring crystals come almost into contact with each other. In this last state the melt confined in very narrow interstices between neighbouring crystals will be deprived of communication from outside, and with most metals, the average value of N_l will become smaller so far as the crystal growth continues, due to the contraction accompanying the crystallization from the melt. As to the manner of the internal structure of the thin liquid layer in such state of reduced value of N_l and consequently of the reduced pressure, we are entirely ignorant, and we cannot make any definite statement. But let us assume for the present that the number of liquid molecules which fall into the lattice point of the crystal at its surface in unit time is still proportional to N_l and is equal to αN_l, keeping the values of α, β and N_c unaltered; and see what follows from this: It follows from the above assumption that the decrease of the average value of N_l at the narrow interstices acts to prevent the further growth of the crystals toward the liquid layer in the narrow interstices; and this crystal growth will be entirely stopped when, with the decreased value of N_l, the value of αN_l becomes equal to βN_c even at a temperature lower than the melting point. This signifies the persistence of a thin liquid layer in the narrow interstices between neighbouring crystals. In addition to the reason given above, the disturbance to the regular crystallizing force at the surface of the crystal by the nearest approach of the other crystal differently oriented will assist at least to some extent the persistence of the thin liquid layer. When the temperature is very much lowered from the melting point, the value of α will increase and that of β will decrease; and by this cause alone the crystal growth will be accelerated. But at the same time the number N_l of free liquid molecules which are to be entrapped into the lattice point of the adult crystals will be remarkably reduced by virtue of the crystal growth and of the enormous increase in number of the cybotactic crystals. As this fact counteracts the crystal growth due to the former cause, the thin liquid layer can still persist in the super-cooled solid state or in a glassy state at very low temperature, even down to absolute zero.

The above argument may be correct only in a statistical sense. When considered microscopically the widths of the narrow interstices between neighbouring crystals will be different from place to place and from time to time; and direct contact between neighbouring crystals will occur at some localities in the narrow interstices, by leaving the major part of the narrow interstices as the liquid or amorphous layer in the manner described above.

In a few cases, as of bismuth and others, where the substance expands on crystallization, the circumstances are different. In this case the decrease of N_l at the narrow irregular interstices between neighbouring crystals by the crystal growth connot be possible. On the contrary various parts of the thin liquid layer will be subjected to enormous and irregular pressure, and this enormous and irregular pressure will act to melt the crystal at its surface partly by lowering the melting point of the crystal and partly by destroying the crystal into finest crystallites and by giving at the same time considerable distortion. Considering this, though the reason is different, the persistence of the amorphous layer is not inconceivable in this case also.

Recrystallization of Cold Worked Metals

Cold worked metal crystals recrystallize at a temperature much lower than the melting point of the metal. As to the ultimate mechanism of this phenomenon the writer and K. Koyanagi[1] proposed a theory several years ago. In that theory the following three assumptions were made: 1) The metal crystals melt at their boundaries in the recrystallization temperature range, and the recrystallization takes place through the growth of the crystal nuclei formed in the melt. 2) The metal crystal is easier to melt at its contact surface with the melt than in its interior. 3) Distorted metal crystals are easier to melt than those without distortion. The third assumption was modified in the previous report[2] as follows:– Distorted crystals and extremely small crystals are much easier to melt than undistorted larger ones. For the first two assumptions some explanation will be given here. It has already been stated that the amorphous layer in the cybotactic state may exist at the boundaries of the crystal grains formed by solidification from the melt. It is also considered

1. U. Yoshida and K. Koyanagi; These Memoirs, A, **18**, 9 (1935).
2. loc. cit.

that the boundaries of the crystallites formed by the process of slipping are cemented to a considerable degree by the amorphous solid layer of the cybotactic state. In the latter case there may still be some part of the boundaries not transformed into the cybotactic state. However the crystallites in these parts would have been smashed into considerable fineness and their lattices would have been distorted to a considerable degree; and these parts, together with the already existing amorphously solidified layer, will be reduced to the liquid state by raising the temperature to a recrystallization range. Thus at this temperature the larger part of the boundaries of the crystallites is changed to the liquid state; and this is nothing but the first part of assumption 1). When this state is reached, the liquid state or the cybotactic state can exist as such for all temperatures in very narrow interstices between neighbouring crystallites or crystals, as is considered before in the case of the crystallization in the melt. This property of the persistency of the liquid or amorphous layer at the crystal boundary seems to play an important rôle in the process of recrystallization of plastically deformed metals.

When a metal is deformed plastically above a certain degree, the majority of the crystallites are to be supposed to have a lattice distortion of various degrees after deformation. Now let us suppose that a crystal nucleus, which has no lattice distortion, is formed spontaneously in the liquid layer between the neighbouring distorted crystallites and has grown to a considerable size without suffering any distortion by the process of recrystallization. Then the molecular exchange between the undistorted and the distorted crystals will be made easily by means of the thin liquid layer between them which, when once formed, can persist for ever. In Fig. 1, suppose A and B to be the undistorted and distorted crystals respectively, which are separated by a thin liquid layer, and let N_c and N_l' be the surface density of the molecules of the crystals and the liquid at the boundary surfaces. Moreover let a be the crystallizing factor and β and β' be the melting factors of the undistorted and distorted crystals respectively. Then, as the distorted crystal is supposed to melt easier than the undistorted one, the value of β' should be greater than β. As to the value of N_l', it is considered to be much lessened from its normal value at a narrow interstice between

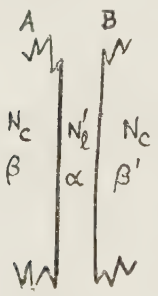

Fig. 1

neighbouring crystals and at a recrystallization temperature which is of course much lower than the melting point of the crystal. Now consider that the growth of the undistorted crystal has reached such a state that the lessened value of $\alpha_{\perp}V_i'$ has just become equal to the value of ${}_{i}\beta_{\perp}V_e$. Then as the value of ${}_{i}\beta'_{\perp}V_e$ is greater than that of ${}_{i}\beta_{\perp}V_e$, that is than that of $\alpha_{\perp}V_i'$, some part of the outer surface of the distorted crystal will be transformed to the liquid phase. This increases the value of $_{\perp}V_i'$, and a further growth of the undistorted crystal will continue again. In this way the growth of the undistorted crystal will proceed further and further by means of the intermediary action of the liquid layer by consuming the distorted crystals, as long as distorted crystals remain. Ordinarily, with a cold worked metal, it is usual to have many undistorted crystal nuclei; and in this case the end of the crystal growth by recrystallization is reached when the undistorted, newly grown crystals have come into contact with each other with only a thin amorphous layers between them. In this way the presence of a persistent thin liquid layer between two neighbouring crystales enables the less distorted crystal to grow by consuming the more distorted one, as long as there is a contrast in the degree of lattice distortion, even of very small degree. It is already stated that very small crystals are much easier to melt than larger ones. Thus the contrast in size between neighbouring crystals acts for crystal growth, in exactly the same way as the contrast in the degree of lattice distortion, and the growth of the larger crystal by consuming the smaller one is more favourable than the growth in the reverse direction. A sharp end of a protuberance of a crystal which is surrounded by another crystal, like a very small crystal, will have the same tendency to melt more easily. This property of the effect of the shape and the size of the crystal may be stated simply as follows: the greater the convexity of a crystal the more easily it melts. The presence of a persistent thin liquid layer between neighbouring crystals seems to be very important in understanding the mechanism of the crystal growth in the process of recrystallization. By virtue of the existence of such a thin liquid layer the growth of the stronger crystal can proceed as long as there is some contrast, even in very small degree, in the melting tendency between two neighbouring crystals, such as is due to the degree of lattice distortion or to the degree of convexity. Thus the final state reached by sufficiently high and prolonged heating in recrystallization,

will be such that there is little contrast in lattice distortion, in convexity and in crystal size between neighbouring crystals. This is in conformity with actual observation in comparative evenness of the size of new crystals formed by recrystallization, and in that their boundaries consist of rather continuous curves or lines without too much ruggedness. In respect to the latter fact T. Sutoki[1] has made a very interesting observation. He observed that a crystal grows, in most cases, on its concave side by consuming the convex side of the neighbouring crystal in the final stage of recrystallization, where the lattice distortion contrast has seemed to have been almost removed. As to the evenness of the crystal size mentioned above, it is no more than a rough statement; and a considerable range of difference in crystal size is of course present. This signifies that the crystal growth cannot be determined by the crystal size contrast alone, but that there are still some other factors affecting this; and the writer's view simply regards the lattice distortion contrast as the most preminent among these factors. In the case of the growth of crystals to a considerable size in a specimen composed of very small crystallites, which have suffered different degrees of lattice distortion by the preceding process of cold working, it seems probable that it took place in many steps, and not in one step directly from all the nuclei to the final crystals by consuming the initial distorted crystals. At first a lot of nuclei will be formed rather evenly in the specimen, then by consuming all the old distorted crystallites situated in the region between them they will grow until they come into direct contact with each other. The release of the internal strain by this first step of crystal growth will of course, be considerable, but it will not be complete for all the new crystals on account of too many new crystals in an irregular manner and the different velocity of crystal growth and melting from crystal to crystal. Thus after this first stage of the crystal growth, there remains still the lattice distortion contrast and the crystal size contrast; and the crystal growth of the stronger and healthy ones will proceed further by consuming the weaker ones in succession, as long as there remains some lattice distortion and crystal size contrast between neighbouring crystals. This is like the players in a tennis tournament, and the final equilibrium is attained among the strongest crystals having almost the same strength. In this way, the displacement of all the initial

1. T. Sutoki: Sci. Rep. Tôhôku Imp. Univ., **17**, 857 (1928).

crystallites by new crystals in recrystallization seems to be explained clearly, with the aid of the idea of a persistent thin liquid layer between the neighbouring crystals.

During the growth of a crystal by recrystallization it may happen sometims that its power of growth is reduced accidentally by some cause, such as by suffering some degree of distortion etc.; and consequently that the crystal, though it has started from a strong nucleus, is consumed by some other which has grown under more favourable circumstances. But statistically the crystals which can survive to the end will be those grown from the strongest nuclei. According to the writer's view, crystal nuclei are formed in the melt at the boundaries of the deformed crystallites. Consequently the strongest nuclei whithin a certain volume, will be formed at the localities in the metal where the crystallites have suffered severest disturbance by the process of cold working and have become easiest to melt. This consideration was stated similarly in a former paper,[1] where a rough calculation was attempted of the number of crystals formed by recrystallization at different temperatures and with different degrees of cold working.

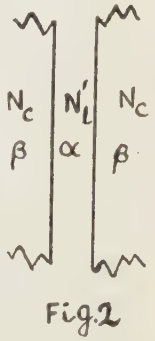

Fig. 2

Next let us consider the effect of temperature on the thin and persistent liquid layer between neighbouring crystals having the same crystallizing power. Suppose that the thin liquid layer exists between two perfect crystals as shown in Fig. 2. In this case the surface density N_c of the molecules situated at the crystal lattice can be considered to be the same for different temperatures. But the other factors α, β and N_l' affecting the crystal growth must be considered to vary with the temperature. When the temperature T is raised α will decrease and β will increase in the manner as is shown in Fig. 3. With most metals, which expand by melting, the proportion of the values of α and β at its melting point will be such as is shown by the proportion of the lengths of the lines AC and BC; α being somewhat greater than β corresponding to the value of N_l' which is smaller than N_c. When two neighbouring crystals are in equilibrium with the liquid layer between them at a temperature below the melting point, we have, corresponding to a reduced value of N_l', $\alpha N_l' = \beta N_c$, and consequently

1. U. Yoshida, S. Nagata and Ch. Mitsuki; These Memoire, A, **19**, 169 (1936).

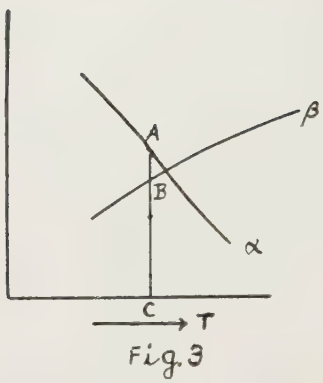

Fig. 3

$\beta/\alpha = N_l'/N_c$. As is seen from Fig. 3, β/α and consequently N_l'/N_c increase with increasing temperature: that is the surface density of the liquid molecules in the thin layer increases gradually with increasing temperature and approaches a normal value at the melting point. As the decrease of N_l' with decreasing temperature is assumed to be caused by the decreasing thickness of the thin liquid layer, the increase of N_l' with increasing temperature signifies the increase of the thickness of the thin liquid layer as it approaches the melting point. When a metal such as aluminium is recrystallized by prolonged heating at a high temperature which is very near the melting point, the crystal boundaries become engraved as narrow grooves, the width of which increases with temperature and attains sometimes to about one mm. at a temperature just below the melting point. The formation of such grooves at the crystal boundaries was ascribed in the previous report[1] to the melting at the crystal boundaries and consequently to the rapid evaporation occurring there. This is in harmony with the present theory.

In the light of these considerations, the mechanism of crystal growth by recrystallization is fully explained by assuming the presence of the persistent thin liquid layer at the crystal boundaries. By any theory which ascribes the crystal growth to sublimation and condesation, the rapid crystal growth at high recrystallization temperatures seems not to be accounted for. The consideration that the contrast in lattice distortion, in convexity and in crystal size between two neighbouring crystals is cancelled by the presence of the thin liquid layer at the crystal boundary in the process of recrystallization is nothing but the assumption 2) in the former paper,[2] that the metal crystal melts more easily at its contact surface with the melt than in its interior. When a metal is cooled to the room temperature after recrystallization, part of the liquid layer existing between two neighbouring crystals will be solidified as the extension of one or both of them, but still a very

1. U. Yoshida and K. Koyanagi; loc. cit.
2. Ibid.

thin layer between them will be left as super-cooled amorphous solid in the cybotactic sense just as it is in the case of crystallization in a melt.

Very recently F. M. Jaeger and A. J. Zuithoff[1] measured at temperatures higher than about 500°C the specific heat of two specimens of cobalt, one composed of comparatively large crystals and the other composed of very fine crystallites deposited by electrolysis. They found that the latter had a smaller specific heat, and moreover that the specific heat of the latter increased and became equal to that of the former when its crystals had grown to a considerable size by recrystallization. Similar observations on cold worked metals and alloys were also made by S. Sato,[2] H. Quinney and G. I. Taylor.[3] According to these authors some amount of energy is imparted as latent energy to the metals and alloys by the process of cold working, and this latent energy is re-emitted by heating the metals and alloys to high temperatures. These facts are in accordance with the writer's view that the latent heat of fusion is smaller with smaller and distorted crystals, and consequently that the smaller and the distorted crystals are easier to melt than the larger and undistorted ones. When the specific heat of the specimen composed of very fine and distorted crystallites is measured at high temperatures, the distortion will be released and small crystallites will melt and gradually recrystallize into larger ones; and by this process of annealing and recrystallization, heat evolution of some amount takes place by virtue of release of the distortion and of the preponderant latent heat of fusion of larger crystals as compared with that of smaller ones which melt and transform into larger ones by the recrystallization. Consequently the specific heat of the specimen will be reduced by this amount of heat evolved by the annealing and recrystallization.

The writer is grateful to the special fund of the Department of Education for the financial support given to the present work.

---

1. Jaeger and Zuithoff: Proc. Amsterdam, **43**, 815 (1940).
2. S. Sato: Sci. Rep. Tôhoku Imp. Univ. **20**, 140 (1931).
3. H. Quinney and G. I. Taylor: Proc, R. S, **163**, 157 (1937).

Change of the Elastic Limit of an Aluminium Rod by Cooling

By **Miyabi Sugihara**

(Received December 16, 1940)

Abstract

An aluminium rod previously heated, is elongated by stretching or by drawing through dies, and then immersed suddenly in liquid air for various durations of time. The elastic limit of such a rod increases rapidly in the beginning of cooling time, and then decreases slowly as the time is lengthened. Instead of being cooled in such a sudden manner, a cold worked rod is immersed in liquid air after being cooled by the cold air above the liquid. The second rod shows a similar tendency to the first in the measure of the elastic limit but gives somewhat smaller values. When the rod cooled at first by liquid air is heated at a temperature somewhat higher than the room, its elastic limit increases slightly.

Experimental Method

A commercial cold-worked aluminium wire about 2 mm in diameter was cut off about 20 cm in length, and the rod was straightened by hammering on a plane iron plate with a wooden hammer. A number of such rods were suddenly put into an electric furnace heated to approximately 500°C and annealed for about 6 hours; then they were taken out of the furnace and cooled suddenly to the room temperature.

In order to calculate the initial cross-sectional area of the rod prepared in different ways, for example, annealed only, or elongated by stretching or by drawing through dies, the diameter of the rod was measured at several different points with a micrometer screw gauge, and then the average value was taken. Next elongation testing of the rod was performed by the extensometer designed by the writer.[1] A curve showing the relation between the stress per unit initial cross-sectional area and the elongation per unit length, was plotted on a section-paper, and then the elastic limit was determined by use of the contact point finder reported previously by the writer.[2] In the present experiment, the following eight different processes were used.

Process I. The rod annealed in the electric furnace was here used as the primary state, and the rod stretched to a certain plastic elonga-

1. These Memoirs, A. **20**, 19, (1937).
2. These Memoirs, A. **20**, 27, (1937).

Pable I

Elastic limit of the rod in the primary state: 1.01×10^{-4}, elastic limit of the rod in the secondary state after being elongated by about 4.7%: 4.81×10^{-4}.

Specimen Group number	Duration of cooling time	Elastic limit		Young's modulus in C. G. S. unit
		Stress per unit area	Elongation per unit length	
1	2 hours	435 $\frac{kg}{cm^2}$	6.28×10^{-4}	6.79×10^{11}
2	7	453	6.61	6.72
3	16	433	6.25	6.79
4	69	405	5.88	6.75

Fig. 1

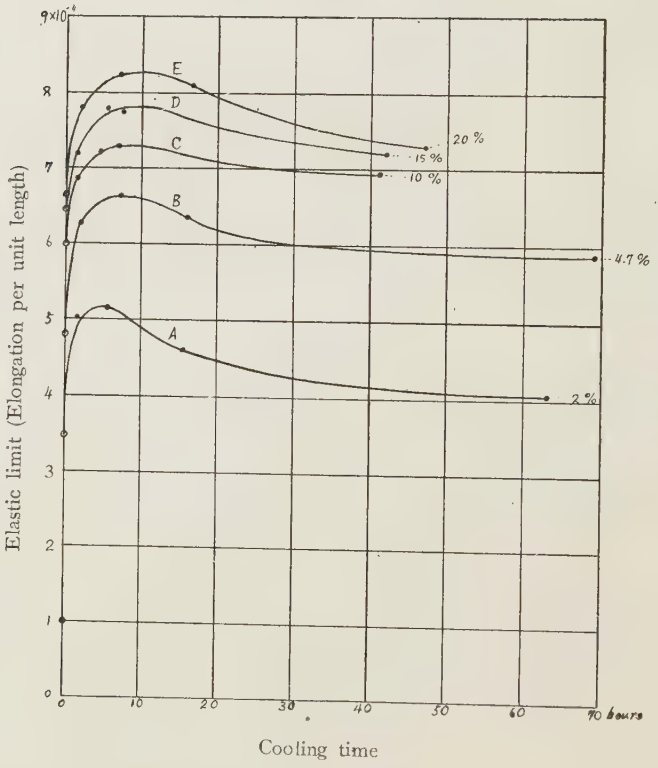

tion after annealing, as the secondary. Ten rods in the same secondary state were classified into five groups of two each, and the elastic limit of one group was measured. The remaining groups were immersed in liquid air separately for various durations of time and taken

out of the liquid air to the room where the elastic limits were measured. As an example the results are given in Table I. Rods stretched to several different plastic elongations were treated in the same manner as the above and the results are shown in Fig. 1.

Process II. Rods in the same primary state as in Process I were elongated, not by stretching, but by drawing through dies. This was the secondary state. Some of these rods were treated in the same way as in Process I. To compare the results in the case of gradual cooling with those obtained in the case of sudden cooling as described above, the remaining rods were classified into several groups each consisting of two in the same secondary state, and such groups were placed together for about 15 hours in the cold air (at about −40°C) above the liquid air. One group was taken out of the cold air to the room

Fig. 2

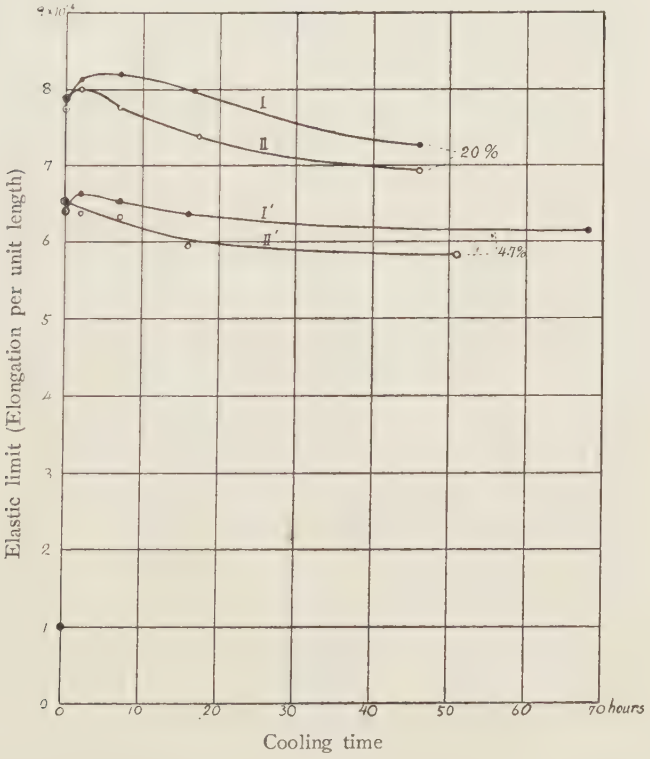

where the elastic limit was measured, while the remaining groups were immersed in liquid air for various durations of time, and then were

taken out of the liquid air to the room where the elastic limits were measured. The results are shown in Fig. 2. The degree of elongation in this case was calulated approximately from the reduction in diameter by assuming that the volume of the rod is constant.

Process III. To compare the result in the case of elongation by tension with that in the case of elongation by drawing through dies, the rods in the same primary state as in Process I were elongated by tension to the same degree as that drawn through dies. Such elongated rods were treated in the same manner as in Process II, and the results are shown in Fig. 3.

Fig. 3

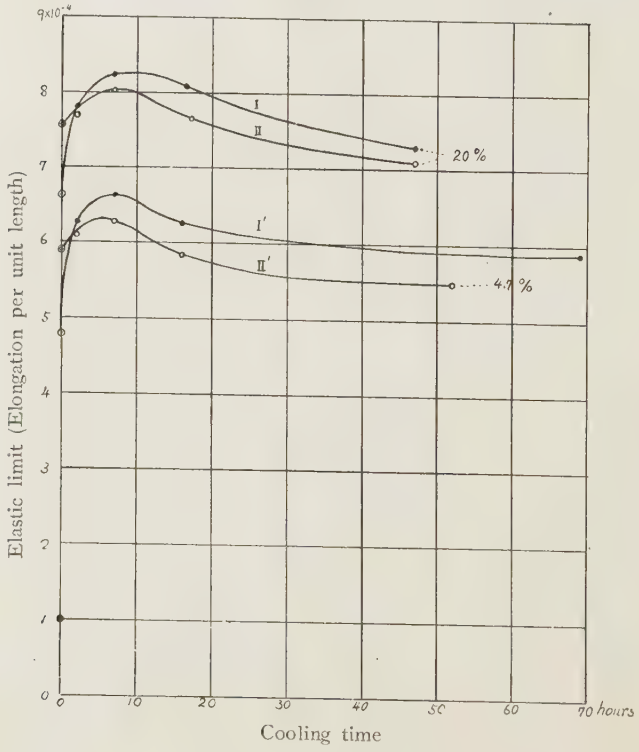

Process IV. A commercial aluminium rod about 5 mm in diameter, and about 20 cm in length was heated in the furnace at approximately 300°C for two days, and then taken out of the furnace. After being elongated by about 1.5 %, the rod was heated again in the furnace at about 600°C for two days. A rod composed of large crystal grains was obtained by this treatment. This was the initial state in

the present process. The elastic limits of several such rods were measured by elongation testing and the average was taken.

Several groups each consisting of two such rods in the initial state, were classified into two series as described in Process II, the one being subjected to the sudden cooling and the other to the gradual. One more group of each series, after being cooled, was annealed in the furnace at about 80°C and 120°C for approximately 10 hours and then the elastic limit was determined. The results obtained in the present process are given in Fig. 4.

Fig. 4

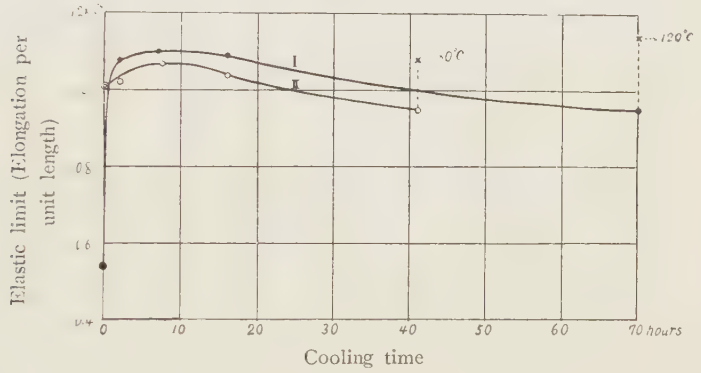

Process V. Several groups each consisting of two rods in the same initial state as in Process IV were classified into two series. Both series were subjected to gradual cooling as described above, the one being employed to measure the elastic limits after being taken out of the liquid air, and the other to do so after being annealed in the furnace

Fig. 5

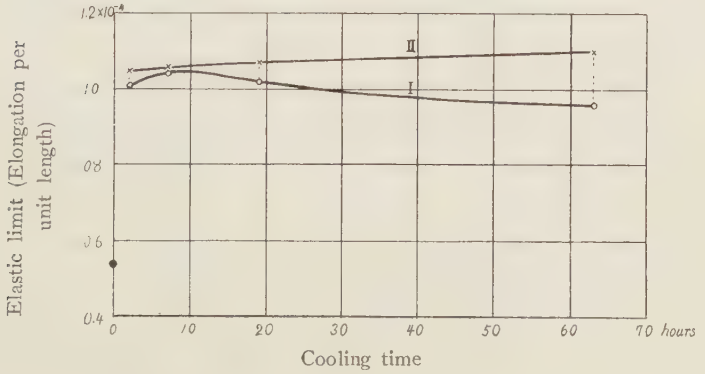

at approximately 90°C for about 10 hours. The results are shown in Fig. 5.

Process VI. The rods in the same primary state as in Process I were elongated by about 6 %. This was the secondary state in the present process. By placing some such rods under elongation testing, the average elastic limit of the rods was determined. Several groups each consisting of two rods in the secondary state were cooled suddenly by liquid air and the average elastic limit of each group was determined after it had been taken out of the liquid air to the room. In the present cooling, three of the groups were cooled for 13.5 hours, one being used to dotermine the elastic limit as described above, and the remaining two for testing after they had been annealed at 51°C for 6.5 hours, and at 95°C for 6 hours respectively. The results are shown in Fig. 6.

Fig. 6

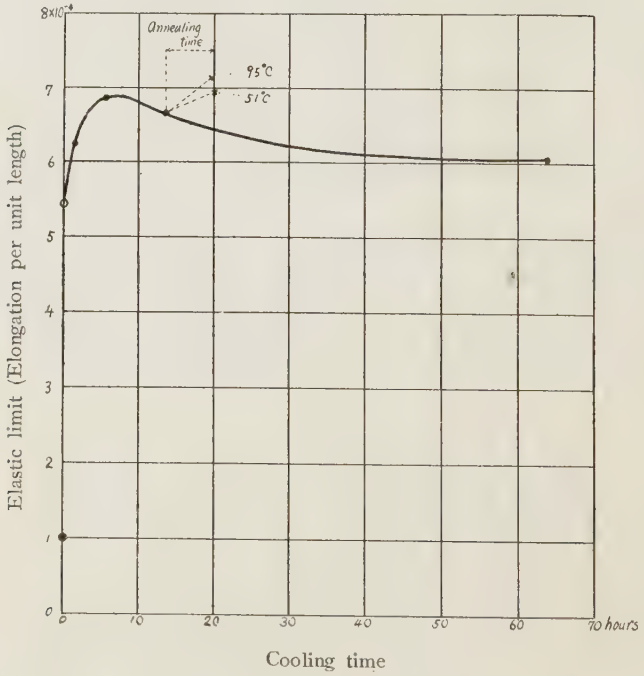

Process VII. Several groups each consisting of two rods in the same primary state as in Process I were cooled suddenly, without applying any cold work, by liquid air and the average elastic limit of each group was determined after being taken out to the room air.

One more group was subjected to such sudden cooling for 16 hours, and the average elastic limit of that group was determined after being annealed at 90°C for 10 hours. In the case of sudden cooling for 68 hours, exactly the same process as before was followed and the results are given in Fig. 7.

Fig. 7

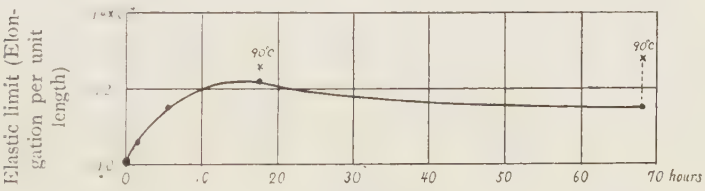

Cooling time

Process VIII. In all the above experiments, the elastic testing was accomplished within 1.5 hour at room temperature, after the specimen had been taken out of liquid air. Accordingly we must expect that the elastic limit might have changed somewhat during this test. The following experiments were performed in order to estimate the degree of this change.

Many rods in the same primary state as in Process I were elongated by 4.5 % by stretching. This was the secondary state in the case of stretching. Several groups each consisting of such rods were cooled suddenly by liquid air for 5 hours, and one group was placed under elastic testing soon after it was taken out of the liquid air, The remaining groups were classified into three series, and after each series was annealed for various

Fig. 8_1

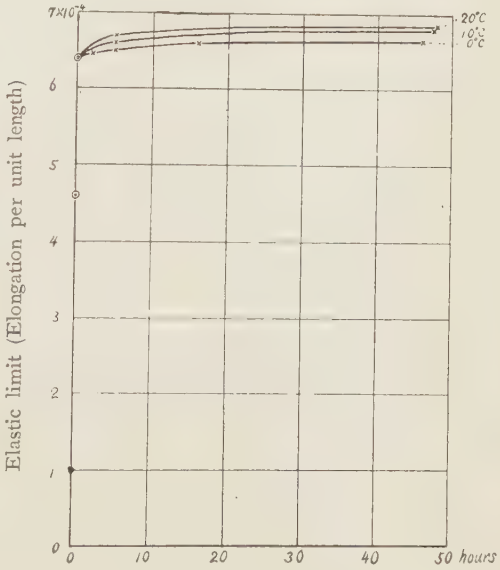

Annealing time

Fig. 8_2

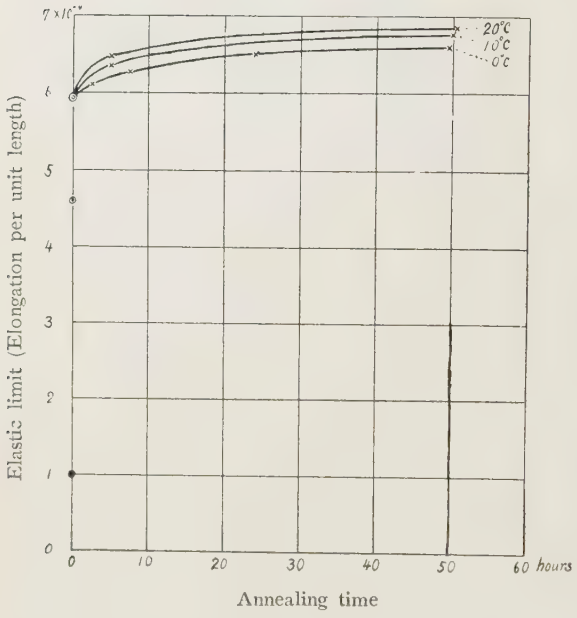

durations of time, at temperatures respectively of 0°C, 10°C and 20°C, it was placed under elastic testing. The results are shown in Fig. 8_1. Instead of being cooled for 5 hours, the rods in the secondary state were cooled for 39 hours and then treated in the same manner as sbove. The results are shown in Fig. 8_2.

In order to compare the results in the case of stretching with those in the case of drawing through dies, rods in the same primary state as in Process I were drawn through dies to the same amount of elongation as above, that is 4.5%. This was the secodary state in the case of drawing through dies. Such rods were subjected to the elastic testing after being treated in the same manner as above. The results are shown in Figs. 8_3 and 8_4.

Fig. 8_3

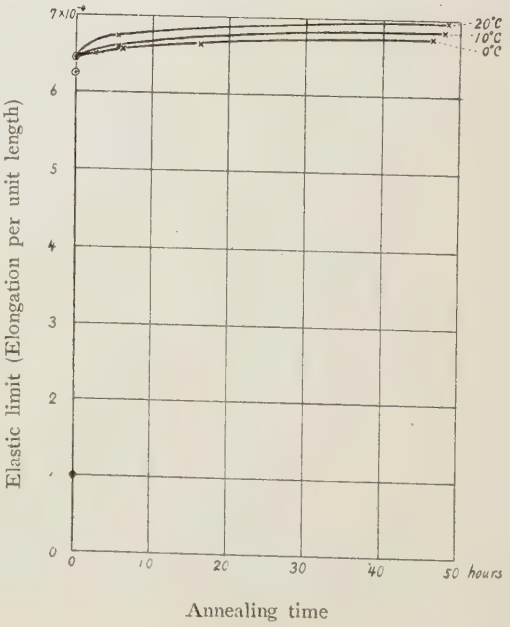

Experimental Results

From Table I, it is found that the elastic limit changes with the duration

of cooling time, but that Young's modulus remains almost constant. This fact is seen also everywhere through the elongation experiments carried out by the writer in room temperature.

Fig. 8₄

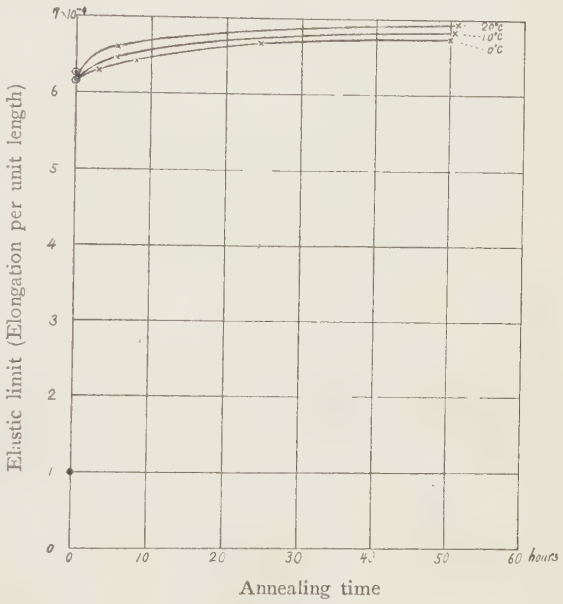

The results obtained in Process I are shown in Fig. 1. In this figure, the elastic limit of the aluminium rod annealed at about 500°C for 6 hours, in the so called primary state, is represented by a large dot •, its value being 1.01×10^{-4}, and that of each group subjected to each different amount of elongation by a circle having a centre ⊙. Further the elastic limit of the specimen cooled by liquid air for different durations of time is represented by a small dot ·. From the marks ⊙, it is seen that the elastic limit increases according to the increase of elongation. This fact was reported in a previous paper.[1] Curves A, B, C, D and E represent the results obtained from specimens elongated by about 2, 4.7, 10, 15 and 20% respectively. From these curves, it is found that the elastic limit increases rapidly at first and then decreases slowly with the cooling time, and that the specimen elongated by a larger amount always takes a larger value for the same cooling time than one elongated to a smaller amount.

Process II used two kinds of rods drawn through dies, the amounts of elongation being about 20% and 4.7%. The results are shown in Fig. 2 where the marks •, ⊙ and · have the same meanings as before. Curves I and I′ which represent the results obtained by sudden cooling, go up at first and then go down slowly according as the cooling time increases.

The elastic limit of a rod placed in the cold air (at about -40°C)

1. These Memoirs, A. **22**, 199, (1939).

above the liquid air, is represented by a double circle ◎, and that of such a rod immersed then in liquid air by a small circle ○. Curves II and II′ represent the results obtained by such gradual cooling, and the former goes up at first and then goes down slowly with the cooling time, but the latter goes down slowly from the beginning. Curves I and I′ are situted higher than Curves II and II″ respectively excepting at the vicinity of the starting points. In comparing Curves I and II with Curves I′ and II′ respectively, we find that the elastic limits in the case of larger elongation are larger than those in the case of smaller.

The results obtained in Process III, the amounts of elongation by stretching being 20% and 4.7%, are shown in Fig. 3 where the marks have the same meanings as in Fig. 2. Curves I and I′ show the results obtained by sudden cooling, and Curves II and II′ those obtained by gradual cooling. The former go up rapidly at first and then go down slowly with the cooling time, while the latter go up gradually at first and then go down slowly. Curves I and I′ are situated higher than Curves II and II″ respectively excepting for about the first 2 hours of the cooling time. The curves in the case of larger elongation are situated higher than those in the case of smaller. On comparing Fig. 3 with Fig. 2, it becomes evident that in general the curves show almost the same tendency.

The results obtained with the specimen composed of large crystal grains are represented in Fig. 4 where the large dot denotes the primary state. The elastic limits obtained by sudden cooling are denoted by Curve I. The elastic limit obtained by leaving the specimen in the cold air at about −40°C for approximately 15 hours is denoted by a double circle. The elastic limits obtained by immersing such cooled specimens in liquid air for various durations of time are denoted by Curve II. The cross × above the end points of the curves denotes the elastic limits obtained when the specimens in the states corresponding to the end points of the curves were annealed for about 10 hours at 120°C and 80°C respectively. Curve I goes up rapidly at first and then goes down slowly with the cooling time, and Curve II goes up gradually at first and then goes down slowly. The latter curve is situated somewhat lower than the former excepting the small region at the starting point. The elastic limit of the specimen annealed after being taken out of the liquid air is somewhat larger.

In Fig. 5 showing the results obtained in Process V, the marks

have the same meanings as described in Fig. 4. Curve I represents the result obtained by gradual cooling and Curve II that by annealing at about 90°C for about 10 hours after cooling. Curve I goes up gradually and then goes down slowly with the cooling time while Curve II goes up slowly. As seen from the curves, the elastic limits represented by Curve II are somewhat larger than those by Curve I.

In Fig. 6 showing the results obtained in Process VI, the marks have the same meanings as mentioned before, and the curve takes a form similar the curves in Fig. 1. When the specimens cooled suddenly by liquid air were annealed at 51°C for 6.5 hours and at 95°C for 6 hours respectively, their elastic limits were found to grow somewhat larger than the maximum value of the curve. Assuming that the annealing time is almost the same in each case, the value at the higher annealing temperature is somewhat larger than that at the lower.

In Fig. 7 representing the results obtained in Process VII, the marks have the same meanings as described before. The curve goes up gradually at first and then goes down slowly with the cooling time. When the specimen in the vicinity of the maximum point of the curve and that at the end point were annealed at about 90°C for about 10 hours, their elastic limits were seen to grow slightly larger in both cases.

The results obtained in Process VIII are represented in Figs. from 8_1 to 8_4 where the marks have the same meanings as before. As is seen from the curves, the elastic limit increases, to be sure, with the annealing time even with anealing temperatures as low as 0°C, 10°C and 20°C. But its amount of increase is very slight at the beginning of the annealing with those temperatures. Thus when the specimen is left at room temperature for about 1.5 hours after being taken out of the liquid air, its elastic limit is found to change only slightly; so that the specimen whose elastic limit was measured in room air in Processes from I to VII as described before, may be considered as almost identical in this respect with the same specimen immedietely after being taken out of the liquid air.

Consideration on the Results of the Experiment

In the present experiment, rods were cooled in three ways: by simply immersing the specimen in the liquid air, by placing it in the cold air (about–40°C) above the liquid air, and by placing it at first in the cold air mentioned above and then immersing it in the liquid air. The elastic testing was carried out within 1.5 hour after the rods were

taken out into the room air. Thus the specimen being annealed during this period of tesring at room temperature, the elastic limit measured is considered to give a slightly elevated value. But as the influence of such annealing upon the elastic limit must be considered to be very small as described above, the elastic limit measured in the room air may be expected in general to take approximately the same value it would just after being taken out of the cold place.

When the cold worked specimen is heated at approximately 500°C for about 6 hours, the crystallites grow considerably larger by recrystallization. If such a specimen is elongated plastically by stretching, the crystal grains are broken by slipping into smaller crystallites on the one hand, and on the other hand the localities of weak cohesion between crystallites and the unevenness of the internal stresses among crystallites will be formed in the structure at the same time. Of these two causes the former increases the elastic limit, and the latter decreases it; and as the former predominates in our case of aluminium at room temperature, the elastic limit increases just after the plastic elongation. This state is shown by the mark ⊙ in Fig. 1.

When the specimen is suddenly immersed in liquid air, it contracts severely and unevenly. Consequently the crystallites are again broken rapidly into smaller pieces, and at the same time the localities of weak cohesion between crystallites and the unevenness of the internal stresses among crystallites are again formed in the structure. This is just the same as in the case of plastic elongation, and the sudden cooling to the temperature of liquid air increases the elastic limit in the beginning of the cooling time as seen in Fig. 1. A certain quantity of crystallites breaks during the early period of cooling, but after that there is scarcely any further destruction of them; but the weak cohesion between crystallites at some localities increases and the unevenness of the internal stresses among crystallites is enhanced gradually with cooling time, by the lack of the recovery observed at temperatures higher than the room temperature. Hence after a certain cooling time, the elastic limit decreases gradually with the cooling time as is seen in Fig. 1.

When the specimen cold worked by stretching is cooled at a somewhat higher temperature, for example–40°C, by the air above the liquid air, it contracts in smaller amount than when cooled by the liquid air, and the destruction of crystallites, the weak cohesion between crystallites at some localities and the unevenness of the internal stresses among crystallites are all smaller than before; and consequently

the increase of the elastic limit is smaller as shown by the starting point ◎ of Curve II or II′ in Fig. 3. In comparing the case when the specimen cooled at first by cold air and then cooled further by liquid air with the case when it is cooled directly by liquid air from the beginning, Fig. 3 shows that the elastic limit is as a whole somewhat smaller in the former case than in the latter. This seems to be due to the smaller amount of destruction of crystallites, of weak cohesion between crystallites and of the unevenness of the internal stresses among crystallites in the former case.

The fact that the starting point ⊙ of Curve I or I′ in Fig. 2 is situated higher than that in Fig. 3 is considered to be due to the severer destruction of crystallites when the specimen is drawn through dies than when it is elongated by stretching. When a specimen prepared by drawing through dies is cooled suddenly or gradually by liquid air, the amount of increase of the elastic limit is smaller than in that prepared by stretching. This fact seems to be caused by the fact that a further destruction of crystallites occurs only to a small extent in the former case. Especially, when the specimen drawn through dies is cooled at first by cold air at about −40°C and then cooled in liquid air, any further destruction of crystallites must be almost imperceptible; and only the weak cohesion between crystallites at some localities and the unevenness of the internal stresses among crystallites increase gradually as a whole on the continued cooling, Thus the elastic limit decreases from the starting point or from its neighbour with the time of cooling as shown by Curves II and II′ in Fig. 2.

When the specimen composed of large crystal grains, which are formed by recrystallization, is cooled suddenly or gradually by liquid air, the destruction of crystallites results; and at the same time localities of weak cohesion between crystallites develop and unevenness of the internal stresses among crystallites is also produced in the structure as in the former cases. As seen in Fig. 4, the influence of those changes upon the elastic limit is similar to that in the former cases. When the specimen cooled by liquid air for a certain time is heated at a relatively low temperature, for example 80°C or 120°C, the elastic limit increases slightly. This fact is due to the recovery to a normal state of the localities of weak cohesion between crystallites and of the unevenness of the internal stresses among crystallites. Such a recovery is seen more clearly in Fig. 5, where the specimen at various stages of cooling time is annealed at approximately 90°C for about 10 hours. As is seen in Fig. 7, where the specimen prepared by heating at about

500°C for about 6 hours is used, and in Fig. 6, where the specimen elongated by stretching after being heated is used, such a recovery as described above makes the elastic limit somewhat higher.

From these considerations, the following conclusions may be drawn. When the specimen composed of relatively small crystallites is cold worked by stretching or by drawing through dies, the crystallites are broken into smaller pieces on the one hand and on the other, the localities of weak cohesion between crystallites and the unevenness of the internal stresses among crystallites occur at the same time somewhere in the structure. The former makes the elastic limit higher and the latter makes it smaller. The elastic limit as measured is thus the resultant of these two effects. The fact that the elastic limit of the specimen of aluminium prepared by cold working becomes greater is due to the predominance of the former effect.

When the specimen prepared by annealing or by cold working is cooled suddenly or gradually by liquid air, the crysallites are broken into smaller pieces by the severe contraction on the one hand and on the other, localities of weak cohesion between crystallites and unevenness of the internal stresses among crystallites result in the structure at the same time. In the beginning of cooling time, the former effect predominates over the latter, so the elastic limit increases. After a certain time, the destruction of crystallites almost ceases, but gradually the weak cohesion between crystallites at some localities increases and the unevenness of the internal stresses among crystallites grows larger, and accordingly the elastic limit decreases slowly with the cooling time.

When the specimen in such a state is annealed at a relatively low temperature, for example 90°C or 120°C, the localities of weak cohesion and the unevenness of the internal stresses gradually recover to the normal state, and accordingly the elastic limit increases.

In conclusion, the writer wishes to express his sincere thanks to Prof. U. Yoshida for his kind guidance in the present experiment.

Plastic Deformation of Metals

By Usaburo Yoshida

(Received January 8, 1941)

Abstract

By the plastic deformation of a metal, the slip along a slip plane of the metal crystal causes the smashing of the crystal into fine crystallites of scattered orientation. The lattice distortion and the uneven internal strain of the crystallites take place simultaneously. As to the boundaries between neighbouring crystallites, some are supposed to be cemented in the cybotactic sense, by the Beilby's amorphous layer, and the rest are considered to be weakened in intercrystalline cohesion. These facts help to explain the change of the mechanical properties of metals, single and polycrystalline, by plastic deformation, and by aging and light annealing.

Destruction of Metal Crystals by Plastic Deformation

Plastic deformation of a metal crystal is usually considered to follow a slip in a slip direction along a slip plane of the metal. Ordinarily the slip process never occurs in an ideal manner; and the crystal is, at the same time, smashed somewhere into fine crystallites of somewhat scattered orientation, the degree of scattering increasing, as is revealed by x-ray examination, with the amount of the slip. This smashing into fine crystallites appears to be caused by an irregular coercionary stress distribution due to imperfection in the internal structure of the crystal and also, in the case of polycrystalline material, to the interaction between neighbouring crystallites near the crystal boundaries. The new crystallites thus formed by the drastic process of smashing will be strained, by being stretched or compressed unevenly, and their lattices will be differently distorted. It is already stated in former papers[1] that the melting point of a very small and distorted crystal of submicroscopic size, can be reasonably supposed to be much lower than that of the adult crystal. Thus when very very fine and distorted crystallites are formed somewhere in the interstices between neighbouring larger crystallites, it may happen that they melt by the local heating occurring here and there during the slip process by the plastic deformation. If this has occurred, very rapid cooling to the normal temperature, which takes place at the

1. U. Yoshida: These Memoirs, A., **23**, 207, 225, 237 (1941).

same time as the melting, will solidify the melt as its supercooled amorphous state, consisting of the cybotactic crystals and free molecules distributed at random as has been recognised before.[1] Such supercooled solid is nothing but the so-called Beilby's layer which, owing to its isotropic strength, binds neighbouring crystallites firmly, except at high temperatures. Though neighbouring crystallites will be, to a considerable degree, cemented by the formation of Beilby's layer, the cementing will not be complete, and there will remain interstices between neighbouring crystallites where Beilby's layer may or may not be formed afterwards by aging or by light annealing. These portions of the interstices between neighbouring crystals which remain uncemented during the process of plastic deformation will be the localities of weak cohesion between neighbouring crystallites. Among these, some can and a few others cannot be transformed to the cementing Beilby's layer by aging or by light annealing after the plastic deformation. Moreover, it may be imagined that very fine fissures of a few atoms in width are formed somewhere between neighbouring crystallites by plastic deformation. These will also be the localities of weak intercrystalline cohesion, most of which can and a few others cannot be mended by aging or by light annealing. In such a way, the mending of most of the localities of weak intercrystalline cohesion by aging or by light annealing will harden the metal as a whole, as was detected by M. Sugihara[2] who noted the elevation of the elastic limit of a cold worked polycrystalline aluminium rod by a slight annealing. Aging or slight annealing will also diminish the uneven internal strain of the crystallites on the one hand, and their lattice distortion on the other. Of these two effects, the latter weakens the metal and the former tends to raise the elastic limit of the metal. As to the presence of a few localities of weak intercrystalline cohesion, which can not be mended simply by aging or by light annealing, they will not have any noticeable effect with moderate plastic deformation ; but they will be the starting points of thicker fissures which give rise to the final failure with continued plastic deformation as observed in static tensile and fatigue tests.

The ideal slip which is supposed to occur in the slip direction along the slip plane does not affect the mechanical properties of metals. Thus the causes which arise from the plastic deformation and affect

1. U. Yoshida, loc. cit
2. M. Sugihara: These Memoirs, A, **21**, 145 (1938); **22**, 195 (1939).

the mechanical properties of metals will be: 1) Destruction of the crystals into smaller crystallites having scattered orientation. 2) Lattice distortion in crystallites. 3) Formation of uneven internal strain among crystallites. 4) Formation of the amorphous layer at the boundaries between crystallites. 5) Formation of localities of weak intercrystalline cohesion. Among these causes, 3) and 5) weaken the metal by making its elastic limit or yield point lower. The lattice distortion in crystallites hardens the metal by hindering the easy slip in the slip direction along the slip plane in the crystallites. 4) combined with 1) also hardens the metal by cementing the boundaries of the new crystallites which are formed by destruction and have different orientations, and thus by making the slip in neighbouring crystallites difficult by virtue of the slip interference at the crystal boundaries. Heating affects differently the above five causes. The small crystallites having scattered orientation mentioned in 1) can be brought to larger ones only by the process of recrystallization which takes place usually at higher temperatures than the aging and light annealing. 2), 3) and 5) can be restored largely, but not completely to the normal state by aging or light annealing as is stated above; and their further complete recovery requires annealing at higher temperatures such as recrystallization temperature range. Formation of Beilby's layer between crystallites denoted by 4) occurs partly, as is stated before, during the process of plastic deformation, but a further approach to completion will follow heating at higher temperatures.

The five causes mentioned above, which take place in crystalline structure by the process of plastic deformation, are not independent, but are intimately connected. However, their individual effect is different in degree from case to case, so that different causes predominate respectively in different cases.

Tensile Deformation of Single Crystals of Metals

By applying a tension or compression of sufficient strength, a single metal crystal deforms by slipping in a slip direction along a slip plane, that is, the weakest crystallographic direction and the weakest plane of the crystal. If the slipping process would happen in an ideal manner, the mechanical property of the crystal would remain unaltered by the slip. But this is not actually the case. The metal crystals harden by a plastic deformation, even with the small amount of plastic deformation caused by tension or compression, where the

slip is supposed to occur mostly in the slip direction along the slip plane. This shows that, as stated before, unideal processes take place together with the ideal slip; as is evident from the destruction of the crystal into fine crystallites of scattered orientation, as is revealed by x- ray examination.

Fig. 1

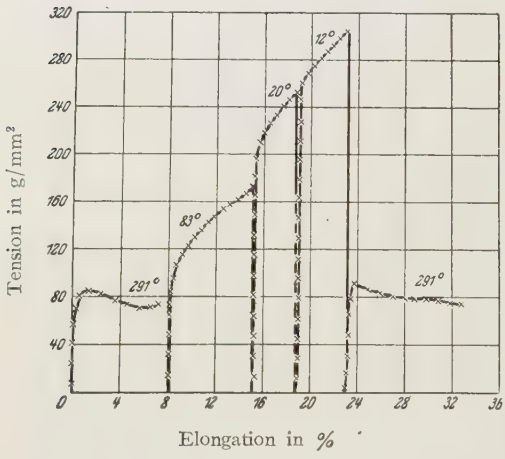

Fig. 1[1] shows the results of the elongation test made on a single crystal of cadmium at various low temperatures. In this case the elongation took place by steps, and the temperature of the specimen was changed when unloaded. As is seen from the figure, the tension which is necessary to sustain a certain amount of elongation increases with the amount of elongation when the temperature is lowered from room temperature to 12° K, and recovers to the original value when the temperature is again raised to the room temperature. This signifies that the cadmium single crystal hardens when elongated plastically at low temperatures, and recovers when its temperature is raised. Now let us consider the reason for this. The amount of destruction of the crystal into fine crystallites of scattered orientation will increase, of course, with the degree of elongation. Their unification to larger crystals cannot take place so long as the temperature is not raised higher to the recrystallization temperature range. Thus the recovery of the elastic and plastic property of the cadmium crystal at room temperature after the plastic deformation

Fig. 2

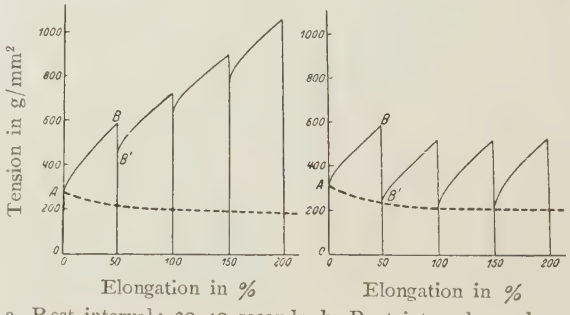

a, Rest interval: 30-40 seconds b, Rest interval: 24 hours

1. E. Schmid und W. Boas: Krystalplastizität, 156 (1935).

made at low temperatures cannot be accounted for by this cause; and consequently, for the hardening by straining at low temperatures, another reason must be sought. Formation of the amorphous layer by plastic deformation at low temperatures increases the elastic limit or the yield point, and it does not accord with the recovery by raising the temperature to the room. Formation of localities of weak intercrystalline cohesion is in direct contradiction to the strain hardening at low temperatures. Increase of the uneven internal strain among crystallites by plastic deformation spoils the proportionality between stress and strain and it lessens the elastic limit. This is especially remarkable in the case of polycrystalline iron and steel as will be considered later. When polycrystalline iron or steel is plastically elongated beyond their yield point at room temperature, and an elongation test is repeated, we see that the elongation does no more increase proportionally with the tension. As the uneven internal strain can be removed by sufficient aging or annealing, its removal at such low temperatures as in the case of Fig. 1 cannot be acceptable. Thus the increase of the proportional part with decreasing temperature seems to be inconsistent with the supposed increase of the uneven internal strain. This inconsistency becomes clearer if we consider the experiment shown in Fig. 2a,[1] where the elongation test on zinc single crystal was repeated stepwise at room temperature by interposing an unloaded rest for about 30–40 seconds. Here, contrary to the supposed decrease due to the increase of the uneven internal strain, the proportional part between tension and elongation increases again with the number of times the test is repeated. Taking these facts into consideration, strain hardening of single crystals of cadmium and zinc can be ascribed, in all probability, to the lattice distortion arising from the plastic deformation. The lattice distortion hardens the crystal by interfering with the crystal slip. Its amount increases with the degree of plastic deformation, and its recovery to the undistorted lattice is hastened by the thermal agitation with rise of the temperature; and the increase of the strain hardening of cadmium crystal at low temperatures with increased elongation and that of zinc crystal with repeated elongation at room temperature seems to be explained by the increase of the lattice distortion with increasing elongation, by being not much recovered at low temperatures, and with insufficient aging at room

1. E. Schmid und W. Boas: Kristalplastizität, 166 (1935).

temperature. Here it must be noted that the increase of interatomic cohesion with decrease of the temperature plays a part also in hardening the cadmium crystal at very low temperature. The strain hardening by lattice distortion recovers gradually with aging. When the time of unloaded rest is increased to 24 hours the zinc crystal hardened by previous loading softens at room temperature, to its original hardness, as in shown by Fig. 2b. The curves drawn in broken lines in Fig. 2 are those calculated on the assumption that the critical shear stress which is just necessary to cause the crystal slip is constant and is independent of the amount of elongation. The fact that the yield point of every one of the repeated elongation tests gets down to the theoretical curve in Fig. 2b shows that the recovery is already perfect with the aging of 24 hours in unloaded rest.

The recovery of the lattice distortion hardening is due to the thermal agitation of the constituent molecules. It is much retarded at very low temperatures, and, as is stated before, is increasingly hastened with rise of the temperature. This point will be more clearly seen from the fact that the yield point of a cadmium single crystal manifests itself more sharply with rise of the temperature as shown in Fig. 3.[1] When the lattice distortion is recovered, the cadmium specimen will behave in tensile test as if it were composed of a single crystal. Beyond the yield point, where the crystal slip begins, it goes on with a tension which is smaller than or at most the same as that at the yield point, by giving a sharp break to the tension-elongation curve at the yield point. The recovery of the lattice distortion with a single crystal of cadmium seems to be almost stopped at such a low temperature as 4.2° absolute as will be seen from the tension–elongation curve in Fig. 4,[2] where the tension which is necessary to cause a further elongation increases with the amount of elongation almost linearly up to 80 % elongation. The dependence of the recovery of the lattice distortion on temperature is more clearly seen in Fig. 5.[3]

Fig. 3

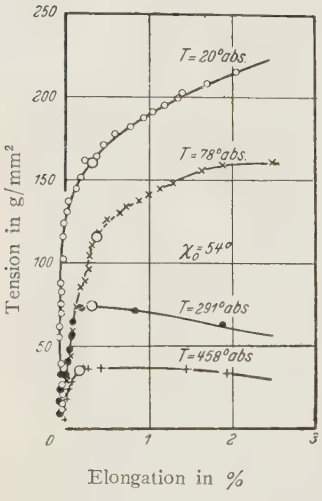

1. E. Schmid und W. Boas: Kristalplastizität, 152 (1935).
2. Ibid. p. 153.
3. Ibid. p. 159.

In this figure are plotted the curves showing the relation between the shear and the shearing stress which is necessary to cause the former in a single crystal of cadmium at different temperatures. The change of the strain hardening with temperature is remarkable at intermediate temperatures, but is only slight at very low and at very high temperatures. At high temperatures where there covery is nearly complete the curves run almost horizontally; and at very low temeratures where the recovery is almost suspended they stand close in a nearly vertical direction. The curves represented by broken lines in the figure show the results obtained with the loading of much higher velocity than those drawn in full lines. The fact that the former curves are situated somewhat higher than the latter seems to be due to smaller amount of recovery of the lattice distortion during the rapid elongation.

Fig. 4

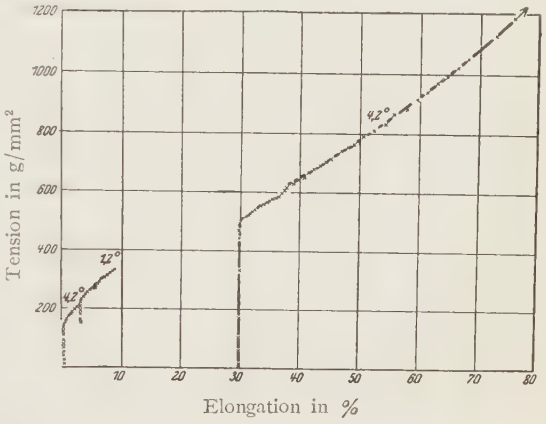

Fig. 5

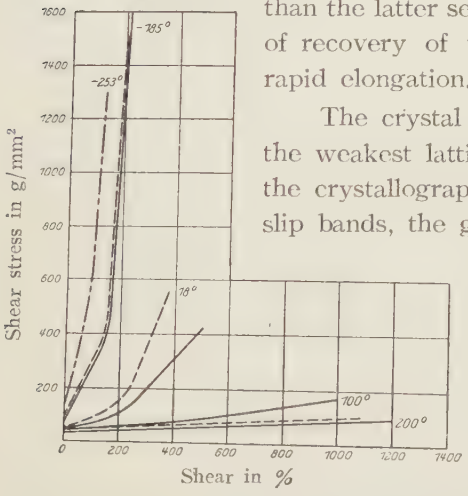

The crystal slip takes place unevenly along the weakest lattice planes which are parallel to the crystallographic slip plane, giving rise to the slip bands, the glide lamellae and glide packets. The coarseness of the glide packets depends upon the temperature and the rapidity of the slip. When the temperature is high or when the slip is very slow it becomes coarse. According to the writer's view some portion of the crystal in a slip band or a glide lamella is smashed by the slipping into extremely fine and distorted crystallites. When the slipping is not very slow some of these fine and distorted crystallites will be melted down to the amorphous layer successively by the local

heating occurring here and there during the slipping. When the temperature is not high the amorphous layer will be solidified immediately and the further slip will proceed along certain remaining virgin lattice planes which are weaker than the solidified layer, making the glide packets finer. On the contrary, when the temperature is high the amorphous layer, when once formed, will remain unsolidified and will be weak for resisting a further slip, so that the subdividing of the glide packets becomes increasingly rare. Next when the slip is very slow the local heating will be so slight that it is insufficient to melt the very fine and distorted crystallites and to transform them to the cementing amorphous solid; and the portion in the crystal where the slip has once taken place remains so weak that a further slipping proceeds along that portion rather than along the remaining virgin lattice planes. Thus the subdividing of the glide packets into finer ones is also prevented in this case.

Above the writer has stated the possibility of formation of the amorphous layer in the portion of the crystal where the crystal slip has taken place. This agrees with the amorphous hypothesis proposed first by Beilby, in that both assume the formation of the amorphous layer on the planes of slip. But the writer's opinion is in many respects quite different from Beilby's, and the objections to the Beilby hypothesis as raised by Elam[1] seem to be avoided by the modified opinion. The main points of her objection are: 1) At the moment that the surface layer melts, the slip direction would presumably be obliterated, and the direction of slip would be the direction of greatest slope in the slip plane; but the actual case contradicts this since the slip direction along the slip plane is not altered up to a very large amount of distortion. 2) The planes upon which slip has taken place, having a greater amount of amorphous material, would be harder than other similar crystal planes, but this is not the case. Plastic deformation hardens the metal as a whole. As to the crystal slip in the slip direction along the slip plane, the writer does not consider it to take place entirely in an ideal manner. Beside the ideal slip, unideal slip is supposed to occur even with a single crystal, by virtue of the presence of some crystal defects. On applying a strong external force, these crystal defects will call forth an irregular internal stress distribution and consequently the destruction of the crystal into fine and

1. C. F. Elam: Distortion of Metal Crystals 166 (1935).

distorted crystallites throughout the crystal. This hardens the crystal as a whole. On the plane of slip such destruction into fine and distorted crystallites will be severest, and in some localities it will be melted by local heating and immediately solidified by rapid cooling during the process of slip. As such local heating and subsequent solidification are supposed to take place only in an instant here and there in the plane of slip, this plane will be hardened even during the slipping process. Moreover the ideal slip, by which the regular molecular arrangement in crystal lattice is not disturbed, is considered to take place at the same time in other localities in the slip plane, guiding the slip in the same slip direction. The localities in the plane of slip where melting and subsequent solidification have taken place will be the localities of new crystal defects, and will call forth a further hardening of the whole of the crystal by continued slipping.

In the above description, the strain hardening of metal single crystals is ascribed mainly to the lattice distortion. This is due to the fact that, with a small amount of plastic deformation, the scattering of orientation of the neighbouring crystallites formed by the process of slip is not remarkable, so that the effect of the lattice distortion is predominant over that of the slip interference at the crystal boundaries. However when a metal single crystal is subjected to plastic deformation of great amount, it takes on a polycrystalline structure, having been composed of small crystallites scattered to a considerable degree in their crystallographic orientation. In this state the effect of the slip interference at the crystal boundaries becomes predominant; the destruction of the crystallites into finer ones of scattered orientation, formation of the amorphous layers between neighbouring crystallites, and the setting up of uneven internal strain among crystallites by a plastic deformation, will play a more important part in changing the mechanical properties of a metal. As to the formation of the localities of weak cohesion between crystallites, it seems to be essential in causing the final fracture by the static tensile and the fatigue tests.

Tensile and Repeated Tests of Polycrystalline Metals

The elastic limit or the yield point of a plastically deformed polycrystalline metal increses by aging or by light annealing, as is seen from the experiments of J. Muir[1] on iron and steel (Fig. 6) and from

1. J. Muir: Phil, Trans, R. S. **198**, 1 (1902).

M. Sugihara's[1] on aluminium. This is different from the case of a metal single crystal, where, as previously described, the yield point decreases by aging. According to Sugihara, the elastic limit of an aluminium rod, which is elevated by a slight annealing, decreases on further heating by the growth of the crystallites caused by the recrystallization. Thus it seems clear that the elevation of the elastic limit or yield point by aging or by light annealing is due primarily to the smashing of the crystallites into finer ones by the plastic deformation. A plastic deformation causes also other processes: formation of the amorphous layers between crystallites, uneven internal strain among crystallites, localities of weak intercrystalline cohesion and lattice distortion in the crystallites. By aging or by light annealing, most of the localities of weak cohesion are healed, uneven internal strain is reduced, amorphous layers increase and the lattice distortion is removed. Among these causes, the first three elevate the elastic limit or the yield point, by making the effect of the presence of finer crystallites greater than that due to the removal of the lattice distortion which softens the metal.

Fig. 6

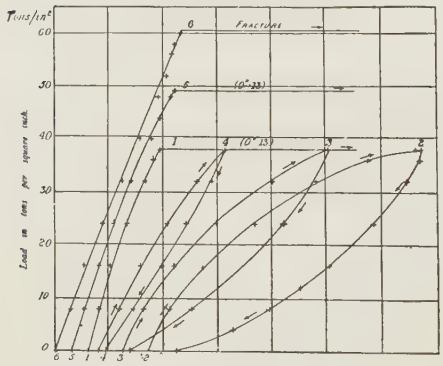

Scale:—1 Unit=$\frac{1}{2000}$th of an inch

Curve No. 1—Primary test.
" " 2—Shortly after No. 1.
" " 3—1$\frac{3}{4}$days " " 1.
" " 4—2 weeks after No. 1.
" " 5—After heating to 200°C.
" " 6— " " 200°C.

When polycrystalline iron or steel is deformed plastically beyond its yield point, it ceases to be elastic. The proportionality between stress and strain is obliterated; and the stress strain curve by loading and unloading develops into a loop, as is seen in Fig. 6. The loop becomes gradually narrower with aging, and at last the material recovers its initial elastic property, by a light annealing, having a higher yield point than before. Such violation of the proportionality between stress and strain seems to be caused mostly by the formation of an uneven internal strain among crystallites

1. M. Sugihara, loc. cit.

by the plastic deformation, by calling forth successively the crystal slip in different crystallites throughout the whole process of subsequent loading and unloading; this point will be considered later.

The effect of plastic deformation is revealed especially prominently in the case of hard metals such as iron and steel, owing to the slow recovery of their elastic property by aging or by light annealing. With soft metals such as aluminium the recovery is so rapid that the proportionality between stress and strain can be detected rather soon after the plastic elongation without any noticeable aging. The effect of aging or light annealing is only to elevate its elastic limit slightly. Moreover Hooke's law indicating the proportionality between stress and strain, is seen by Sugihara to be satisfied almost exactly by the tensile test with aluminium. This seems also to be due to the rapid and rather complete recovery of the elastic proporty by aging or by light annealing with this metal, the uneven internal strain among crystallites which are developed by a previous plastic deformation being mostly lost by the aging alone. However, in the case of iron and steel, of which the recovery of the elastic property is very slow, the exact proportionality between stress and strain below the yield point cannot be detected even after an annealing. This seems to show that the uneven internal strain among crystallites is very difficult to remove and, with these metals, some remains even after annealing.

Bauschinger was the first to show that the limits of proportionality between stress and strain under repeated stresses are not only the quantities characteristic of the material. but that their positions could be modified by the application of cyclical variations of stress. Under such applications both limits could be lowered or raised, but not necessarily by the same amounts. Bauschinger then proposed a theory that the range of these new limits of proportionality constituted a safe range of stress which the material could resist for an indefinitely large number of repetitions– "fatigue range". He called the elastic limits, as found by a primary loading, the "primitive" elastic limits, and gave the term "natural" elastic limits to those obtained by the material after undergoing cycles of stress. Bauschinger's theory has been supported by Bairstow's classical experiment.

C. F, Jenkin[1] ascribed the cause of non-proportionality between stress and strain to the crystal slip occurring during the tensile test

1. C. F. Jenkin: Proc. R. S., A, **103**, 121 (1923).

in some of the constituent crystallites of the material which have internal stresses in them before any load is applied. He supposed that all crystallites expand or contract elastically up to their own elastic limit with increase of the applied stress, then they slip along the slip planes in them with a resistance which is the same as or somewhat smaller than the cohesive force at the elastic limit. To test this idea, he constructed a spring-model and carefully explained the formation of the hysteresis loop by a cyclic extension-compression testing below the yield point, of some metals such as wrought iron, steel, etc. However, Jenkin's theory cannot cover the plastic behavior of metals beyond their yield point. By the continued plastic extension or compression beyond the yield point, all the crystallites would be slipping against the same resistances throughout, constant stress being sufficient to cause a continued deformation. Moreover the internal strain would be equalized among the crystallites rather than made uneven by the plastic deformation. These two conditions do not occur, usually, in the actual case; and some modification of Jenkin's idea is required. The resistance to the crystal slip in a crystallite, which takes place by extension or compression beyond its elastic limit, will be considered much smaller than the cohesive force at the elastic limit; and we shall regard it as approximately nil in comparison with the latter. Thus as soon as the crystal slip is started in a crystallite with negligible resistance, it will be at the same instant finished; and the two parts of the crystallite which have slipped on each other will be reunited as tightly as before the slip, by being released from the internal strain which has existed before the start of the slip, Consequently after the slip the crystallite will be ready anew for further elastic deformation. Generally such sudden slips in the crystallites will not happen simultaneously but in succession, moving from some to another. Moreover as the smashing of crystallites into finer ones and the production of the lattice distortion, act to elevate the elastic limit of the crystallites in a case when the localities of weak intercrystalline cohesion are recovered approximately during the plastic deformation, the plastic deformation does not necessarily cause strain softening, but rather strain hardening.

In the case of the plastic deformation of a metal single crystal, the crystal slip in the slip direction along the slip plane will not take place simultaneously along the whole portion of the slip plane. The slip will proceed in succession from some localities to others in the

manner supposed by the dislocation theory of Taylor and others; and no sudden decrease in the shearing stress for the slip at the yield point will be noticeable; and this is actually the case.

With some kinds of steel the yield point in tensile test is very sharp. At the yield point the load which is necessary to give a further extension lessens suddenly and then causes jerks in the load-elongation curve in the succeeding course of extension. It seems probable that with these metals the mutual interference for the crystal slip between neighbouring crystallites is especially remarkable, so that every one of the crystallites can withstand with mutual interaction an applied stress stronger than their own. When a sufficient stress is applied to such a test piece, and the crystal slip is caused in the crystallites at several localities in the test piece, then the crystal slip of smaller resistance will spread suddenly and pulsatorily throughout the whole portion of the test piece, travelling from one crystallite to the next in succesion due to the successive release of the interfering action for the slip.

With Jenkin's idea modified as before, Bairstow's experiments[1] of applying repeated cycles of tension and compression to a test piece of axle steel seem to be clearly understood. His experiments were carried out in the following way: To the test piece are applied direct tension and compression, the values of the range and mean stress of the cycle being adjusted as desired. The amounts of extension and compression of the specimen were measured by means of a mirror-extensometer. The first range of stress was certainly below the yield point observed in a static tensile test, and the first cycle loading indicated that the material was elastic.

Fig. 7

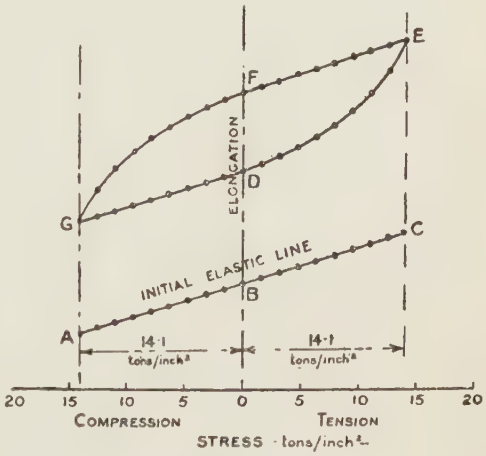

On further repetitions of stress, the straight line developed into a hysteresis loop. Fig. 7 illustrates the form of this loop obtained by giving the same range for the tension

1. L. Bairstow: Phil. Trans. R. S., A, **210** (1910).

and the compression (mean stress=o). In this case the loading was carried out in the direction DEFGD, and EF and GD were found to be parallel to ABC. At the first cycle, where the stress is proportional to the strain, the majority of the crystallites are supposed to be free from internal strain; and they can be compressed and extended equally well elastically. However, it may be imagined at the same time that a few of the crystallites have suffered the crystal slip in this cycle, owing to the presence in them from the beginning of internal strain to a considerable amount. Though the slipped crystallites are few in number on the first cycle loading, they will cause added internal strain in their neighbours; and in the following cycles these strained neighbours will suffer the crystal slip in succession. Thus after the repetition of a very large number of the cycles, the majority of the finer crystallites will come to have internal strain of different amounts and of different signs even at the state of no load. Now let us consider the cycle DEFGD, and suppose the state at D. At this state about one half of the crystallites will be stretched and the rest compressed; and the greater part of them, having only a small amount of internal strain, will follow the cycle elastically. As the D state is attained by expansion from the G state by unloading in compression, we cannot expect that there will be crystallites of noticeable number which are still considerably compressed at this state. However, the crystallites which are considerably stretched will be much more numerous, and these crystallites will slip along the loading curve DE in tension. On passing the point E, where the majority of the crystallites are supposed to be in a stretched state, they will contract elastically to the point F along the unloading curve EF in tension. At this point the circumstances are similar to those at the point D. Some crystallites which are severely compressed at this point will slip along the loading curve FG in compression. Lastly, after passing the point G, where the majority of the crystallites are supposed to be compressed, they will expand elastically to the point D along the unloading curve GD in compression. The formation of the Bairstow's hysteresis loop seems thus to be understood clearly.

Bairstow made his experiment with steel. Steel is a material whose natural elastic limits for reversed stresses are less than the primitive limits of proportionality. This is due to its slow recovery of the elastic property by aging. By a plastic deformation the crystallites are smashed into finer ones, having the lattice distortion and the

uneven internal strain. And at the same time localities of weak intercrystalline cohesion and amorphous cementing layers are produced here and there in the specimen. The recovery is a process which removes the lattice distortion and the uneven internal strain, and heals the weak intercrystalline cohesion merely by the thermal agitation or by increasing the amorphous layer. Thus by applying repeated stresses of sufficient strength to a test piece of such a metal as steel, it gradually loses its elastic property as is seen in Bairstow's experiment, on account of inability to recover with sufficient rapidity. This is in marked contrast to the case of such material as copper, where the recovery is remarkable even at room temperature. Fig. 8 shows the results of the experiment made by Gough,[1] by applying reversed bending stresses to a test piece of annealed copper. Annealed copper has no primitive elastic limit, and describes a wide hysteresis loop on first reversal. As the number of reversals increases, the width of the loop diminishes gradually, and at last the metal becomes elastic. As the recovery is rapid with copper, the lattice distortion of the crystallites and the uneven internal strain among the crystallites are both to a large degree removed during the course of the testing, and at the same time the localities of weak cohesion are almost healed; so only the effect of the presence of much finer crystallites is left and this elevates the elastic limit considerably by means of the slip interference at the crystal boundaries.

Fig. 8

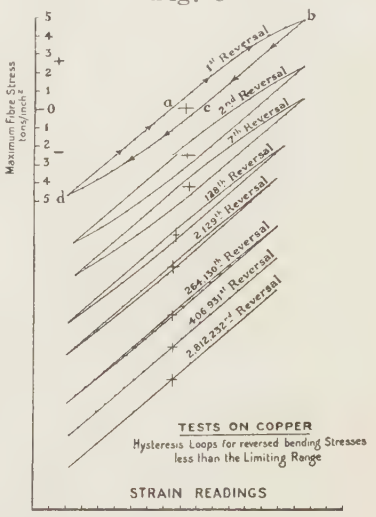

Creep, After-Working and Recovery

When a metal test piece is plastically deformed by applying a given load the deformation is not completed at the same time with the application of the load, but it continues to proceeds slowly and ceases only after the lapse of a considerable period. This is the creep phenomenon. On the contrary, when the test piece is unloaded

1. H. J. Gough: The Fatigue of Metals; p. 129 (1924).

after it has been deformed plastically, the final settling of its form requires a considerable time. This is termed after- working. These two phenomena are essentially the same, and signify that in a plastic change of material, it takes a long time to attain the state of structural equilibrium. As to the mechanism of these phenomena a clear explanation has already been given by Gough and Hanson.[1] When crystal slips occur in some of the crystallites, their effects will be transmitted to their neighbours in succession and will call forth slips in other crystallites of the specimen. Such effects are reciprocal to each other, and the final settling to structural equilibrium will be reached only after a long time. Recovery by aging or by light annealing is also a phenomenon of settling down to structural equilibrium, and is essentially the same as the creep and after-working. The only difference is that creep and after-working refer to the outer form and size of the material, and recovery relates mainly to its mechanical property. By aging or light annealing the lattice distortion of the crystallites diminishes, uneven intrnal strain among crystallites lessens, amorphous layers cementing the neighbouring crystallites are increased and the localities of weak intercrystalline cohesion are largely healed. These recovering actions will not necessarily take place simultaneously in all portions of the material, but will start at many distinct localities and spread to the other portions by passing through the intervening neighbours in succession. As is stated above the creep and the after-working are essentially the same phenomenon. The only difference is that, the former takes place on the loading and the latter occurs on the unloading. The effects of plastically deforming a solid and of the recovery of its mechanical property seem to stand entirely in the same relation as creep and after-working. Thus structurally considered, the recovery is essentially the same process as the plastic deformation; and it seems not unreasonable to imagine that such severe processes as the crystal slip and the formation of the amorphous layer, which are supposed to occur usually with the plastic deformation, take place also in the recovery, though very slowly.

Fatigue Test and Fracture

It is already stated that the elastic limit of a metal changes on applying repeated cycles of tension and compression, and that it rises or falls according to the kind of metal, and reaches the so called

1. H. J. Gough and D. Hanson: Proc. R. S., **104**, 538 (1923).

natural elastic limit. When the range of stress applied is within the natural elastic limit, the metal can withstand an infinite number of reversals of stress without fracturing. In this case all the crystallites are stretched and compressed elastically without suffering any crystal slip which brings about structural change in the material. On the contrary, when the stress applied is above the natural elastic limit, the metal suffers a plastic deformation on each reversal of stress. In this case fissures will be ceaselessly produced in the test piece during the course of the fatigue test. Many of them may be healed by the recovery or by the application of succeeding reversals of stress, but there will be some which widen gradually to be fatal with the progress of the test. Such fatal fissures, though only few at the beginning, will become so numerous at last that a greater part of the interior of the test piece is sectioned by their net-work, making the material very brittle. At this state the fracture of the test piece will occur immediately along a part of the net-work which offers macroscopically the least resistance to the stress applied, when a further cycle loading is repeated. The local contraction in cross sectional area at the fractured part, which is ordinarily observed in a static tensile test, does not commonly occur in the fatigue test. This fact accords well with the above view. In the case of the static tensile test, where the plastic deformation of the test piece before the fracture is great, the number of the fatal fissures will be only a few, and the major part of the material will be deformed plastically in a ductile and tenacious state, so that the contraction in the cross sectional area accompanies the elongation of the test piece. In this case, the stress concentration at the edges of such fatal fissures acts to develop the fissures and weakens the material. The portion of the test piece where the fatal fissures accumulate will be more stretched and consequently more slender than elsewhere, bringing finally the fracture at that point.

According to the static tensile and fatigue tests carried out at high temperatures, the tensile strength of a metal diminishes with increase of temperature, but its fatigue limit remains nearly unaltered up to a certain temperature. Generally the interatomic and intercrystalline cohesions weaken with rise of temperature, and this acts to diminish both the tensile strength and the fatigue limit in the same way. However the rapid healing of the localities of weak intercrystalline cohesion and of the primitive fissures at higher temperatures

prevent the metal from losing its ductility and tenacity, the qualities whose loss is fatal in the fatigue test. This recovering action counteracts to the reduction of fatigue limit of the material with rise of temperature, and helps it to maintain its health. In the case of a static tensile test, the tensile strength relates mainly to the strain hardening, which the material will acquire during the test. The diminution of such strain hardening, caused by quicker recovery and recrystallization at higher temperatures, assists in lessening the tensile strength with rise of temperature.

The writer is grateful to the special fund of the Department of Education for financial support to the present work.

Vol. XXIII, No. 5, Published, July 31, 1941

Price - - - - Yen 2.20

These Memoirs are on Sale at

MARUZEN COMPANY, LTD.
TOKYO, OSAKA, KYOTO, NAGOYA, YOKOHAMA,
FUKUOKA & SENDAI

昭和十六年八月二十五日印刷
昭和十六年八月三十一日發行

編纂兼發行者　京都帝國大學理學部

印刷者　須磨勘兵衞
京都市下京區北小路通新町西

印刷所　內外出版印刷株式會社
京都市下京區西洞院通七條南

賣捌所　丸善株式會社
東京、大阪、京都、名古屋、横濱、福岡、仙臺

CONTENTS

On the Refined Structure of the Silver-rich Aluminium-Silver Alloys
By Hajime Kotô 285
On the Refinement of the Eutectic-structure of Some Alloys by the Addition of a Small Quantity of Foreign Metal
By Kaoru Kase and Hajime Kotô 297
On the Crystalline Configurations of Zinc and Cadmium Deposited by Electrolysis
By Hideki Hirata, Hajime Kotô and Mituo Hara . . . 309
On the Constitution of the so-called Intermetallic Compound, "Ag_3Al" in the Silver-rich Aluminium-Silver Alloys
By Hajime Kotô 321
Structure of the Crystal Boundaries of Metals and the Phenomenon of Recrystallization
By Usaburo Yoshida 325
Change of the Elastic Limit of an Aluminium Rod by Cooling
By Miyabi Sugihara 337
Plastic Deformation of metals
By Usaburo Yoshida 351